

FINAL REPORT

Using Electrical Resistivity Imaging to Evaluate Permanganate Performance
During an In Situ Treatment of a RDX-Contaminated Aquifer

ESTCP Project ER-0635

AUGUST 2009

Steve Comfort
University of Nebraska, Lincoln

Vitaly Zlotnik
University of Nebraska, Lincoln

Todd Halihan
Oklahoma State University



Environmental Security Technology
Certification Program

This report was prepared under contract to the Department of Defense Strategic Environmental Research and Development Program (SERDP). The publication of this report does not indicate endorsement by the Department of Defense, nor should the contents be construed as reflecting the official policy or position of the Department of Defense. Reference herein to any specific commercial product, process, or service by trade name, trademark, manufacturer, or otherwise, does not necessarily constitute or imply its endorsement, recommendation, or favoring by the Department of Defense.

Standard Form 298 Report Documentation Page

REPORT DOCUMENTATION PAGE		<i>Form Approved OMB No. 0704-0188</i>
Public reporting burden for this collection of information is estimated to average 1 hour per response, including the time for reviewing instructions, searching existing data sources, gathering and maintaining the data needed, and completing and reviewing this collection of information. Send comments regarding this burden estimate or any other aspect of this collection of information, including suggestions for reducing this burden to Department of Defense, Washington Headquarters Services, Directorate for Information Operations and Reports (0704-0188), 1215 Jefferson Davis Highway, Suite 1204, Arlington, VA 222024302. Respondents should be aware that notwithstanding any other provision of law, no person shall be subject to any penalty for failing to comply with a collection of information if it does not display a currently valid OMB control number. PLEASE DO NOT RETURN YOUR FORM TO THE ABOVE ADDRESS.		
1. REPORT DATE (01-12-2008)	2. REPORT TYPE Report	3. DATES COVERED (From - To) May 21, 2007 – August 30, 2007
4. TITLE AND SUBTITLE Using Electrical Resistivity Imaging to Evaluate Permanganate Performance during an In Situ Treatment of an RDX-Contaminated Aquifer	5a. CONTRACT NUMBER	
	5b. GRANT NUMBER	
	5c. PROGRAM ELEMENT NUMBER ESTCP Project Number ER0635	
	5d. PROJECT NUMBER	
	5e. TASK NUMBER	
	5f. WORK UNIT NUMBER	
6. AUTHOR(S) Todd Halihan Steve Comfort Vitaly Zlotnik	8. PERFORMING ORGANIZATION REPORT NUMBER	
7. PERFORMING ORGANIZATION NAME(S) AND ADDRESS(ES) University of Nebraska, Lincoln Oklahoma State University	10. SPONSOR/MONITOR'S ACRONYM(S)	
9. SPONSORING / MONITORING AGENCY NAME(S) AND ADDRESS(ES)	11. SPONSOR/MONITOR'S REPORT NUMBER(S)	

12. DISTRIBUTION / AVAILABILITY STATEMENT					
13. SUPPLEMENTARY NOTES					
14. ABSTRACT <p>The difficulty and cost of groundwater remediation are compounded by our inability to directly observe the subsurface. Traditionally, boreholes and monitoring wells have been used to characterize sites and assess the performance of remedial efforts. These techniques are expensive and, by themselves, are effectively random samples guided by the training and experience of the investigator. Electrical resistivity imaging (ERI) is a geophysical technique that infers subsurface water and soil electrical properties. Where the soil, the contaminant, and remediation compound are suitable, ERI quickly and economically provides the investigator with a spatially extensive, high-density, high-quality model of subsurface conditions. ERI has earned success in research and applications by reliably locating contaminant targets where traditional drilling and direct push methods have failed to locate contamination.</p> <p>In this demonstration project, ERI was used to monitor injection of in situ chemical oxidation (ISCO): an injection of sodium permanganate to mineralize RDX at the former Nebraska Ordnance Plant near Mead, Nebraska. Monitoring wells showed that the ISCO demonstration was, indeed, transforming RDX, but samples from seventeen available wells and eight direct push profiles at different locations did not provide enough data to construct the distribution and flow of the injected permanganate. ERI showed that the permanganate injection flowed against the regional groundwater gradient, and that the solution was able to sink below the monitoring well screens. Without geophysical observations, no information would have been available to explain the permanganate and RDX concentrations observed in the wells. The same data were used to guide the boring of additional holes; unguided drilling would be a costly and inefficient option, based on essentially random location choices. ERI demonstrated its usefulness and value in monitoring a permanganate injection. The technology should be further explored and developed for use in pre-amendment tracer tests and quantitative remedial assessments.</p>					
15. SUBJECT TERMS					
16. SECURITY CLASSIFICATION OF:		17. LIMITATION OF ABSTRACT	18. NUMBER OF PAGES	19a. NAME OF RESPONSIBLE PERSON	
a. REPORT				b. ABSTRACT	c. THIS PAGE

Standard Form 298 (Rev. 8-98)
 Prescribed by ANSI Std. Z39.18

Table of Contents

<i>Standard Form 298 Report Documentation Page</i>	<i>i</i>
<i>Table of Contents</i>	<i>1</i>
<i>Acronyms</i>	<i>3</i>
<i>List of Figures</i>	<i>5</i>
<i>List of Tables</i>	<i>9</i>
<i>Acknowledgements</i>	<i>10</i>
<i>Executive Summary</i>	<i>11</i>
<i>1. Introduction</i>	<i>14</i>
1.1 Background	14
1.2 Objectives of Demonstration.....	15
1.3 Regulatory Drivers	16
1.4 Stakeholder/End-User Issues.....	16
2.1 Electrical Resistivity Development and Application	17
2.1.1 Existing techniques.....	17
2.1.2 Electrical Resistivity Imaging Theory.....	17
2.1.3 Halihan/Fenstermaker ERI Technology	19
2.1.4 ERI Data Collection and Processing	21
2.1.5 Potential Applications	22
2.2 Previous Testing of the Technology (ERI).....	22
2.3 Factors Affecting Cost and Performance of ERI.....	23
2.4 Advantages and Limitations of the Technology of ERI.....	24
<i>3. Demonstration Design</i>	<i>24</i>
3.1 Performance Objectives	24
3.2 Selecting Test Site	25
3.3 Test Site Description	27
3.3.1 General Hydrogeology	28
3.3.2 Former NOP Site Hydrogeology	31
3.3.3 Soil Electrical Conductivity (SEC) Logging and Correlation with Grain Size Analyses	37
3.4 Pre-Demonstration Testing and Analysis.....	39
3.5 Testing and Evaluation Plan.....	42
3.5.1 Demonstration Installation and Start-Up	42
3.5.2 Period of Operation.....	45
3.5.3 Amount/Treatment Rate of Material to be Treated.....	46
3.5.4 Residuals Handling	46
3.5.5 Operating Parameters for the Technology	46

3.5.6 Experimental Design.....	47
3.5.6.1 ERI Data Collection	47
3.5.6.2 Injection Planning	53
3.5.6.3 Injection Procedures.....	53
3.5.7 Sampling Plan.....	54
3.5.7.1 Sample Collection.....	54
3.5.7.2 Sample Analysis.....	55
3.5.7.3 Experimental Controls	55
3.5.7.4 Data Quality Parameters	55
3.5.7.5 Data Quality Indicators	55
3.5.7.6 Calibration Procedures, Quality Control Checks, and Corrective Actions.....	57
3.5.8 Demobilization	57
3.6 Selection of Analytical/Testing Methods	58
3.7 Selection of Analytical/Testing Laboratory	58
4. <i>Performance Assessment</i>	58
4.1 Performance Criteria	58
4.2 Performance Confirmation Methods	63
4.3 Data Analysis, Interpretation, and Evaluation.....	67
4.3.1 ERI Data.....	67
4.3.2 Injectate Data.....	75
4.3.3 Data Comparison.....	81
5. <i>Cost Assessment</i>	87
5.1 Cost Reporting.....	86
5.2 Cost Analysis.....	88
5.2.1 Cost Comparison	88
5.2.2 Cost Basis	88
5.2.3 Cost Drivers.....	90
5.2.4 Life Cycle Costs	91
6. <i>Implementation Issues</i>	92
6.1 Environmental Checklist	92
6.2 Other Regulatory Issues	92
6.3 End-User Issues	92
6.4 Lessons Learned for ERI Monitoring of Injections.....	93
7. <i>References</i>	95
8. <i>Points of Contact</i>	102
<i>APPENDICES</i>	103
<i>Appendix E: ERI 2D and 3D Data</i>	204

Acronyms

ARDC	Agricultural Research and Development Center
ASTM	American Society for Testing and Materials
ATSDR	Agency for Toxic Substances and Disease Registry
BAZE	Biologically Active Zone Enhancement
bgs	Below ground surface
CERCLA	Comprehensive Environmental Response, Compensation, and Liability Act
CoC	Chain of custody
d	Day
DO	Dissolved oxygen
DoD	U.S. Department of Defense
Eh	Redox potential
EPA	Environmental Protection Agency
ERI	Electrical Resistivity Imaging
ESTCP	Environmental Security Technology Certification Program
EW	Extraction well
ft	linear foot
gpd	gallons per day
gpm	gallons per minute
HASP	Health and safety plan
HPLC	High pressure liquid chromatograph
h	Hour
IC	Ion chromatograph
ISCO	In situ chemical oxidation
IW	Injection well
L	Liter
lb	Pound
lpm	liter per minute
mg	Milligram
min	Minute
MLST	multi-level slug test
MW	Monitoring well
NOP	Nebraska Ordnance Plant (former)

OSHA	Occupational Health and Safety Administration
OSU	Oklahoma State University
PI	Principal Investigator
Ppb	parts per billion
PPE	Personal protective equipment
Ppm	parts per million
QA	Quality assurance
QC	Quality control
RDX	Royal demolition explosive (hexahydro-1,3,5-trinitro-1,3,5-triazine)
RMS	Root Mean Square
SARA	Superfund Amendments and Reauthorization Act
SOP	Standard operating procedures
TCE	Trichloroethene
TNT	Trinitrotoluene
Mg	microgram (1×10^{-9})
UNL	University of Nebraska-Lincoln
USACE	United States Army Corps of Engineers

List of Figures

Figure 2.1-1. Field setup of ERI equipment. Metal stakes extend approximately 6 inches into the ground and are connected to an acquisition instrument via cables. Photo courtesy of Aestus, LLC.....	18
Figure 2.1-2. Evaluation of the performance of the Halihan/Fenstemaker method (commercial available as Geotrax Survey™). This method successfully mapped the horizontal and vertical extent of contamination at the site in a semiquantitative manner (Halihan et al., 2005): Left - comparison to core samples of LNAPL (gasoline) contaminated soil in Golden, OK. Right - ERI image at the location of the boring (warmer colors on the image represent more resistive material.	21
Figure 3.2-1. A) Site well map showing location of wells for original BAZE site. B) Wells added in 2007 for this project.....	27
Figure 3.3-1. Regional water table elevations of the Todd Valley Aquifer (modified from US Corps of Engineers, 1989 modified from Souders, 1967). Purple rectangle indicates location of pilot-scale permanganate injection site.	31
Figure 3.3-2. Water table elevations within the BAZE Study Site (October 2006).	31
Figure 3.3-3. Hydraulic conductivities within the study area.	32
Figure 3.3-4. Configuration of multi-level slug test system including packers and pressure transducer in riser pipe, connected to datalogger (from Zlotnik and Zurbuchen, 2003). Note 62 cm (2-ft) tested interval.	33
Figure 3.3-5. Hydraulic conductivity K_h observed in MW-15 using single- and double-packer multi-level slug test configurations.	34
Figure 3.3-6. Hydraulic conductivity, K_h , obtained from pre and post-injection multi-level slug tests on MW-15.	37
Figure 3.3-7. Soil electrical conductivity (SEC) measurements with depth at the permanganate injection site.	38
Figure 3.4.-1. Scaled contour plot of RDX concentrations ($\mu\text{g/L}$) within the injection site. Sampling occurred on 12/6/06.....	39
Figure 3.4-2. Geometry of the injection analysis	40
Figure 3.4-3. Testing well capacity: Upper row: head changes for re-injection to well IW-1; lower row: head changes for re-injection to well IW-2.....	42
Figure 3.5-1. Map of 12 primary ERI line locations and monitoring wells for the site. Heavy blue ERI lines C and 2 were used as monitoring ERI lines during injection. Purple ERI lines 3 and 4 were not collected during the background period.....	43
Figure 3.5-2. Schematic of injection setup showing photo of Aquifer Solutions, Inc. trailer.....	44

Figure 3.5-3. Photo of injection and extraction wells and safety fence setup. Location of ERI lines 2 and C are indicated with white dashed lines.....	45
Figure 3.5-4. Location of additional 6 meter ERI lines relative to original 10+2 line grid of 3 meter lines.....	52
Figure 3.5-5. Reciprocal and repetition error for ERI data collected at the BAZE site. The data represents data for one complete ERI dataset.....	57
Figure 4.3-1. 2D ERI pseudosection of ERI line D with location of wells on the line. The location of crossing lines are indicated with black vertical lines.....	67
Figure 4.3-2. Six-meter 2D ERI pseudosection of ERI line D with location of wells (if present) on the line. The location of crossing lines are indicated with black vertical lines.....	68
Figure 4.3-3. Geometric average of ERI datasets for location of screened intervals of monitoring wells compared with the hydraulic conductivity at the wells. The trend (solid black line) indicates a general increase in hydraulic conductivity with increases in resistivity. The dashed line indicates the expected trend when factoring in the results of the tracer test which supported a conclusion that the high resistivity areas (>3000 ohm-m) were less hydraulically conductive.....	69
Figure 4.3-4. A) Resistivity of ERI Line 2 (through injection plane) showing location of wells used to develop permanganate curtain, and the lithology develop for the site using other techniques B) Resistivity difference after injection.....	70
Figure 4.3-5. A) Resistivity of ERI Line C (parallel to natural gradient) showing location of extraction well used to develop permanganate curtain and monitoring wells. B) Resistivity difference after injection.....	71
Figure 4.3-6. A) Resistivity of ERI Line 2 (parallel to injection curtain) showing location of extraction and injection wells used to develop permanganate curtain. Heavy overlay indicates area of greatest resistivity change after injection. B) Resistivity of ERI Line C (perpendicular to injection current) showing location of extraction well used to develop permanganate curtain and monitoring wells. Heavy overlay indicates area of greatest resistivity change after injection.....	72
Figure 4.3-7. ERI differences along ERI lines B, C, and D. Data collected for lines B and D by differencing datasets where stakes were replaced instead of being held constant.....	73
Figure 4.3-8. 3D representation of full 3 meter ERI datasets of BAZE site. Transparent areas are interpreted to correspond to areas of higher hydraulic conductivity and thus preferential pathways for the injection.....	74
Figure 4.3-9. RDX and permanganate breakthrough curves observed in field monitoring wells. Open circle symbols with crosses were used to calculate RDX degradation kinetics (i.e. fitted lines).	77

Figure 4.3-10. Sodium permanganate and Bromide breakthrough curves obtained from MW-12, MW-14, and MW-15.....	78
Figure 4.3-11. Permanganate and RDX groundwater concentrations with depth as obtained through multi-level sampling.	79
Figure 4.3-12. Permanganate profile concentrations in monitoring wells prior to pumping for groundwater sampling.	80
Figure 4.3-13. ERI resistivity versus sodium permanganate concentrations in monitoring wells one month after injection. Best fit line represents slope, intercept and R^2 value for the single time period.....	83
Figure 4.3-14. Slope of best fit line for ERI resistivity versus sodium permanganate concentrations in monitoring wells from the time of injection to 63 days following injection. The average slope value from 14 to 45 days is highlighted with a thick line..	83
Figure 4.3-15. Intercept of best fit line for ERI resistivity versus sodium permanganate concentrations in monitoring wells from the time of injection to 63 days following injection. The average slope value from 14 to 45 days is highlighted with a thick line..	84
Figure 4.3-16. R^2 values for best fit line for ERI resistivity versus sodium permanganate concentrations in monitoring wells from the time of injection to 63 days following injection. The average slope value from 14-45 days is highlighted with a thick line.....	85
Figure E1. Orientation of ERI datasets at BAZE site.....	205
Figure E2. 2D ERI pseudosection of ERI line 1 with location of wells (if present) on the line. The location of crossing lines are indicated with black vertical lines.....	207
Figure E3. 2D ERI pseudosection of ERI line 2 with location of wells (if present) on the line. The location of crossing lines are indicated with black vertical lines.....	208
Figure E4. 2D ERI pseudosection of ERI line 3 with location of wells (if present) on the line. The location of crossing lines are indicated with black vertical lines.....	209
Figure E5. 2D ERI pseudosection of ERI line 4 with location of wells (if present) on the line. The location of crossing lines are indicated with black vertical lines.....	210
Figure E6. 2D ERI pseudosection of ERI line 5 with location of wells (if present) on the line. The location of crossing lines are indicated with black vertical lines.....	211
Figure E7. 2D ERI pseudosection of ERI line 6 with location of wells (if present) on the line. The location of crossing lines are indicated with black vertical lines.....	212
Figure E8. 2D ERI pseudosection of ERI line 7 with location of wells (if present) on the line. The location of crossing lines are indicated with black vertical lines.....	213
Figure E9. 2D ERI pseudosection of ERI line A with location of wells (if present) on the line. The location of crossing lines are indicated with black vertical lines.....	214
Figure E10. 2D ERI pseudosection of ERI line B with location of wells (if present) on the line. The location of crossing lines are indicated with black vertical lines.....	215

<i>Figure E11. 2D ERI pseudosection of ERI line C with location of wells (if present) on the line. The location of crossing lines are indicated with black vertical lines.....</i>	<i>216</i>
<i>Figure E12. 2D ERI pseudosection of ERI line D with location of wells (if present) on the line. The location of crossing lines are indicated with black vertical lines.....</i>	<i>217</i>
<i>Figure E13. 2D ERI pseudosection of ERI line E with location of wells (if present) on the line. The location of crossing lines are indicated with black vertical lines.....</i>	<i>218</i>
<i>Figure E14. 2D ERI pseudosection of ERI line F with location of wells (if present) on the line. The location of crossing lines are indicated with black vertical lines.....</i>	<i>219</i>
<i>Figure E15. 2D ERI pseudosection of ERI line G with location of wells (if present) on the line. The location of crossing lines are indicated with black vertical lines.....</i>	<i>220</i>
<i>Figure E16. Six-meter 2D ERI pseudosection of ERI line 6 with location of wells (if present) on the line. The location of crossing lines are indicated with black vertical lines.....</i>	<i>221</i>
<i>Figure E17. Six-meter 2D ERI pseudosection of ERI line D with location of wells (if present) on the line. The location of crossing lines are indicated with black vertical lines.....</i>	<i>222</i>
<i>Figure E18. Six-meter 2D ERI pseudosection of ERI line E with location of wells (if present) on the line. The location of crossing lines are indicated with black vertical lines.....</i>	<i>223</i>
<i>Figure E19. Six-meter 2D ERI pseudosection of ERI line G with location of wells (if present) on the line. The location of crossing lines are indicated with black vertical lines.....</i>	<i>224</i>
<i>Figure E20. 3D representation of full 3 meter ERI datasets of BAZE site. Transparent areas are interpreted to correspond to areas of higher hydraulic conductivity and thus preferential pathways for the injection.....</i>	<i>225</i>
<i>Figure E22. 3D representation of full 3 meter ERI datasets of BAZE site. View looking from northeast towards southwest.....</i>	<i>227</i>
<i>Figure E23. 3D representation of full 3 meter ERI datasets of BAZE site.....</i>	<i>228</i>
<i>Figure E24. 3D representation of full 3 meter ERI datasets of BAZE site.....</i>	<i>229</i>

List of Tables

<i>Table 3.3-1: Design Performance Objectives</i>	25
<i>Table 3.3-1: Pre- and post-injection hydraulic conductivity</i>	35
<i>Table 3.3-2: Soil Core Grain size Analysis</i>	38
<i>Table 3.5-1: Field Activity Dates and Duration</i>	46
<i>Table 3.5-2: ERI Datasets</i>	51
<i>Table 4.1-1: Process Performance Criteria</i>	58
<i>Table 4.2-1: Project Performance Confirmation Methods</i>	64
<i>Table 5.1-1: Cost Tracking</i>	86
<i>Table 5.1-2 Permanganate and Contractor Costs</i>	89

Acknowledgements

We would like to thank the students and staff from UNL and OSU who contributed to the field work for the project including Jeff Albano, Sathaporn Onanong, Chanat Chokeyaroenrat, Greg Federko, Chris Mace, Robert Meyer, Kathleen Thompson, and Tim Sickbert. Dr. Halihan has an ownership interest in Aestus, LLC, which has licensed the technology reported in this document.

Executive Summary

The former Nebraska Ordnance Plant was a military loading and packing facility that produced bombs, boosters, and shells during World War II and the Korean War. Wastewater discharges to unlined ditches during ordnance production contaminated soil and groundwater. To prevent the contaminated plume from migrating offsite and in the direction of municipal well fields, an elaborate series of extraction wells and piping networks were constructed to hydraulically contain the leading edge of the RDX/TCE plume. This extracted groundwater is currently pumped to a \$33 million dollar treatment facility where approximately 4 million gallons of ground water are filtered through granular activated carbon (GAC) each day. Recent estimate indicate that this pump and treat facility will need to operate in excess of 125 years to manage the RDX/TCE plume.

This ESTCP-funded research was conducted in conjunction with an EPA-funded project. The overall goal was to demonstrate that electrical resistivity imaging (ERI) could be used to monitor and facilitate an in situ chemical oxidation (ISCO) demonstration designed to treat RDX with permanganate at the Nebraska Ordnance Plant. ERI is a geophysical technique that rapidly and economically collects data using an array of electrodes on the surface, and then creates a model and an image of subsurface electrical resistivity. In appropriate environments and with appropriate materials, ERI shows the distribution of materials of interest, either contaminants, amendments, or both. With a good ERI image, investigators can drill for specific, observed, subsurface targets.

The pilot-scale demonstration consisted of a grid of 12 wells, specifically an extraction well (EW-1), two injection wells (IW-1 and IW-2), and nine monitoring wells. To create a permanganate curtain across the injection wells, sodium permanganate (NaMnO_4) was injection into the field via a proportional mixing-injection trailer system. Groundwater was extracted from a center extraction well (EW-1) via a submersible pump at a rate of 151.6 L/min (40 gpm) and delivered to an intake manifold located onboard the trailer system. Approximately 1707.2 L (451 gal) of 40% (w/w) sodium permanganate, spiked with potassium bromide, was pumped at 3.79 L/min (1 gpm) to an intake manifold where extracted groundwater and sodium permanganate were mixed at a ratio of 40:1. The mixed eluent was then gravity fed into each of two neighboring injection wells, IW-1 and IW-2, at approximately 77.7 L/min (20.5 gpm).

The site was monitored with electrical resistivity imaging (ERI) prior to, during, and after the injection. The ERI applied at the site uses arrays of easily-placed, non-invasive surface electrodes to measure apparent subsurface electrical resistivity. This data is then processed and

correlated to subsurface properties that cause changes in the electrical properties of the subsurface such as grain size or formation fluids.

Results showed that permanganate was effective in reducing groundwater RDX concentrations under pilot-scale conditions and that ERI was successful in imaging the initial size and distribution of the injected permanganate plume. ERI also quantitatively mapped the hydraulic conductivity distribution.

RDX concentrations temporally decreased in wells closest to the injection wells (IW-1, IW-2) as the permanganate migrated down gradient. We observed RDX degradation rates of 0.12 1/d and 0.087 1/d in wells immediate downgradient of the injection wells. These rates were lower than what was observed under laboratory batch conditions at 11.5°C (0.20 1/d) and likely a result of a lower initial permanganate concentration (6000 versus 15000 mg/L). RDX concentrations decreased between 70 and 80% in monitoring wells immediately downgradient from the injection wells. Monitoring wells farther downgradient did not show a true breakthrough or significant changes in RDX concentrations.

Results from spatial monitoring of permanganate verified that monitoring wells only captured fingers of permanganate and that the groundwater sampling procedures likely mixed treated with non-treated groundwater during pumping. This mixing of permanganate treated and untreated groundwater would explain why initial permanganate concentrations were less than target values. Moreover, the observed decreases in RDX concentrations during permanganate breakthrough (73-80%) may have been higher if we could have selectively sampled only the permanganate treated groundwater. Despite problems encountered in getting the permanganate uniformly distributed across the injection well and throughout the well screen interval, pilot-scale results provide proof-of-concept that permanganate can degrade RDX *in situ* and support permanganate as a possible remedial treatment for the RDX-contaminated groundwater.

RDX concentrations did not decline below the EPA health advisory for drinking water nor did the permanganate injection influence all the anticipated wells downgradient from the injection zone. The ERI datasets provided an explanation for this failure. When the permanganate was injected, small differences in the ability of the material to conduct water forced the injectate to flow upgradient away from the monitoring wells. Furthermore, the ERI data showed that the permanganate solution descended below the monitoring wells.

The ERI demonstration successfully observed the initial permanganate flow, although with unexpected time and monetary expense. The demonstration did not evolve as planned and anticipated: locating and tracking the permanganate required an additional data collection event, and additional processing. ERI protocols can be altered to more economically and efficiently respond to unanticipated results.

Costs for the ISCO demonstration included sodium permanganate (\$9,950), contracted ISCO injection (\$17,463), analytical costs (\$15,000), sampling equipment (\$5,825) and well construction (\$7,900). The ISCO demonstration was able to reduce its costs by using existing wells (installed by former BAZE project) that would have cost \$8,000 to install. The estimated cost of the ISCO demonstration was \$64,635 (See Draft Cost and Performance Report). RDX concentrations in the test area ranged from $34 \mu\text{g L}^{-1}$ to $63.8 \mu\text{g L}^{-1}$ (average $46.85 \mu\text{g L}^{-1}$). Given that the initial of curtain of permanganate was designed to comprise 60,900 L (16,088 gallons), the mass of RDX within the initial injection zone was 2853 mg of RDX.

The ERI demonstration including collecting background data, concurrent data, and post-injection data. With data processing and visualization, the demonstration cost \$ 51,892 and produced model images of $250,000 \text{ m}^3$ of subsurface material at four different times. Additional data was collected to look deeper into the formation but was not part of the original proposal. Of this core data volume, $125,000 \text{ m}^3$ was crucial to understanding the permanganate's fate. To collect a comparable number and distribution of data would require approximately 204 wells or boreholes spaced every 10 meters in the core data area to a depth of 30 m (98 ft). At a cost of \$3,500 per hole, the well installation would cost \$714,000 before sampling. This would not include the examination for the deeper aquifer portions.

ERI geophysical techniques provide the advantages of economically acquiring large, spatially extensive data sets to track the distribution and flow of injectate. Site assessment following groundwater remediation efforts typically involves discrete point sampling using wells or multilevel piezometers along anticipated flowpaths. Small variations in hydraulic conductivity can divert groundwater flow away from anticipated flowpaths, frustrating efforts to monitor remediation efforts with pre-placed wells. Without a dense network of multilevel piezometers throughout and surrounding the area of interest, point sampling cannot reliably determine the spatial distribution of contaminant nor the flow of injectate.

1. Introduction

1.1 Background

The former Nebraska Ordnance Plant (NOP, Mead, NE) was a military loading, assembling, and packing facility that produced bombs, boosters, and shells during World War II and the Korean War. Ordnance was loaded with TNT, amatol (TNT and NH_4NO_3), tritonal (TNT and Al), and Composition B (~60% RDX and 40% TNT) (Comfort, 2005). During ordnance production, wastewater was routinely discharged into sumps and drainage ditches. These ditches became contaminated with TNT and RDX with concentrations exceeding 5000 mg kg^{-1} (Hundal *et al.*, 1997). Water ponded in the drainage ditches became saturated with explosives before percolating into the soil. This process proceeded unabated for more than 40 years. Extensive use of trichloroethylene (TCE) to degrease and clean pipelines by the U.S. Air Force in the early 1960s added to the groundwater contamination.

Groundwater underneath and downgradient from the site has hexhydro-1,3,5-trinitro-1,3,5-triazine (RDX) concentrations as high as $534 \mu\text{g/l}$ and trichlorethene (TCE) concentrations as high as $4800 \mu\text{g/l}$ (EPA, 1997). An estimated twenty-three billion gallons of water under approximately 6,000 acres have concentrations RDX and/or TCE above the EPA health advisory levels of $2 \mu\text{g/l}$ for RDX and $5 \mu\text{g/l}$ for TCE. The former NOP site Operating Unit 1 (OU 1) was listed on the National Priorities List under the Comprehensive Environmental Response, Compensation, and Liability Act (CERCLA) on August 30, 1990 (Elmore and Graff, 2001); the groundwater contamination was listed on April 7, 1997 (EPA, 1997). The current hydraulic containment system is expensive and provides no short-term solution: the granular activated carbon (GAC) pump-and-treat system is currently operating at a cost of \$800,000 per year and is projected to require more than 125 years to complete the remediation.

The US EPA in 2005 provided a Federal Earmark Grant to S.D. Comfort (*Field-Scale Demonstrations of Innovative Remediation Techniques for Contaminated Soil and Water*) to assess the efficacy of in situ chemical oxidation (ISCO) with permanganate to remediate groundwater contaminated with RDX from the former NOP.

This Department of Defense Environmental Security Technology Certification (ESTCP) project assesses the efficacy of electrical resistivity imaging (ERI) to monitor ISCO permanganate plume development, movement, and changes in concentration.

ISCO is a class of remediation technologies that delivers oxidants on-site and in-place to groundwater or the vadose zone. ERI is a well-established method of measuring and modeling subsurface electrical resistivity. The *imaging*, in this case, is a visual representation of the distribution of resistivity in the subsurface. Geological materials and subsurface fluids have differing electrical resistivities that show up as contrasting regions in model images. Thus, the images are useful for exploring the subsurface for patterns such as depth and thickness of an alluvial deposit, and also for anomalies such as channels, faults, and contaminant plumes. ERI was proposed with the expectation that the injectate's electrical resistivity would be sufficiently different from the ambient groundwater to show up as a transient feature.

Site assessment following groundwater remediation efforts typically involves discrete point sampling. Considerable time, effort, and money can be consumed by initially delineating a contaminated plume or assessing the performance of an ISCO treatment. ERI produces images of injected oxidant showing areas of influence which can then be used to assess efficacy of the treatment and to plan subsequent injections. This in turn minimizes over-application and avoids untreated zones in the contaminated plume.

1.2 Objectives of Demonstration

The objective of this pilot-scale field ESTCP demonstration was to show the utility of ERI to track the flow of permanganate in the subsurface during the demonstrated ISCO project.

The scope of this pilot-scale demonstration included:

- acquiring a baseline ERI dataset prior to ISCO injection
- acquiring multiple ERI datasets during the injection of approximately 451 gallons NaMnO₄ (40%) at a rate of 151.6 L/m (40 gpm) over 413 minutes into approximately 61 m³ of aquifer material during the initial injection/extraction phase
- subsequently acquiring ERI datasets monitoring of approximately 1000 m³ of the aquifer—about 300 m³ of contaminated water containing about 18 g of RDX—over 72 days
- point sampling of groundwater within and immediately surrounding the demonstration volume
- spatially and temporally dense ERI imaging of the aquifer volume anticipated to be affected during the injection, with prior background and subsequent imaging over 72 d.

ERI geophysical techniques provide the advantages of economically acquiring large, spatially extensive data sets to track the distribution and flow of injectate. Site assessment following groundwater remediation efforts typically involves discrete point sampling using wells or multilevel piezometers along anticipated flowpaths. Immeasurably small variations in hydraulic

conductivity can divert groundwater flow away from anticipated flowpaths, frustrating efforts to monitor remediation efforts with pre-placed wells. Without a dense network of multilevel piezometers throughout and surrounding the area of interest, point sampling cannot reliably determine the spatial distribution of contaminant nor the flow of injectate. ERI uses arrays of easily-placed, non-invasive electrodes to measure apparent subsurface electrical resistivity. Remedial concentrations of permanganate in solution can have resistivities one-third of the ambient groundwater value, a difference great enough to be measured by ERI techniques. Once the array of electrodes is in place, ERI data acquisition is rapid relative to the time required to collect groundwater samples. ERI cannot entirely replace subsurface sampling, but it can greatly reduce the number of holes required; provide specific, observation-based targets for new holes; and economically provide observations of the volume surrounding the anticipated domain of the remediation effort.

1.3 Regulatory Drivers

The U.S. Environmental Protection Agency (EPA) determined that actual or threatened releases of contaminants from this site, if not addressed by remedial action, may present a current or potential threat to public health, welfare, or the environment (U.S. EPA, 1997). Further, SARA specifies a preference for the use of permanent solutions and innovative treatment technologies (42USC9660, b). ERI improves the efficiency and effectiveness of ISCO by economically monitoring the changes in subsurface resistivity that result from injections.

1.4 Stakeholder/End-User Issues

This pilot-scale demonstration showed that ERI provides invaluable information about the fate—
influenced areas, migration and evolution—of injectate. In showing that the injectate quickly moved upgradient and then descended into the aquifer below its field of view, ERI data potentially prevented numerous, random, expensive, and necessarily futile attempts to locate the injectate by drilling or direct-push point sampling. ERI, as with any suitable geophysical technique, provides dense and spatially extensive data of subsurface characteristics at a fraction of the cost of point sampling. These achievements address the DoD's need for scientific information regarding the real-world application of alternative technologies as agency personnel evaluate available remediation options.

2. Technology Description

2.1 Electrical Resistivity Development and Application

The electrical resistivity imaging (ERI) technology employed in this project was developed as a response to inadequacies of standard techniques used for characterizing and monitoring environmental sites. Much of this summary was drawn from Halihan et al. (2005a).

2.1.1 Existing techniques

Historical methods of site assessment relied primarily on two detection and monitoring strategies, both of which relied on multiple boreholes. The first strategy involves discrete point sampling of fluids drawn from wells or multilevel piezometers whose data are interpreted by hydrogeologists, civil engineers, and other scientists. The second strategy uses indirect measurements through surface or borehole geophysical techniques.

The difficulties with point sampling are the cost and time of drilling; and sample collection, analysis, and interpretation time. Further, point sampling methods typically provide low data density and thus miss contaminants transported on flow paths or stored in clay lenses not sampled by wells. This is especially problematic if the contaminants are moving non-uniformly, such as density-driven fingering or in isolated flow paths in heterogeneous media. In some settings, the very act of probing and monitoring the aquifer can create additional heterogeneity and new preferential flow paths for solutes. Attempts to improve data quality by increasing data density requires additional boreholes, increasing already high initial costs.

2.1.2 Electrical Resistivity Imaging Theory

Electrical resistivity imaging (ERI) provides more complete and more economical data coverage than borehole-dependent methods. A temporary, surficial ERI system can be used to evaluate a 2-D or 3-D portion of the subsurface; the resulting ERI images can then be used to choose specific targets for traditional investigation methods (Figure 2.1-1). ERI systems can support long-term monitoring with the installation of cables in boreholes or shallow trenches.



Figure 2.1-1. Field setup of ERI equipment. Metal stakes extend approximately 6 inches into the ground and are connected to an acquisition instrument via cables. Photo courtesy of Aestus, LLC.

Electrical resistivity measurements have been used since the 1830s to interpret the geology of the subsurface (Van Nostrand and Cook, 1966). The technique introduces current into the ground and measures the resulting potential field. ERT (Electrical Resistance Tomography) is a method of obtaining resistivity measurements using subsurface electrodes (Daily et al, 2004). In contrast, a multielectrode resistivity array uses electrodes only on the surface. An ERI image is an inverse model of the data: that is, it shows a synthetic distribution of resistivity that predicts values measured in the field. ERI is a generic term for the results from any arrangement of electrodes.

Electrical resistivity imaging begins with data acquisition using a series of electrodes placed either on the surface or in boreholes. Two-dimensional data is collected using a linear array of electrodes; three-dimensional data can be collected using electrodes placed as a two-dimensional array or as a three-dimensional electrode grid. The size and resolution of an image is defined by the distance between electrodes and their location in space. A rough estimate for a two-dimensional image is that the resolution is half of the electrode spacing and the image depth is one fifth of the total surface line length. Three-dimensional data collection is more expensive and difficult as most contaminated sites do not have sufficient open area available; acquisition and processing times are also longer. ERI borehole data is also costly since the majority of boreholes constructed for sampling aquifers are not designed with the electrical properties

necessary to collect robust ERI data. All subsequent discussion here describes two-dimensional ERI imaging.

Acquisition algorithms define the set of measurements collected to create an image. The algorithms are generally defined by the spatial geometry of the two current electrodes relative to the two potential electrodes used to collect a single measurement. For example, a dipole-dipole array uses two adjacent current electrodes and two adjacent potential electrodes (Reynolds, 1997). A Wenner array uses four equally spaced electrodes with the potential pair inside the current pair. Many such algorithms are available to acquire an ERI dataset in one-, two-, or three-dimensions. The raw collected data are referred to as apparent resistivity data.

The image is developed using an inversion algorithm. The inversion algorithm uses the collected apparent resistivity data to create a model space of resistivity values that would replicate the collected data. Like many methods measuring potential fields, these models suffer from problems of nonuniqueness (Reynolds, 1997).

If multiple datasets are collected at different times from the same locations, resistivity differencing can be employed. Resistivity differencing is more sensitive to variations than are standard ERI surveys. Since standard ERI surveys collect data that detects properties of the subsurface sediments and fluids at a time point, differencing can be used to evaluate isolated changes that are independent of sediment properties.

Common geophysical techniques are limited by several factors as outlined by Stollar and Roux (1975). Signal quality and resolution decrease with depth and, for resistivity surveys, the target must significantly contrast with background values. Although resistivity techniques may cost less than point monitoring (i.e., wells) for long-term projects, the results are often difficult to correlate with objectives and still require traditional ground water sampling. A major problem with the application of electrical techniques to contaminant detection is that many contaminants of interest to site managers, such as NAPLs (petroleum products usually), are electrical insulators. ERI works best for identifying conductors, making it difficult to image relatively resistive NAPLs.

2.1.3 Halihan/Fenstemaker ERI Technology

The Halihan/Fenstemaker technology is based on conventional electrical resistivity imaging. The technology was developed examining sites in Oklahoma using a direct push ERT method developed by Dr. Halihan in conjunction with Advanced Geosciences, Inc. (Halihan et al, 2005b). However, OSU's proprietary data collection algorithms and software achieve more comprehensive data collection, higher data quality, and increased image resolution relative to other researchers using similar equipment (Halihan and Fenstemaker, 2004) (Figure 2.1-2). In

most cases, the resolution is increased by approximately one order of magnitude. In addition, the Halihan/Fenstermaker technology is able to image subsurface anomalies at sites where competing technologies (ground penetrating radar, conventional electrical resistivity imaging techniques, and electromagnetic surveys) either fail to perform or do not have sufficient resolution to achieve the project objectives. The Halihan/Fenstermaker technology is capable of semi-quantitative analysis of gasoline in the subsurface (Halihan et al., 2005). Nyquist et al. (1999) provided proof-of-concept for permanganate detection using standard ERI techniques by measuring a twenty-fold increase in electrical conductivity following injection of a 1% potassium permanganate solution.

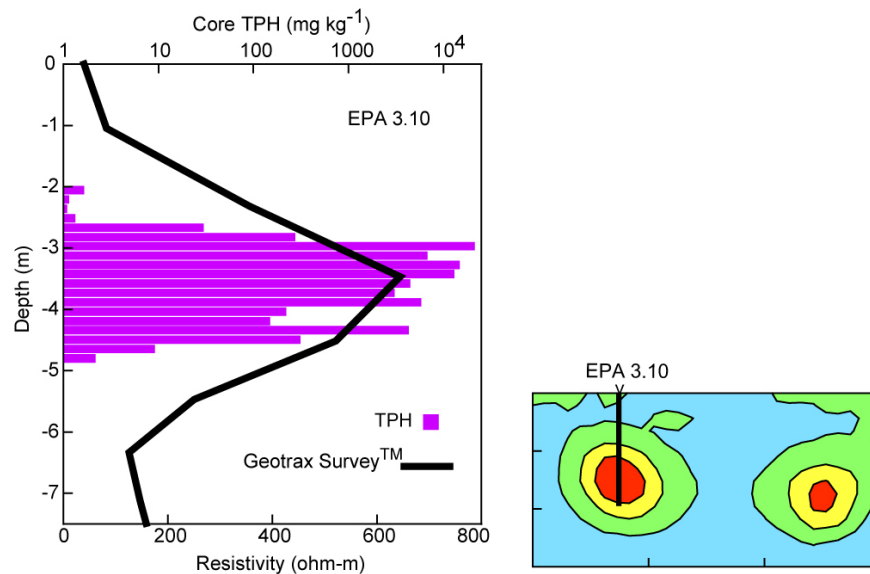


Figure 2.1-2. Evaluation of the performance of the Halihan/Fenstemaker method (commercial available as Geotrax Survey™). This method successfully mapped the horizontal and vertical extent of contamination at the site in a semiquantitative manner (Halihan et al., 2005): Left - comparison to core samples of LNAPL (gasoline) contaminated soil in Golden, OK. Right - ERI image at the location of the boring (warmer colors on the image represent more resistive material).

2.1.4 ERI Data Collection and Processing

Data is collected by placing electrodes in contact with the ground (Figure 2.1-1). A cable is attached to the electrodes and connected to a resistivity instrument that induces the current, measures the potential, and stores the data. The low-energy direct current does not create sparks, damage vegetation, or create a hazard for animals.

Collected data is processed to produce a two-dimensional image of electrical resistivity along a vertical plane. A geophysicist then interprets the image for irregularities in the distribution of electrical resistivity that indicate areas of interest. These anomalies may represent contaminant plumes, but also may represent geological heterogeneities or non-contaminant anthropogenic material. Metal pipelines, in particular, can introduce anomalies sufficiently large to entirely mask other subsurface variations. In common with other geophysical methods, electrical resistivity values are not unique: different materials may have the same resistivity, and a

particular contaminant's resistivity values may span a broad range depending on concentration, co-contaminants, and state of degradation. ERI—and geophysical data in general—requires confirmation by ground-truthing observations. The advantages of ERI remain: more and higher density data providing visual images of the subsurface distribution of a meaningful and significant physical parameter. ERI cannot replace all drilling and point sampling, but it does leverage the cost of drilling by providing drillable images: ERI replaces random drilling.

2.1.5 Potential Applications

ERI technology as described here potentially adds value to any relatively shallow—up to a few hundred meters—subsurface investigation. While theory indicates that ERI is capable of imaging to extreme depths, electrical cable length, manpower, time, and cost constraints make it limited in uses such as deep petroleum exploration, where seismic methods are well-established.

Many features of interest occur within the top few hundred meters of Earth's surface, and ERI techniques may economically provide valuable information on these. Most obvious are the hydrogeological and environmental applications: ERI is particularly well-suited to detecting variations in water saturation, non-aqueous phase liquid (NAPL) saturation, distribution of lithology, and saltwater intrusion. ERI techniques can also potentially provide information for geological engineering, such as the depth and attitude of geological contacts and faults, location of potential sinkholes in karsted carbonates, slip surfaces underlying wasting masses, etc.

2.2 Previous Testing of the Technology (ERI)

The Halihan/Fenstermaker ERI technique has been successfully used for a number of applications including mapping geology, locating zones of increased groundwater flow, and locating subsurface environmental impacts, leaking pipelines, buried tanks and landfill and burial pit boundaries (Figure 2.1-2). OSU has also conducted transient research observing a heap leach pit undergoing wetting over time, and injection of phosphate for groundwater research (Webb, et al., in press; Sima, 2008).

The technique has been used commercially by Aestus, LLC for several years and has been employed in both the U.S. and internationally. Dr. Halihan has a conflict of interest management agreement in force with Oklahoma State University to allow data to move between Aestus, LLC and OSU. Aestus, LLC has a research agreement with OSU to allow for Dr. Halihan's participation. The ERI images produced are confirmed through fluid or soil sampling and have always been confirmed to be a true representation of subsurface conditions. The technique has been applied at approximately 60 sites to date.

The research in recent years has been working to extend the image depth and to model fluid behavior in the subsurface using both single image and transient ERI. This project is an opportunity to evaluate the ability to detect changes in fluid chemistry over time for a reasonable imaging target at an intermediate depth.

2.3 Factors Affecting Cost and Performance of ERI

The cost of ERI depends primarily on the spatial and temporal scope of the investigation. ERI survey costs are specific to each site. Base costs for each survey include:

- research and design of the ERI survey
- personnel travel and equipment transport to the site
- integration, visualization, analysis, and interpretation of datasets.

Incremental costs include:

- daily overhead
- installation and recovery of stakes and cables
- dataset acquisition
- data processing (inverse modeling)

Incremental costs vary depending on the field conditions. For example, in a brownfield stripped of structures, foundations, and concrete pads, with good transportation access, and with no restrictions, no hazardous materials, and no traffic concerns, it might be possible to collect five (5) 275 m lines on a clear summer day. For such a specific site, incremental costs per ERI line would be minimal. In contrast, in a heavily traveled commercial area where a hole must be drilled (and patched) in pavement for each stake, traffic must be diverted and controlled, and weather is inclement, it might be reasonable to collect only two, or even one, 165 m line in a day. In such an environment, the cost for acquiring each ERI line would be considerably higher than the brownfields case.

ERI performance depends most heavily on the electrical resistivity of the geological materials and the substance of interest. Extreme and chaotic heterogeneity in the electrical resistance of the geological materials will confound any effort to use ERI or other electrical-property-based geophysical technique. So long as heterogeneities are generally self-consistent, e.g., horizontal beds, ERI has the potential to distinguish significant anomalies within the electrical resistivity field. Secondly, the material of interest must alter the resistivity field as a function of its concentration, and the concentration must vary along the plane or within the area of the survey.

2.4 Advantages and Limitations of the Technology of ERI

Relative to traditional point-sampling in monitoring wells, ERI provides the advantages of relatively low-cost, high-density two-dimensional, non- or minimally-intrusive surveying. A monitoring well provides point or, with packers, one-dimensional spatial data.

An apparent disadvantage of ERI is, as with all geophysical techniques, that resistivity data is non-unique. That is, an anomaly in the electrical resistivity field may or may not indicate the presence or absence of the material of interest. Geophysical techniques require at least some minimal number of direct physical observations to ground-truth and calibrate the indirect observations. This apparent disadvantage, however, should be compared against the utility of monitoring wells alone. Without guidance from geophysical data such as ERI, monitoring wells are placed essentially at random relative to the distribution of subsurface features. ERI provides specific targets for drilling with a very high correlation between target anomalies and material of interest.

A disadvantage of ERI is that it is not suitable for all project objectives, and that it is not always possible *a priori* to determine its suitability. Extreme and chaotic heterogeneities in the subsurface resistivity field may make it impossible to identify material of interest.

Anthropogenic metal below or at the surface may partially or completely short-circuit the electrical paths and partially or completely mask subsurface features. And although ERI is intrinsically less intrusive than multiple monitoring wells, it may be more disruptive to shut down or install cable ramps on several lanes of a heavily-traveled road for ERI cable and stakes than to divert one lane at a time for a small drilling or direct-push rig.

Ground-penetrating radar (GPR) is another geophysical technique appropriate for contaminant site assessment. GPR offers the advantages of acquiring shallow, high-resolution data faster and with less intrusion than ERI. Disadvantages include less depth penetration, longer processing times involving more individual interpretation, and the greater possibility that high-conductivity features in the shallow subsurface will totally mask deeper features.

3. Demonstration Design

3.1 Performance Objectives

The objective of this demonstration was to show that ERI can identify and track the ISCO permanganate plume. The demonstration was designed to identify and verify the economic,

operational, and performance data that will be used to transfer the technology to potential users. The major factors being evaluated are performance and cost.

Through this technology demonstration, issues such as ease of implementation and cost-effectiveness were studied. Site-specific information about these issues were also identified.

Table 3.3-1: Design Performance Objectives

Type of Performance Objective	Primary Performance Criteria	Expected Performance (Metric)	Actual Performance Objectives Met
Qualitative	1. Identify initial permanganate plume following injection	2-D image corresponds with well data	Yes
	2. Track temporal changes in permanganate plume's size and location	2-D image corresponds with downgradient monitoring well data	Mixed Results
Quantitative	1. RMS of ERI data sets	<20%	Yes

3.2 Selecting Test Site

An ideal test site for demonstrating the ability of ERI to monitor an ISCO treatment would be both electrically and hydrogeologically homogenous. That is, ERI would show a consistent distribution of resistivity in background images acquired before the treatment, and the local hydraulic gradient would uniformly drive groundwater flow. Additionally, a test site should be contaminated either uniformly throughout the domain of the test, or with a clearly identifiable plume. The contaminant, the treatment, or the degradates of either must cause a change in electrical resistivity large enough to be detected by ERI.

It is additionally desirable to test the technology at a site large enough to accommodate a meaningful pilot-scale demonstration with negligible impact on water supply to local users, and minimal additional intrusion to the aquifer or disruption to local activities. Also, existing infrastructure would reduce costs of conducting the demonstration. Finally, collaboration with investigators working on ISCO techniques is essential.

The former NOP appeared to fulfill the criteria listed above. Based on the regional geology (Condra and Reed, 1943; Piskin, 1971), the materials were described as reasonably homogenous and could be expected to hydrogeologically homogenous. The test site is located approximately in the middle of an existing large, contained, and well-characterized contaminant plume with contaminant distribution uniform within an area large enough for the demonstration. Injection, extraction, and monitoring wells had already been constructed for a previous study. Water levels in the existing wells showed the local groundwater gradient to be consistent with the regional

regime. The proposed permanganate ISCO demonstration would inject an amendment that should clearly reduce the electrical resistivity, especially with the addition of bromide as a conservative tracer. The size of the demonstration site is small relative to the area contaminated at the former NOP, and a downgradient containment system was operating, so any potential impact to groundwater users would be negligible.

The site selected is located south of Load Line 2 at N41° 9' 20" by W96° 27' 17". This test site was previously used in an ESTCP-funded research project (the BAZE study, ESTCP#0110) several years ago. The natural hydraulic gradient of the test site has allowed RDX concentrations to rebound and any residual effects of the biodegradation study appear to have been minimized. By conducting the ISCO/ERI demonstration at the same site, a direct comparison of technologies was possible.

The BAZE project constructed a grid of 12 wells: two-four inch injection wells, one-six inch extraction well, and nine-two inch monitoring wells (Figure 3.2-1). The well grid is spaced over a 30 ft x 200 ft rectangle elongated parallel to groundwater flow (V_{GW}). Groundwater velocity determined by previous tracer experiments indicates a groundwater velocity of approximately 1.8 ft/d. Depth to the water at the site averages 50 feet below ground surface with a hydraulic gradient sloping southeast.

Aquifer Solutions Inc. was the private contractor responsible for permanganate injection. Based on discussions with the contractor, additional monitoring wells were installed between the injection wells (IW1, IW2) and the first set of monitoring wells (Fig. 3.2-1). These additional monitoring wells allowed capture of the breakthrough of permanganate as it moved downgradient and allowed us to monitor temporal decreases in RDX concentrations.

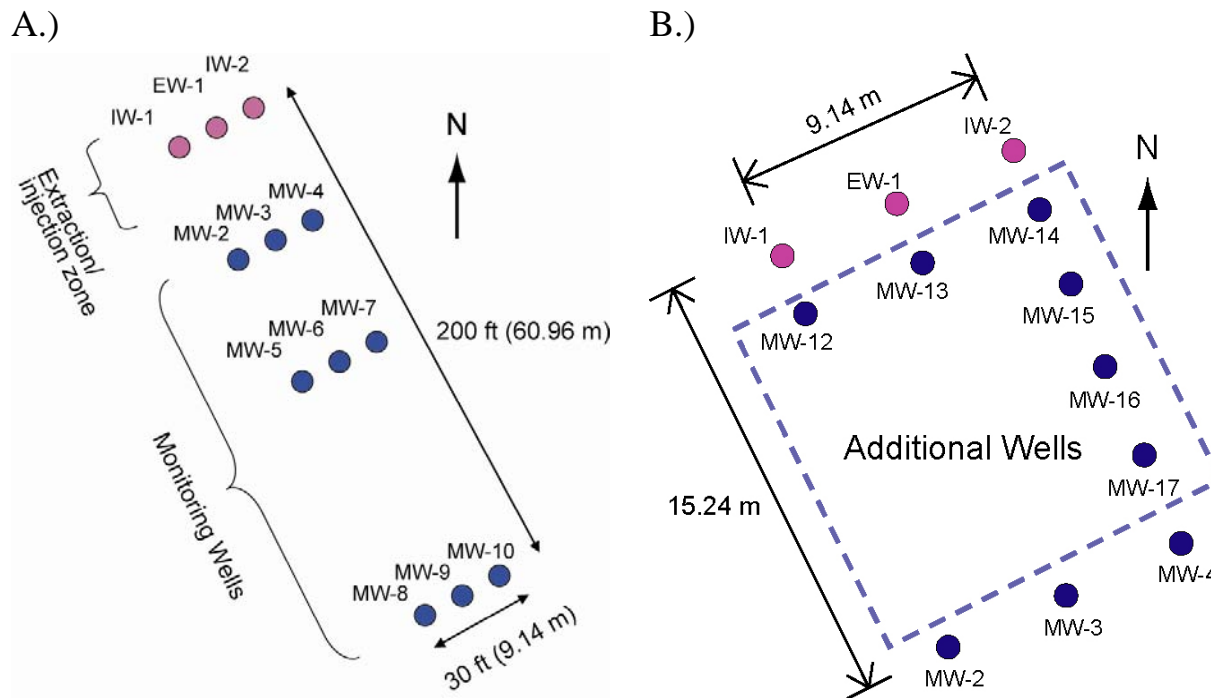


Figure 3.2-1. A) Site well map showing location of wells for original BAZE site. B) Wells added in 2007 for this project.

3.3 Test Site Description

The former Nebraska Ordnance Plant (NOP, Mead, NE) was a military loading, assembling, and packing facility that produced bombs, boosters, and shells during World War II and the Korean War. Ordnance was loaded with TNT, amatol (TNT and NH_4NO_3), tritonal (TNT and Al), and Composition B (~60% RDX and 40% TNT) (Comfort, 2005). During ordnance production, wastewater was routinely discharged into sumps and drainage ditches. These ditches became grossly contaminated with TNT and RDX with concentrations exceeding 5000 mg kg^{-1} (Hundal *et al.*, 1997). Water ponded in the drainage ditches became saturated with explosives before percolating into the soil. This process proceeded unabated for more than 40 years. Extensive use of trichloroethylene (TCE) to degrease and clean pipelines by the U.S. Air Force in the early 1960s added to the groundwater contamination.

Groundwater underneath and downgradient from the site has hexhydro-1,3,5-trinitro-1,3,5-triazine (RDX) concentrations as high as $534 \mu\text{g/l}$ and trichlorethene (TCE) concentrations as high as $4800 \mu\text{g/l}$ (EPA, 1997). An estimated twenty-three billion gallons of water under approximately 6,000 acres have concentrations RDX and/or TCE above the EPA health advisory levels of $2 \mu\text{g/l}$ for RDX and $5 \mu\text{g/l}$ for TCE. The former NOP site Operating Unit 1 (OU 1) was

listed on the National Priorities List under the Comprehensive Environmental Response, Compensation, and Liability Act (CERCLA) on August 30, 1990 (Elmore and Graff, 2001); the groundwater contamination was listed on April 7, 1997 (EPA, 1997). The current hydraulic containment system is expensive and provides no short-term solution: the granular activated carbon (GAC) pump-and-treat system is currently operating at a cost of \$800,000 per year and is projected to require more than 125 years to complete the remediation.

3.3.1 General Hydrogeology

The former NOP is entirely within the Todd Valley, located near the western edge of the Dissected Till Plains section of the Central Lowland physiographic province. The Todd Valley is an ancestral Platte River valley that has been filled with unconsolidated Pleistocene sediment, the Todd Valley Formation. About 3 m to 6 m of late Pleistocene Peoria Loess (medial Wisconsinan) mantles the Todd Valley Formation. The Todd Valley Formation comprises an upper fine sand unit that ranges from about 11 m to about 27 m thick, and a lower sand and gravel unit that ranges from 0 m to about 17 m thick. The Todd Valley Formation unconformably overlies Cretaceous Dakota Group continental shales and sandstones, which ranges from about 12 m to 34 m thick. The thickness of the Todd Valley upper fine sand unit varies with the erosional paleotopography of the lower sand and gravel unit, which likewise preferentially fills in the paleotopographic valleys of the underlying Dakota.

At NOP, the Dakota Group ranges from 12.5 to 33.8 m (41-111 ft) thick. Thickness varies due to post-Cretaceous erosion that formed a southeasterly sloping paleotopographic surface (Piskin, 1971). In Nebraska, the Dakota Group is subdivided into three formations, Dakota Sandstone, Fuson Shale, and Lakota Sandstone. For simplicity the term Omadi was assigned to the Dakota Formation by Condra and Reed (1943) to define the strata between the basal formation of the Colorado Group, the Graneros Shale, and the underlying Fuson Shale of the Dakota Group.

The Pleistocene deposits near Mead, NE consist of sands and gravels of the Todd Valley Formation that range in thickness from 20.1 to 45.1 m (66 to 148 ft) (Piskin, 1971). The unconsolidated sands and gravels are valley fill sediments that were deposited in multiple stages during the Pleistocene epoch. The sands and gravels consist of 95 percent quartz and feldspars and the remaining 5 percent consists of heavy mineral including zircon, magnetite, illmenite, hornblende, tourmaline, and hematite (Schuett, 1964). Possible sources for the Pleistocene sands and gravels include Cretaceous sediments within the area, local Pleistocene tills and associated outwash materials, and alluvial sediments of western origin (Stanley, 1971).

The Pleistocene sands and gravels are divided into two units, from bottom to top these are the sand and gravel unit, and the fine sand unit. The sand and gravel unit consists of poorly to

moderately sorted, subrounded to rounded clasts (Piskin, 1971). Clasts are composed of mostly fine and medium to coarse gravel with fine to very coarse sand (Piskin, 1971). The sand and gravel unit ranges in thickness from 0 to 16.8 m (0 to 55 ft) with maximum thicknesses located within the Cretaceous bedrock channels. The paleotopography of the sand and gravel unit indicates post-depositional erosion. The fine sand unit ranges in thickness from 10.7 to 27.4 m (35 to 90 ft) with thicknesses determined by the underlying sand and gravel unit's paleotopography and post-depositional erosion. Clasts in the fine sand unit coarsen downward and range from very fine to coarse sand but predominantly consist of fine to medium sand.

Overlying the fine sand unit and present at the surface at the NOP is the eolian Peoria Loess. The Peoria Loess consists of brownish-yellow clayey silt to silty clay that ranges from 6.1 to 12.2 m (20 to 40 ft) thick at the northwest end of Todd Valley, which become thinner to the southeast. The Peoria Loess is medial Wisconsinan in age and is characterized by vertical fractures and root holes (Piskin, 1971).

Data for the permanganate injection site (N 41° 9' 24", W 96° 27' 117") were obtained from borehole logs (wells MW-31, MW-28, T63-1). Results from these investigations (Woodward-Clyde, 1995) indicated that approximately 6.1 m (20 ft) of Peoria Loess is mantled over the Todd Valley Formation, which is comprised of approximately 15.2 m (50 ft) of fine sand and approximately 13.7 m (45 ft) of coarse sand.

The two streams present at the NOP, Johnson Creek and Silver Creek, provide drainage to Salt Creek, a tributary to the Platte River. Salt Creek discharges into the Platte River east of Ashland near the southeastern corner of Saunders County. Drainage for Todd Valley is mainly southeast through Wahoo Creek located southwest of the NOP. The flat topography of Todd Valley supports a poorly defined drainage pattern (Woodward-Clyde, 1995). Supplemental man-made ditches were added to enhance natural surface drainage. A man-made ditch created at Load Line 1 discharges into Silver Creek. Load lines 2 and 3 also had man-made ditches built that flowed through former high explosive storage areas. Man-made ditches built to drain Load Line 4 discharge into Johnson Creek. Drainage from the Burning Grounds discharges directly into Johnson Creek. In 1975, the Natural Resource District (NRD) dam was built on Johnson Creek creating the NRD reservoir. The reservoir was built for flood control and covers approximately 78 acres.

The Omadi Sandstone aquifer, Todd Valley aquifer, and the Platte River alluvial aquifer, Pennsylvanian shales, and the Omadi shale make up the aquifer system at the former NOP site. The Todd Valley aquifer is hydraulically connected to the Platte River alluvial aquifer. The Platte River aquitard is the upper semi-confining layer that impedes flow beneath the ground surface and the aquifer. The Platte River aquitard consists of silts and clays. The Omadi

Sandstone is hydraulically connected to the Todd Valley and Platte River alluvial aquifers where the Omadi shale is not present. The Todd Valley aquifer and the Platte River aquifer behave as a single aquifer system without hydraulic barriers.

The Omadi Sandstone Aquifer is composed of fine- to medium-grained sandstone. Mineralogy of the Omadi Sandstone Aquifer is dominantly quartz with ferrugeneous cement found locally (Piskin, 1971). Transmissivities of the Omadi Sandstone Aquifer calculated by grain size range from $49.6 \text{ m}^2/\text{d}$ ($4 \times 10^3 \text{ gpd/ft}$) to $429 \text{ m}^2/\text{d}$ ($3.46 \times 10^4 \text{ gpd/ft}$) with a mean of $272.8 \text{ m}^2/\text{d}$ ($2.20 \times 10^4 \text{ gpd/ft}$) (Piskin, 1971).

The regional water table associated with the NOP slopes southeast with an average gradient of 2.27 m/km (0.00227 , or 12 ft/mile) (Woodward-Clyde, 1995). Depth to groundwater ranges from 11.6 m (38 ft) to 15.24 m (50 ft) (Woodward-Clyde, 1995). Historical data in relatively undisturbed conditions indicates water table elevations ranging from 384 m (1260 ft) to 323.1 m (1060 ft) (Figure 3.3-1). Note that the permanganate injection site used in this research is located between water table elevations 335.3 m (1100 ft) and 341.4 m (1120 ft).

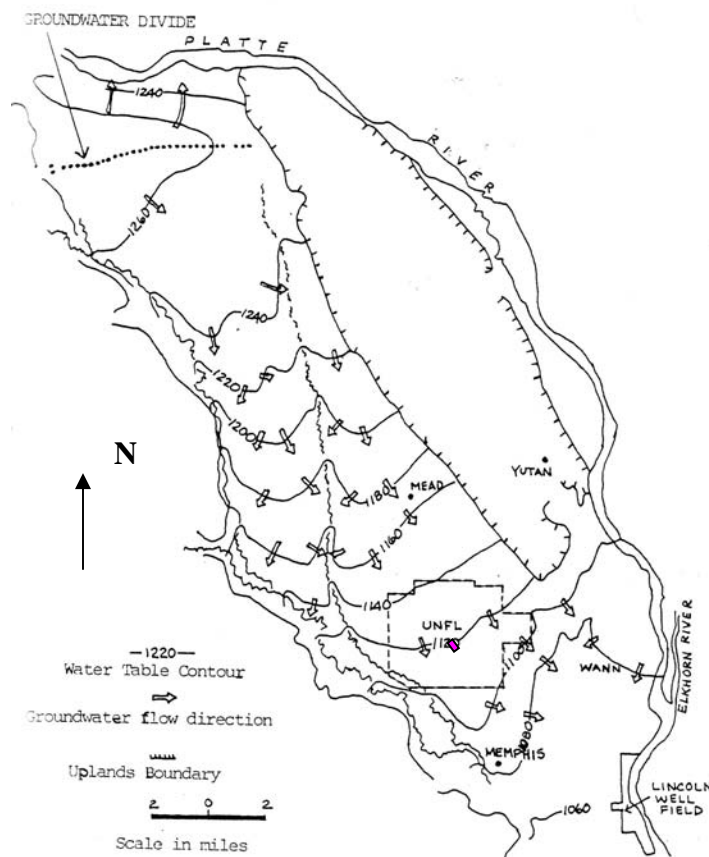


Fig 3.3-1. Regional water table elevations of the Todd Valley Aquifer (modified from US Corps of Engineers, 1989 modified from Souders, 1967). Purple rectangle indicates location of pilot-scale permanganate injection site.

3.3.2 Former NOP Site Hydrogeology

Water table elevations were surveyed in October 2006 on wells installed by previous research at the site (the BAZE project, Wani et al., 2007). A total of 11 long-screen monitoring wells (MW-1 to MW-11), injection wells IW-1 and IW-2, and extraction EW-1 well were used for water table mapping. All wells had continuous screens over the same depth range preventing measurement of vertical head gradients. However, flat topography of the site suggests low vertical gradients, and piezometric data from monitoring wells were taken as proxies for water table elevations. Water levels ranged from 339.558 m (1113.75 ft) to 339.405 m (1113.25 ft) with an overall southeasterly hydraulic gradient of 0.0025 (Figure 3.3-2).

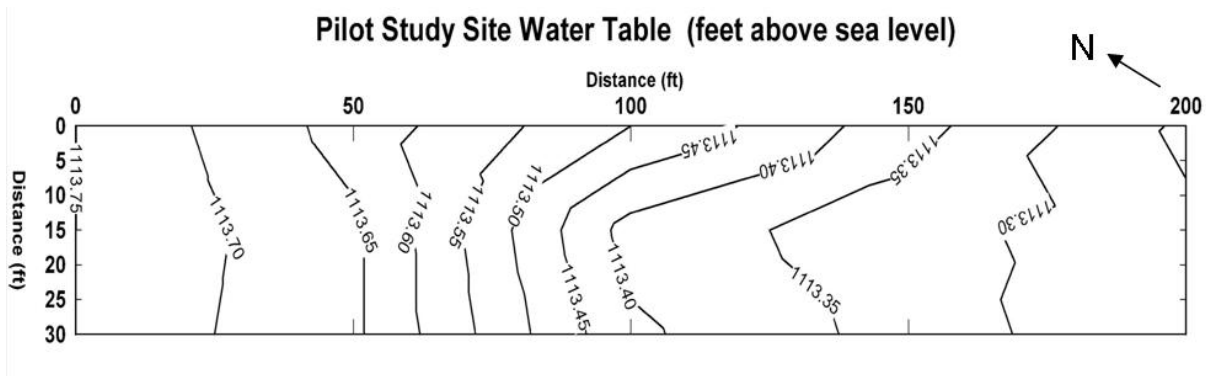


Figure 3.3-2. Water table elevations within the BAZE Study Site (October 2006).

Aquifer characterization relied on slug tests without packers, with double-packers, and single packer. In addition, pre- and post-ISCO comparisons were been performed on monitoring wells. To characterize the site more effectively and to monitor RDX degradation more adequately, six additional monitoring wells (MW-12 to MW-17) were installed at the site. Except for the 10 cm (4 in)-diameter MW-15 well, the wells had a 5 cm (2 in) diameter. All wells were installed using a hollow stem auger to a depth of 22.86 m (75 ft) and screens were deployed from 16.76 m to 22.86 m (55 to 75 ft). All had 6-m long screens located in the upper fine sand layer of the Todd Valley aquifer. The wells were constructed with gravel packs.

This well array was used for characterizing areal and vertical distribution of hydraulic conductivity at the site. Slug tests (Zurbuchen et al., 2002) for obtaining horizontal hydraulic conductivity (specifically, horizontal hydraulic conductivity K_h) were conducted on thirteen existing BAZE (Wani et al. 2007) wells and the additional monitoring wells. Water level

displacements were initiated using pneumatic level depressor (Zlotnik and McGuire, 1998). All responses were monotonic, and drawdown curves were interpreted using Bouwer-Rice (1976) method implemented in software package Aqtesolv[®]. The slug tests showed the average well horizontal hydraulic conductivity values (K_h) ranged from 4 m/day to 20 m/day (Figure 3.3-3). These values are in agreement with average hydraulic conductivity of the upper fine sand layer previously reported at 15 m/day by the Army Corp of Engineers (Woodward-Clyde, 1995). Considering the presence of the gravel pack, hydraulic conductivity data obtained from all wells represent large volume-averaged characteristics. The actual range of hydraulic conductivity values could be wider than found from slug tests in these long-screen wells.

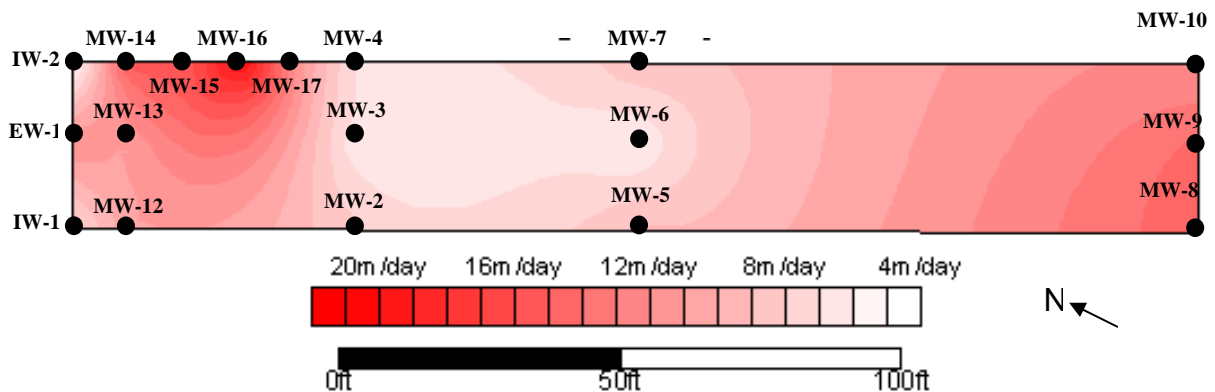


Figure 3.3-3. Hydraulic conductivities within the study area.

To delineate vertical variations in hydraulic conductivity, multi-level slug tests (MLST) were performed on the 10-cm well MW-15 following the procedures of Zlotnik and McGuire (1998), and Zlotnik and Zurbachen (2003). Using an air-inflatable double-packer system with extendable riser pipe (Figure 3.3-4), each 60-cm (2-ft) interval of the 6-m (20-ft) screen interval was isolated and tested.

Vertical variations of horizontal hydraulic conductivity for MW-15 ranged from 3 m/day to 27 m/day with highest conductive intervals between 18.9 m (62 ft) and 19.8 m (65 ft) bgs (Figure 3.3-5). These data show that the range of K_h values in vertically distributed points is slightly wider than obtained from 6-m long screens. Further delineation of vertical hydraulic conductivity was limited due to the lack of additional 10-cm wells.

To assess scale effects due to differences in tested screen interval length, a set of single-packer tests was performed. Using one packer, the lower part of the aquifer was isolated and tested. For each packer elevation, transmissivity of the isolated part was estimated using Bouwer-Rice

(1976) method and Aqtesolv© software. Hydraulic conductivity of each interval Δz was assessed using formula

$$K_{h,i} = (T_{i+1} - T_i) / \Delta z \quad (\text{Eq 3.3-1})$$

where T_{i+1} and T_i are transmissivity values of intervals, isolated in two consecutive packer positions, where $i+1$ -th is a deeper one, and i -th is a more shallow (see Halihan and Zlotnik, 2002).

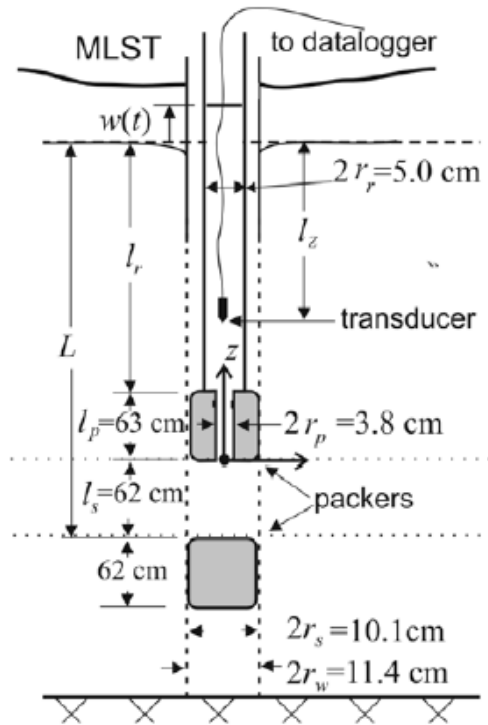


Figure 3.3-4. Configuration of multi-level slug test system including packers and pressure transducer in riser pipe, connected to datalogger (from Zlotnik and Zurbuchen, 2003). Note 62 cm (2-ft) tested interval.

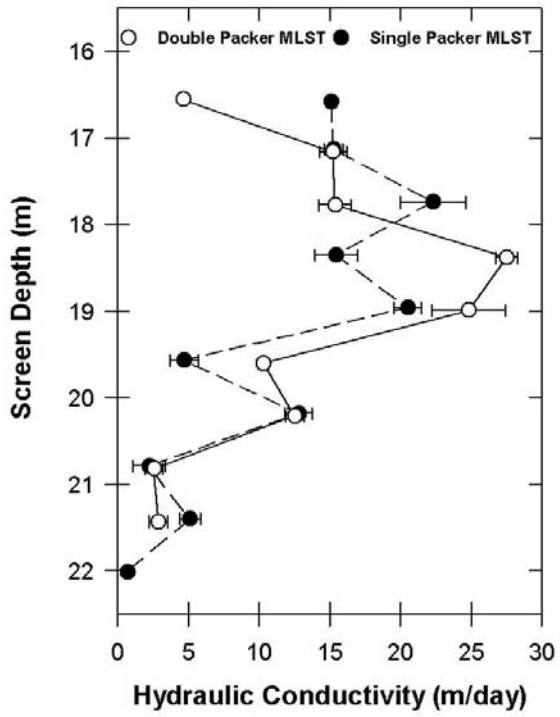


Figure 3.3-5. Hydraulic conductivity K_h observed in MW-15 using single- and double-packer multi-level slug test configurations.

Data in Figure 3.3-5 indicate slightly lower values of K_h from single-packer tests than from double-packer tests, although the presence of preferential flow zone at depth 58-63 ft (17.5-19 m) is clearly shown by both tests. Preferential flow pathways are likely ubiquitous in this paleoalluvial environment, contrary to the expectation and assumption of hydrogeological homogeneity.

This hydraulic characterization study was repeated after completion of the injection test in the injection, extraction, and monitoring wells, including results from a 10 cm (4") well that are presented separately (Fig 3.3-6). Post-injection K_h values exhibited slight changes in most wells with post-injection to pre-injection K_h ratios ranging from 0.9 to 1.3 (Table 3.3-1.)

Table 3.3-1: Pre- and post-injection hydraulic conductivity

Well ID	Pre-injection K_h (m/day)	Post-Injection K_h (m/day)	Post-injection / Pre-injection
IW-1	4.4	5.5	1.2
IW-2	12.0	4.7	0.4
EW-1	7.1	1.8	0.2
MW-12	10.8	10.9	1.0
MW-13	10.9	11.5	1.1
MW-14	15.6	16.9	1.1
MW-15	15.1	13.9	0.9
MW-16	20.7	18.4	0.9
MW-17	11.5	15.6	1.4
MW-2	8.2	7.6	0.9
MW-3	6.4	8.2	1.3
MW-4	7.0	14.0	2.0

Wells IW-2, EW-1 and MW-4 exhibited post- injection to pre-injection K_h ratios of 0.4, 0.2, and 2.0 respectively. Reduced hydraulic conductivity in EW-1 may be attributed to the fact that upon the completion of permanganate injection and sampling, we re-injected the accumulated purged groundwater containing permanganate. The re-injected groundwater may have had suspended fine grain sediments and possible MnO_2 colloids, which could have accumulated at the bottom of the well and sealed of portions of the well screen.

The K_h reduction in IW-2 could be attributed to MnO_2 colloid production during permanganate reactions, although this was not observed in IW-1 and it is unlikely that permanganate reactions with soil and RDX would be much different in both IW-1 and IW-2. Nevertheless, water level observations in the well IW-2 indicate that flow became significantly impaired during injection (see well water level observations during pre-injection tests and injection). Another possibility

for the reduced hydraulic conductivity values could be undetected problems of design, construction, and conservation of wells in BAZE project. For example, lack of integrity of the bentonite seal was found in spring, 2007, that had to be fixed later. The increase in hydraulic conductivity observed in MW-4 is most likely due to the intense sampling regime (Wani et al., 2007).

Data obtained from post-injection MLSTs in MW-15 indicates an increase of K_h at all elevations (Figure 3.3-6) and no reduced hydraulic conductivities due to MnO_2 colloids. However, significant changes are present only in the preferential flow elevations. We believe that intense bi-weekly sampling regime (purging 3 to 4 well volumes twice a week) resulted in further well development, removal of fine grains, and therefore, increase of K_h . However, after uniform weighting of all changes, the overall average K_h has not change dramatically. Slug tests conducted over the entire screen length indicates a small decrease of post-injection K_h , but overall changes in monitoring wells seem insignificant (Table 3.3-1).

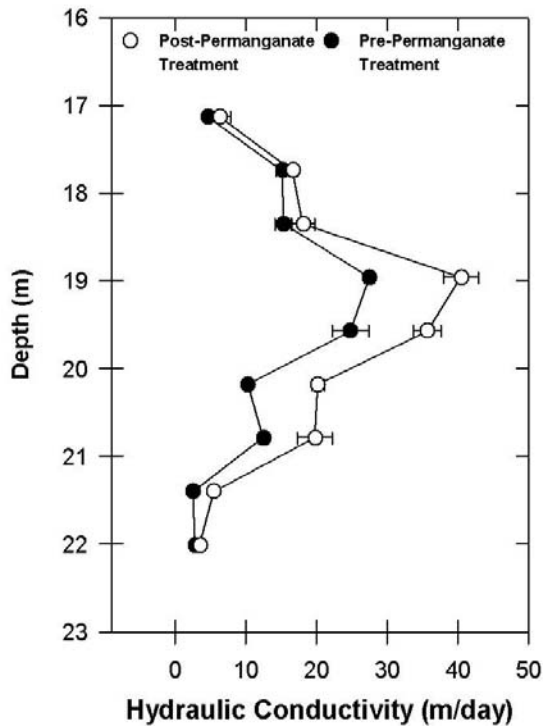


Figure 3.3-6. Hydraulic conductivity, K_h , obtained from pre and post-injection multi-level slug tests on MW-15.

3.3.3 Soil Electrical Conductivity (SEC) Logging and Correlation with Grain Size Analyses

Data on stratigraphy were collected using soil core and soil electrical conductivity data analyses. Results indicate roughly 5.5 m (18 ft) of Peoria Loess above at least 16.2 m (53 ft) of medium to fine sand (maximum soil core depth was 22.3 m (75 ft) below ground surface). Soil cores taken from the Todd Valley Formation were analyzed for grain-size (Table 3.3-2). Soil electrical conductivity sampling (SEC) was performed at the site via direct push technology (Geoprobe® Model 6610DT) and SC400® soil conductivity probe consisting of a four-electrode Wenner array with an inner-electrode spacing of about 2.5 cm (1 in). SEC was logged every 1.5 cm (0.6 in) as the probe was pushed through the soil. SEC analysis showed changes in conductivity at approximately 5.5 m (18 ft), 10.1 m (33 ft), and 18.3 m (60 ft). The SEC data is in agreement with the grain-size analyses and indicates roughly 5.5 m (18 ft) of Peoria Loess is located above a coarsening downward sand sequence (Fig. 3.3-7; Table 3.3-2)

Table 3.3-2: Soil Core Grain size Analysis

Sample Depth (m)	Size Class	Sorting
6.7-7.6	Fine Sand	moderately sorted
9.1-10.7	Medium-Fine Sand	moderately well sorted
11.0-12.2	Fine Sand	moderately well sorted
13.7-15.2	Fine Sand	moderately sorted
15.2-16.2	Medium-Fine Sand	moderately well sorted
18.3-19.2	Medium-Fine Sand	moderately sorted
21.3-22.9	Medium-Fine Sand	moderately sorted

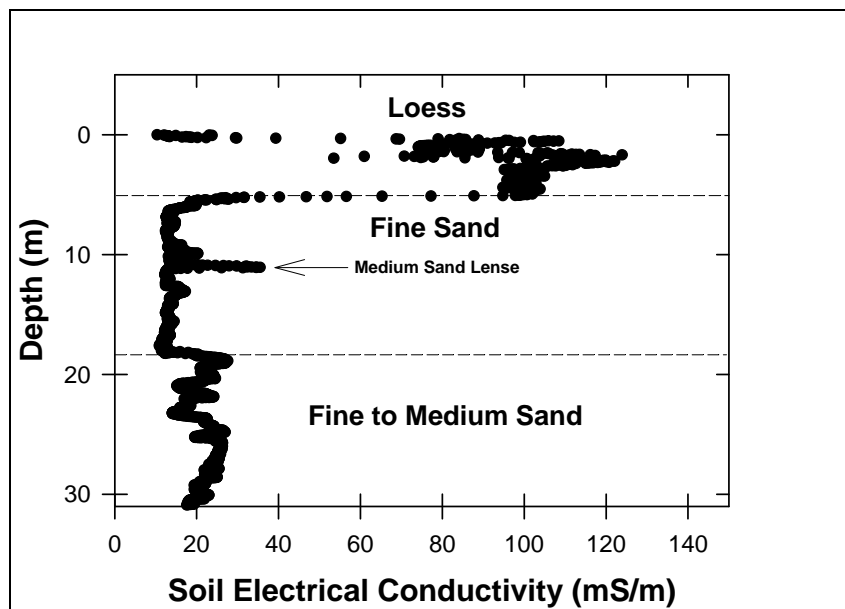


Figure 3.3-7. Soil electrical conductivity (SEC) measurements with depth at the permanganate injection site.

3.4 Pre-Demonstration Testing and Analysis

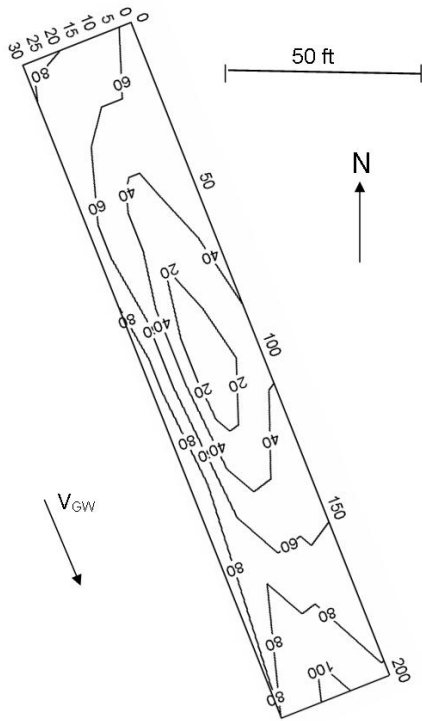


Figure 3.4.-1. Scaled contour plot of RDX concentrations ($\mu\text{g/L}$) within the injection site. Sampling occurred on 12/6/06.

To maximize area of contact between permanganate solution and background groundwater, the vertical curtain between two injection wells was designed. To simplify design calculations, the following assumptions were made:

- The aquifer is homogenous and isotropic
- Permanganate velocity is horizontal
- Velocity near screen is uniform
- Convection does not play role in groundwater flow
- Plume drift due to natural groundwater flow during the short injection time is negligible
- Water extracted from well EW is equally split over injection wells IW-1 and IW-2 after dilution of permanganate
- Curtain is complete when breakthrough of permanganate is observed in an extraction well (EW-1)
- Groundwater recirculation rapidly reaches steady state (Zlotnik and Ledder, 1994).

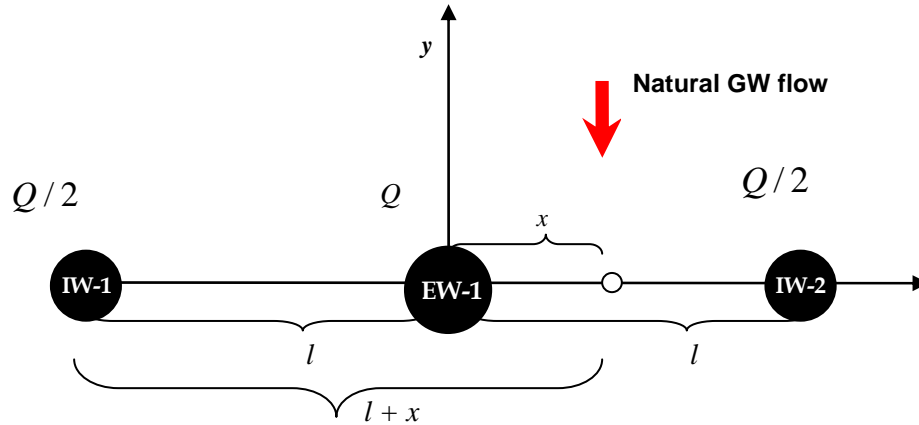


Figure 3.4-2. Geometry of the injection analysis

In the schematic diagram (Figure 3.4-6), the center circle represents the extraction well (EW-1) at coordinate $x=0, y=0$, and is flanked by injection wells IW-1 and IW-2 with coordinates $x=-l, y=0$ and $x=+l, y=0$, respectively. To calculate the volume of water impacted by this delivery technique, we evaluated Darcian and linear velocity (Q and v) along the x -axis using superposition of effects from all three wells with appropriate signs:

$$q(x) = - \left[\frac{Q}{2\pi b x} + \frac{Q/2}{2\pi(l-x)b} - \frac{Q/2}{2\pi(l+x)b} \right] \quad (\text{Eq 3.4-1})$$

$$v(x) = \frac{q(x)}{n} = \frac{-Q}{2\pi b n} \cdot \frac{l^2}{x(l^2 - x^2)} \quad (\text{Eq 3.4-2})$$

Here, we assumed that steady-state velocity is uniform over the screen length b . The time T required for curtain completion can be evaluated as a time required for a particle to arrive from location of IW-1 (or IW-2) to EW-1, was obtained as follows:

$$T = \int_l^0 \frac{dx}{v(x)} = - \int_l^0 \frac{dx}{Q/2\pi b n} \cdot \frac{x(l^2 - x^2)}{l^2} = \frac{2\pi b n l}{Q l^2} \int_0^l x(l^2 - x^2) dx = \frac{\pi b n l^2}{2Q} \quad (\text{Eq 3.4-3})$$

Pumping with discharge Q for this time produces the volume of groundwater V that is impacted with permanganate.

$$V = Q \cdot T = \frac{\pi b n l^2}{2} \quad (\text{Eq 3.4-4})$$

Note that these estimates strongly depend on the unknown parameter of effective porosity. Note that travel time, T , is pumping-rate dependent, while total volume of injectate is independent of Q . Therefore, pumping rate selection is independent of the pump capacity.

The approximated time T and volume V required for creating a continuous curtain of permanganate were estimated using the following parameter estimates. Considering b equal to well screen length (20 ft. or 6.096 m), porosity n approximately 0.3 for sand, and l is the distance between the extraction well and the injection well (15 ft. or 4.6 m), one obtains.

$$T = \frac{\pi b n l^2}{2Q} = \frac{\pi \cdot 6.096m \cdot 0.3 \cdot 4.6^2 m^2}{2 \cdot 216 m^3 / day} = 0.28 \text{ day} = 6.8 \text{ hours} \quad (\text{Eq 3.4-5})$$

$$V = \frac{\pi b n l^2}{2} = \frac{\pi \cdot 6.096m \cdot 0.3 \cdot 4.6^2 m^2}{2} = 60.9 m^3 = 60,900 L \quad (\text{Eq 3.4-6})$$

These estimates may be on the high end considering that effective porosity is commonly less than full porosity by a factor of approximately 2. In addition, travel time may be further reduced by the presence of preferential pathways of the injectate. This means that the likely breakthrough time might be on the order of 2-3 hours. After the breakthrough, the injectate recirculation between wells will provide a broader aquifer coverage.

A pre-permanganate injection test was performed to explore the injection wells' (IW-1 and IW-2) ability to accept injected groundwater, and to monitor drawdown within the extraction well (EW-1) (Figure 3.2-1). Injection wells were tested one at a time. Prior to pumping, 3.81 cm (1.5 inch) PVC piping was lowered approximately 3.05 m (10 ft) below the static water level in wells IW-1, IW-2, and EW-1 to shield pressure transducers and dampen water level noise caused by cascading water. One PTX-161 pressure transducer (In-Situ Inc.) was lowered down the PVC pipe in each well and connected to a Hermit 2000 datalogger (In-Situ Inc.). Prior to pumping/injection, all three transducers were zeroed and the datalogger was initiated. Groundwater was pumped via a submersible pump (Aermotor A+ 75-500, Delavan, WI) a rate of 151.6 L/min (40 gpm) from EW-1 through a flow meter and PVC pipe into one injection well. Drawdown was recorded in EW-1 and in the injection well which was not being tested. Head build up was recorded in the injection well being tested. The injection test was conducted until the head build up stabilized, which occurred in a very short time (Figure 3.4-7).

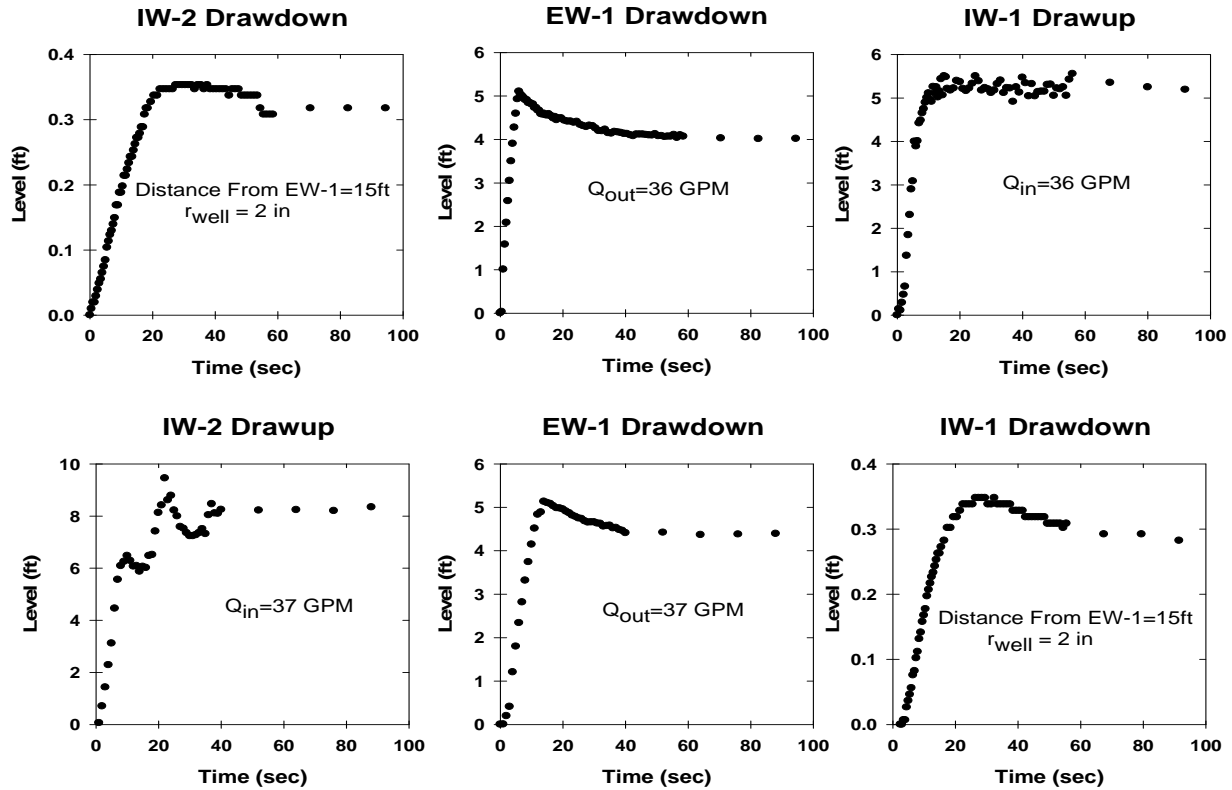


Figure 3.4-3. Testing well capacity: Upper row: head changes for re-injection to well IW-1; lower row: head changes for re-injection to well IW-2.

3.5 Testing and Evaluation Plan

3.5.1 Demonstration Installation and Start-Up

Extraction, injection, and eleven monitoring wells were in place from the previous BAZE experiment. The additional monitoring wells illustrated in Fig 3.2-1B were installed in April, 2007. ERI measurements were collected during May 21-23, 2007 (Figure 3.5-1) along ten lines to obtain background imaging of the site prior to permanganate injection. ERI electrode installation consisted of installing metal stakes approximately 15 cm (6 in) into the ground. The site preparation consisted of determining ERI line locations. Power was supplied by a deep-cycle 12 volt battery. Traffic was controlled on the unpaved site road during this time with traffic cones. The site for the monitoring wells was mowed in limited areas to improve site access. ERI lines needed to cross an unpaved road west of the injection site and into a soybean field.

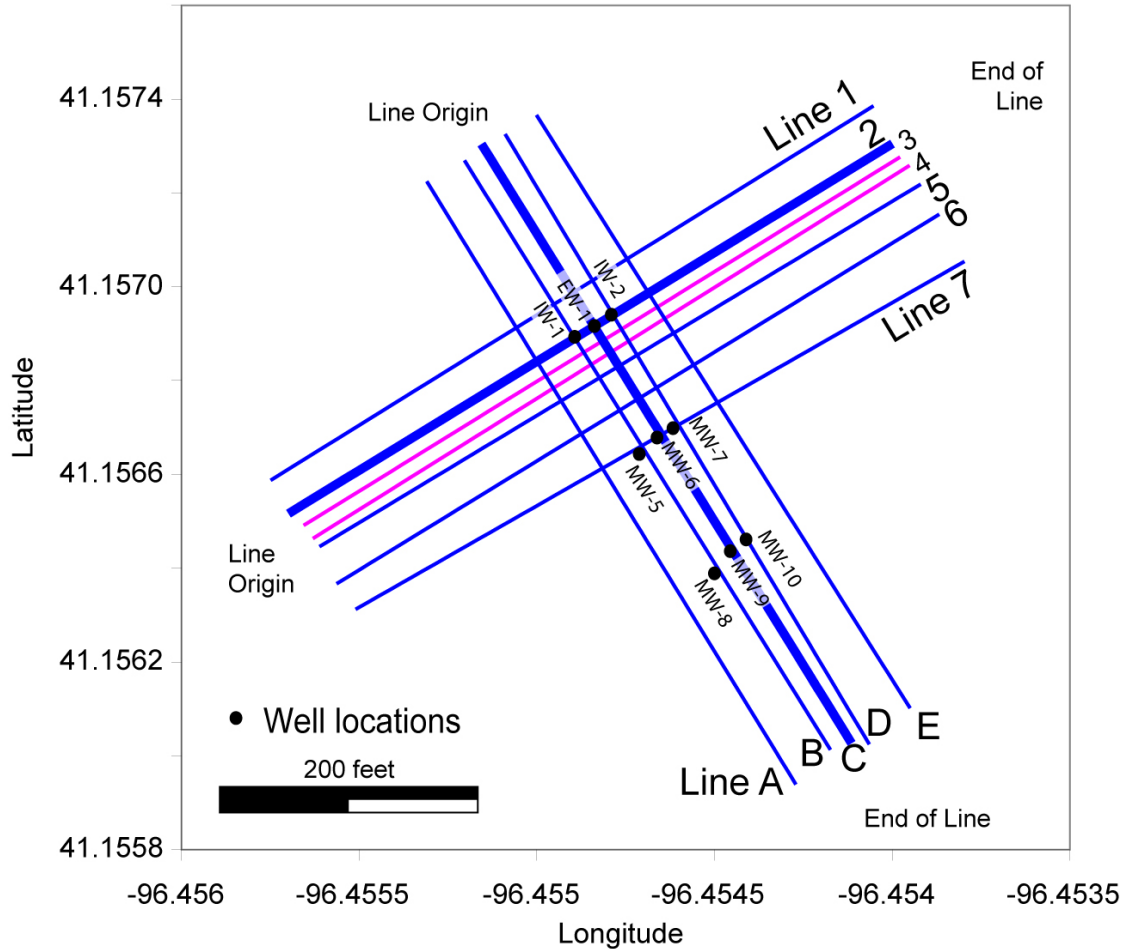


Figure 3.5-1. Map of 12 primary ERI line locations and monitoring wells for the site. Heavy blue ERI lines C and 2 were used as monitoring ERI lines during injection. Purple ERI lines 3 and 4 were not collected during the background period.

The ISCO injection experiment was performed on June 19th, 2007. The previous day, Aquifer Solutions, Inc. connected their injection trailer to the pumping and injection wells (Figure 3.5-2). A safety fence was established around the area where concentrated permanganate was accessible. A field safety (decontamination) shower was installed on site. Two ERI lines were established: Line 2 over the well curtain area and Line C perpendicular to the curtain over the extraction well (Figure 3.5-3). The injection occurred for approximately 8 hours. ERI data was collected continuously and repeatedly during, and immediately following the injection until 25 hours after the injection began. After this initial monitoring period, the two original ERI lines were moved to collect data along the remaining 8 lines. Based on observations at the monitoring wells, data

was also collected along two additional lines (ERI lines 3 and 4). While the larger set of ERI data was being collected, the permanganate injection system was removed from the site.

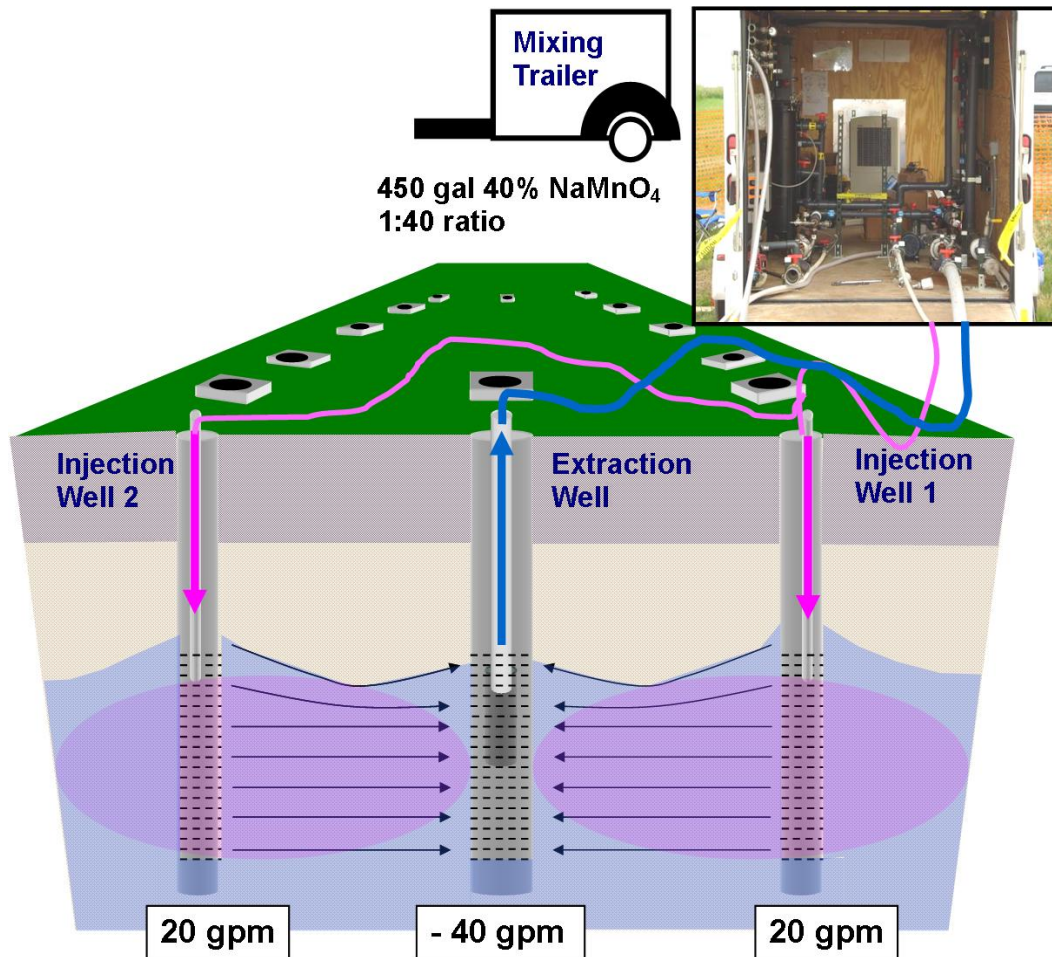


Figure 3.5-2. Schematic of injection setup showing photo of Aquifer Solutions, Inc. trailer.

On July 20 through the 22, 2007, a 12-line ERI dataset was collected from the site. Mobilization and demobilization was performed the same as the original background dataset. At this time, grassy areas that had been mowed had not grown significantly, but the soybean field was established.

Geoprobe fluid samples were collected 24, 56, and 72 d after injection. Discrete groundwater samples were taken at 122 cm intervals (4 ft) in one borehole on July 17th, 2007, two boreholes on August 14th, 2007 and three boreholes on August 30th, 2007.

The final ERI sampling period occurred between August 29th through the 31st, 2007. The sampling evaluated 10 specific ERI lines. Selected lines were imaged twice as deep to determine

if injectate had moved vertically below the previous datasets, and to confirm whether the ERI technique could distinguish the injectate from the geological materials.

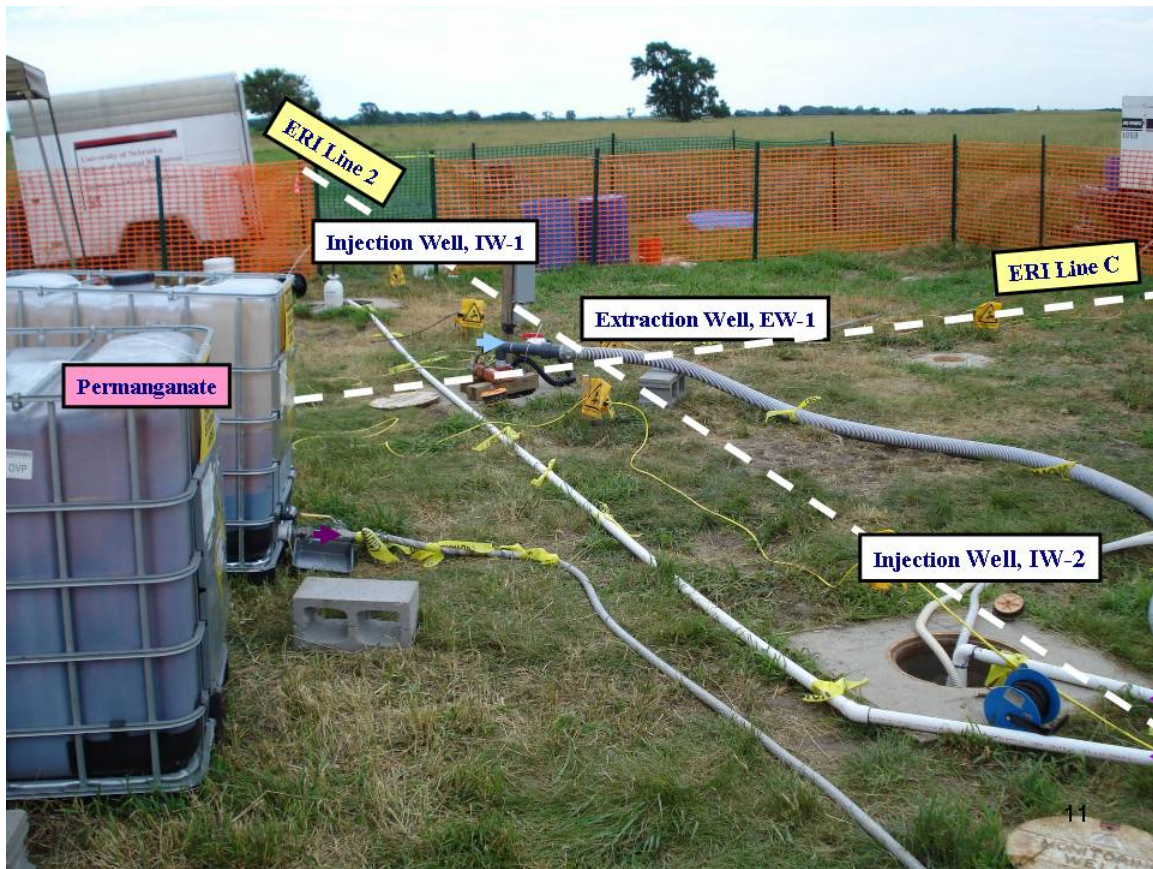


Figure 3.5-3. Photo of injection and extraction wells and safety fence setup. Location of ERI lines 2 and C are indicated with white dashed lines.

3.5.2 Period of Operation

The ERI project field work and confirmation borings were completed between May 21, 2007 and August 31, 2007 (Table 3.5-1).

Table 3.5-1: Field Activity Dates and Duration

Activity	Start Date	End Date	Number of ERI datasets	Number of Borings
Background Data	21/05/2007	23/05/2007	11	
Injection Preparation	18/06/2007	19/06/2007	2	
Injection	19/06/2007	20/06/2007	23	
Post Injection	20/06/2007	21/06/2007	10	
1 Month after Injection	20/07/2007	22/07/2007	12	
Geoprobe Sampling #1	13/8/2007	14/08/2007		3
2 Months after Injection	29/08/2007	31/08/2007	10	
Geoprobe Sampling #2	30/08/2007	30/08/2007		3

3.5.3 Amount/Treatment Rate of Material to be Treated

The permanganate injected could transform and mineralize RDX. Based on the volume of groundwater initially treated (16,200 gallons or 61324 L), the mass of RDX present could be estimated. From four monitoring wells (i.e., MW-12, MW-14, MW-15, and MW-16), RDX concentrations before injection ranged from 34.0 ug/L to 63.8 ug/L (i.e., average 46.85 ug/L). This average concentration times the volume equals 2,873 mg of RDX. The ERI site characterization treats no materials.

3.5.4 Residuals Handling

ISCO, because it treats on site and in place, produces no recoverable residuals. Sodium permanganate reduction will produce MnO₂ as a colloid that may precipitate, and sodium ions (Na⁺) that will remain in solution. ERI site characterization produces no residuals.

3.5.5 Operating Parameters for the Technology

For ERI data collection, an experienced three person team can effectively collect the data. Once lines are placed, a single person can monitor the equipment and collect data for transient analysis. Although not used in this experiment, the system can be operated remotely for long term or higher risk environments.

The equipment used to collect the ERI data includes standard survey gear to locate the array of electrodes in three-dimensional space. In addition, approximately \$50K worth of acquisition equipment is required to collect the data. This includes stakes for coupling to the earth, cables to

communicate to the individual stakes, and a control system with resistivity meter to collect the data (Figure 2.1-1).

3.5.6 Experimental Design

The design of the ISCO demonstration is fully described in two UNL graduate students Masters theses. Specifically, Jeff Albano's thesis (Albano, 2009) focused on the field-scale injection as well as bench-scale confirmation and measurement of RDX mineralization by permanganate over a range of concentrations and temperatures. Additional information on site selection, regional and local geology and hydrogeology, calculation of the injection parameters (permanganate mass, injectate solution concentration, flux, and time) are also presented. Chanat Chokejaroenrat thesis (Chokejaroenrat, 2008), conducted over the same time frame, provides in-depth analysis of the mechanisms associated with the permanganate-RDX reaction.

3.5.6.1 ERI Data Collection

The ERI data was used to track the distribution of injectate. The primary depth of interest was 17 to 23 m (55-75 feet). For imaging from the surface, the primary issue is the detection limit of the injectate. It was anticipated that the injectate would cause a large change in conductivity in the subsurface. It was also assumed that since the test site had been used previously, that the hydraulic properties were reasonably well understood. It was also assumed that the movement of injectate from the original well locations would be slow, with movement occurring on the order of months.

The ERI data was collected with a 56 electrode array on the surface with a 3 meter spacing during four visits to [the site] in 2007 (May 21-23, June 18-21, July 20-22, and August 29-31) using an Advanced Geosciences, Inc., *SuperSting R8* system. This spacing generated a 165 meter (541 feet) long line that imaged approximately 33 meters (108 feet) deep. This arrangement was selected to vertically center the volumes surrounding the well screens within the measured domain. This image depth also allowed the imaging to capture downward movement during injection. The ERI method measures apparent resistivity with a resolution equal to half the electrode spacing, in this case 1.5 m (4.9 ft) both horizontally and vertically. Additional data were collected during the August 29 – 31, 2007 site visits using 6 m (19.7 ft) spacing to explore deeper geological materials and investigate the possibility that the injectate had flowed downwards.

ERI can be collected under different protocols that may be designed to fulfill different needs and priorities. In this investigation, two different protocols were used:

- a proprietary (“standard”) protocol designed to efficiently acquire and process high-resolution data, which is used for characterizing sites, and for outlining contaminant plumes to within the half-electrode resolution;
- a high noise protocol that performs better in high noise environments by acquiring a greater number of data at the expense of longer collection times. This protocol is useful for environments where data will be lost due to anthropogenic interference.

The initial background survey explored the related issues of surface coupling and data quality. Surface coupling, or contact resistance, describes the quality of the electrical connection between the electrode stakes and the ground. Tests performed for each data line showed that the site provides good coupling with low contact resistance. This allowed standard approaches to be used. This also allowed data to be collected without adding salt water or additional materials to the stakes which may alter coupling over time.

ERI data quality was explored by determining data repeatability and inversion error. Background testing indicated that the data repeatability was excellent, and the inversion error was low (3.1-4.8% RMS error). This allowed data to be collected more quickly without the use of the high noise protocol. The background data indicated that more spatial variation could be evaluated by collecting 10 to 12 lines of data instead of the six proposed lines. The site was an active agricultural area, so electrodes were replaced in the lines during each sampling interval instead of being installed for the duration of the experiment. A summary of the lines collected can be seen in Table 3.5-2.

Six temporally discrete ERI datasets were collected at the site:

1. background data (5/21 – 5/23/2007);
2. immediately prior to injection (6/18/2007);
3. during injection (6/18/2007);
4. immediately post-injection (6/19 – 6/21/2007);
5. one month post-injection (7/20 – 7/22/2007); and
6. two months post-injection (8/29 – 8/31/2007).

These are described in further detail below.

1. 5/21 – 5/23/2007: Background survey.

During the visit, the site was evaluated and a data collection protocol was finalized. Visible site characteristics, well-placement, and guidance from Drs. Comfort and Zlotnik were considered and supported the decision to arrange multiple lines along (ERI Lines 1-7, southwest to northeast) and perpendicular to (ERI Lines A - E, northwest to southeast) the injection-extraction well plane (Figure 3.5-1).

Of the southwest-northeast numbered lines, Line 1 was hydraulically upgradient (northwest) of the injection-extraction well plane, the second (Line 2) was along the injection well plane, and the remaining three (Lines 5 through 7) were downgradient (southeast) of the well plane. The last of these (Line 7) was along a line of previously installed southwest-northeast trending monitoring wells. Note that line number 3 and 4 were included after the injection demonstrated limited horizontal flow. Of the five northwest-southeast trending lettered lines, the three interior lines were placed so as to intersect the injection (Lines B and D) and extraction wells (Line C). The remaining two lines were placed approximately 10 m to the southwest (Line A) and northeast (Line E) of the injection wells. Data were collected along all lines using the standard protocol with 3-m stake spacing.

During the visit, ERI survey line endpoint coordinates were collected using a GPS to support future acquisition of ERI data along the same lines along without placing markers along the lines. (Note that re-placement of lines on separate visits may not strongly support quantitative data quality assessment because stake placement is imprecise and resistivity characteristics of geologic materials vary over time with change in, for example, soil moisture. Overall, non-quantitative quality can be assessed by visual inspection of images for similar distributions.)

2. 6/18/2007: Immediately prior to injection

On the day prior to the injection, Line 2 (southwest-northeast, through the injection-extraction well plane) and Line C (northwest-southeast, along the groundwater gradient and intersecting the extraction well) were emplaced. This arrangement was left in place for the duration of and for approximately twenty hours following the injection. A preliminary dataset (MEAD 13) was collected using the high noise protocol.

3. 6/19/2007: During and immediately following injection

Using the arrangement installed on 06/18, data was collected continuously during and following the injection. Data was collected alternately on Line 2 (southwest-northeast) and Line C (northwest-southeast) without moving electrodes or cables. During the injection, six datasets (file names MEAD14 through MEAD19) were collected in hopes of observing rapid changes in resistivity as the injectate flowed within the system. As the injection ended, dataset MEAD18 and MEAD19, were collected using the standard protocol. Two additional datasets (file names MEAD20 and MEAD21) were collected using the high noise protocol. Finally, dataset MEAD22 was collected using standard protocol along Line 2 and Line C before moving the stakes. Note that data quality is

suspect for dataset MEAD21 due to decreasing battery voltage during protocol execution, which took place overnight.

4. 06/20/2007: ~1 day (26.5h) subsequent to initiating injection, ~17h subsequent to completing injection (1 day)

Upon completing repetitive data collection on Line 2 and Line C, a full site survey of seven southwest-northeast lines (Line 1 through Line 7) and five northwest-southeast lines (Line A through Line E) using *standard* protocol, except Line 2 which was collected with high-noise protocol (dataset MEAD22). In addition, data were collected along Line E using a standard with reciprocal protocol, with the reciprocal data used as a field-check of instrument and technique precision.

5. 07/20/2007: ~31 days post injection (1 month)

Approximately one month after the injection, the twelve ERI lines (southwest-northeast Line 1 through Line 7, and northwest-southeast Line A through Line E) were re-established, stakes were installed at the same 3 m spacing along each of the recovered lines, and ERI data was collected using the standard protocol.

6. 8/30/2007: ~72 days post injection (2 months)

Approximately ten weeks after the injection, using the same technique as on the prior visit, ERI data were collected along southwest-northeast Line 6 and Line 7; and along northwest-southeast Line D and Line E using standard protocol. In addition, the stakes were extended from 3 m to 6 m spacing—extending in each direction from the center of the line—to explore deeper features along Line 6, Line D, and Line E (Figure 3.5-4). Further, to explore the possibility of a highly preferential flowpath to the east, two additional northwest-southeast trending lines were established: Line F, from which data was collected with 3-m stake spacing; and Line G, from which data was collected with both 3- and 6-m stake spacing, both using standard protocol. The objective was to determine if the lower formation would allow imaging of deep permanganate.

Table 3.5-2: ERI Datasets

Line	Background	Injection		One month	Two month	
		Pre-	Injection	Post-		
1	X			X	X	
2	X	X	X	X	X	
3				X	X	
4				X	X	
5	X			X	X	
6	X			X	X	X
7	X			X	X	X
A	X			X	X	
B	X			X	X	
C	X	X	X	X	X	
D	X			X	X	X
E	X			X	X	X
F						X
G						X

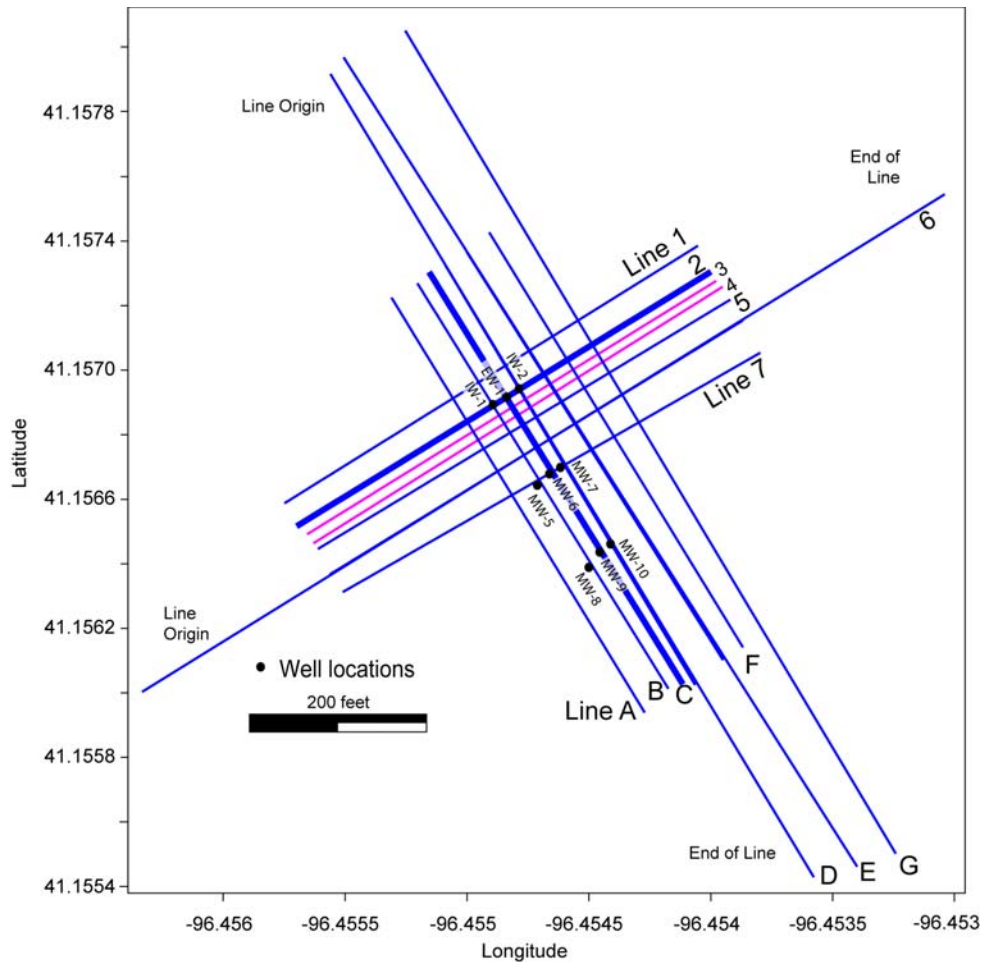


Figure 3.5-4. Location of additional 6 meter ERI lines relative to original 10+2 line grid of 3 meter lines.

Comparing multiple ERI datasets requires using a consistent color scheme. The color scheme that best shows the resistivity distribution may not be the best scheme for showing transient changes in side-by-side images: that is, meaningful changes may not cause a perceptible change in the colors of the images. To explore for and show meaningful changes requires differencing between the datasets. Repetitive ER datasets—sets collected along the same line, using the same electrode configuration and spacing, and the same protocol—may be differenced to reveal transient changes.

Differencing may be performed on both raw data and on inverted model data. Raw data differencing directly compares two datasets recorded by the instrument in the field. Inverted model differencing compares the results of two independently executed inversions as described above.

3.5.6.2 Injection Planning

Tradeoffs between costs, time, availability of facilities, and uncertainty of the permanganate delivery were taken into account. Two injection options for delivery of permanganate were considered. In both cases, it was assumed that plume would drift with natural groundwater flow after injection; the option of continuous recirculation for several weeks that would keep plume in place was judged prohibitively expensive (e.g. Siegest et al., 2001).

An alternative method of delivering permanganate would have used temporary direct-push injection wells. However, the rental costs of a direct push rig, time required to inject, small well diameter (less than 2"), and risks of screen clogging with colloidal permanganate were too high to consider this option. In addition, EPA recommendation of utilizing a previous experiment site (BAZE) and available long-screen 6"-diameter wells implied that extraction-injection scheme seemed less risky and more economical (Figures 3.5-2 and 3.5-3).

Drift of permanganate during curtain development was estimated by natural groundwater flow linear velocity from porosity $n=0.3$, water table slope $i=0.0025$, and $K_h=20$ m / day. Linear velocity was estimated on the order of 0.15 m/day, and the permanganate drift during injection was on the order of 5 cm and could be safely neglected.

Post-injection drift of the curtain with natural groundwater flow was monitored using breakthrough curves in wells downgradient from initial curtain location (e.g., MW-14, MW-15) and will be discussed based on results of groundwater sampling in the following section. When considering this drift, note that the actual permanganate travel distance is shorter than distance between IW-1 and these wells because injection creates a zone around IW-1 that has a significant width.

3.5.6.3 Injection Procedures

Sodium permanganate (NaMnO_4) was injected into the groundwater via a trailer-mounted proportional mixing-injection system (Aquifer Solutions, Inc. Evergreen, CO) (Figure 3.5-2). Groundwater was extracted from well EW-1 via a submersible pump (Aermotor A+ 75-500, Delavan, WI) at a rate of 151.6 L/min (40 gpm) and delivered to an intake manifold located onboard the trailer system (Figure 3.5-3). Approximately 1707.2 L (451 gal) of 40% (w/w) sodium permanganate, spiked with potassium bromide (concentration), was pumped at 3.79 L/min (1 gpm) from 1041 L totes to an intake manifold where extracted groundwater and sodium permanganate were mixed at a ratio of 40:1. The mixed effluent was then gravity fed into each of two neighboring injection wells, IW-1 and IW-2 (Fig. 5.), at approximately 77.7 L/min (20 gpm). Sodium permanganate was continuously injected for 413 minutes with the exception of a 10 min interval at 260 min when sodium permanganate totes were switched. Following the

sodium permanganate injection, extracted groundwater from EW-1 was recirculated to wells IW-1 and IW-2 for 42 min.

Sodium permanganate concentrations were periodically measured on site with a portable spectrophotometer (Hach model DR 2800, Loveland, CO) to monitor the concentration delivered to the injection wells and breakthrough at the extraction well. Specific conductivity was measured using a YSI 3000 T-L-C meter (Yellow Springs, OH) during each sodium permanganate measurement to establish a calibration curve to relate specific conductivity to sodium permanganate concentration.

To monitor groundwater levels and buildup of a permanganate head during the 7-hour injection, 20 m of continuous PVC pipe (3.8 cm diameter) was placed into each injection well to shield and dampen water level variations created by the cascading permanganate solution. A water level meter (Solinst Model 101) was periodically lowered into the PVC pipes to record water levels.

3.5.7 Sampling Plan

3.5.7.1 Sample Collection

The objective of sampling at the demonstration site was to provide data for evaluation of the effectiveness of the ISCO/ERI process. Sampling included monitoring RDX degradation and permanganate consumption. Groundwater was sampled pre-injection to establish ambient groundwater chemistry and initial RDX concentrations. Post-injection groundwater samples were sampled to monitor and track RDX degradation, bromide movement, and permanganate consumption. Groundwater was sampled using a Grunfos Redi-Flo2 submersible environmental sampling pump with Teflon hose. A minimum of three well volumes were purged from each well before the samples were taken to ensure a true representation of the groundwater. Samples were analyzed for permanganate on site using a Hach model DR 2800 Portable Spectrophotometer and off site using a Shimadzu model UV-2101PC UV/VIS Spectrophotometer at 525 nm. Samples analyzed for RDX were quenched on site using manganese sulfate (MnSO_4) to prevent further RDX degradation. Because the quenching of permanganate with MnSO_4 produces sulfate, and sulfate interferes with Br^- analysis during analysis by ion chromatography, this quenching agent may not have been suitable for samples taken for Br^- analysis. Samples taken for Br^- analysis were quenched with hydrogen peroxide. All water samples were kept in a cooler, chilled with blue ice on site and during transport, and refrigerated within the UNL soil environmental chemistry laboratory upon delivery. RDX was analyzed by the UNL water science laboratory via a liquid chromatography/mass spectrophotometer (LC/MS) (Cassada *et al.*, 1999).

The depth to water in each well was measured by an electronic depth meter. The logs of depth-to-water and other direct real-time readings such as temperature, conductivity, Eh, pH and DO were kept in a field log book.

3.5.7.2 Sample Analysis

All groundwater samples collected from monitoring and injection wells were analyzed using standard methods approved by US EPA and /or ASTM.

ERI data were analyzed with standardized protocols developed at Oklahoma State University (Halihan et al, 2005). There are no standard US EPA and/or ASTM standards for collection and analysis of ERI data.

3.5.7.3 Experimental Controls

The experimental control (baseline data) for the ISCO and ERI demonstrations was collected prior to permanganate injection. In addition, a dedicated monitoring well (MW01), which is located upstream of the injection wells, was sampled to determine the RDX concentration flowing into the demonstration area. The samples from this monitoring well were analyzed following the same protocol as the samples obtained from the other monitoring wells. The background ERI data collected during May 2007 allowed for experimental control of electrical conditions that existed prior to the injection.

3.5.7.4 Data Quality Parameters

Prior to sampling, each well was thoroughly purged (three well volumes) to remove the stagnant groundwater in order to collect representative samples. Ten percent of the total field samples were used for QA/QC for data completeness as well as accuracy. Appendices A, B, and C contain the QAPP and SOP for laboratory and field sampling, which were developed for the permanganate injection.

3.5.7.5 Data Quality Indicators

ERI allows three primary tools to assess data quality. These tools were used in various degrees throughout the project depending on the objective of the sampling period. These tools are:

- Repetition: the degree to which a sequential series of observations provide the same values; typically, the observation protocol is executed twice, preserving the configuration of the equipment from one measurement to the next. The repetition error is measured as an error between the two identical measurements. This is commonly used since it does not significantly alter the total measurement time period.

- Reciprocity: the degree to which resistivity measured in one current direction matches the resistivity measured in the opposite direction; typically, a “forward” protocol is run followed by a “reverse” protocol, preserving the configuration of the equipment. This protocol is not as commonly used since it requires doubling the survey time to run the survey with complete current pairs. For this reason, only one complete reciprocal set of data was collected.
- Inversion RMS error: The iterative inversion process of creating a model image of resistivity distribution, described above, isolates individual ER data points that cannot be reconciled with the inversion model. Such points may be anomalous but correct measurements; or may result from, for example, instrument error or poor electrode coupling (i.e., hard rock, concrete, or dry sand). A small number of such points are generally present in any ER dataset; the proportion of such data points indicates data quality: the smaller the proportion, the higher the data quality. Prior work has demonstrated that 5 to 15 % is a typical range for good quality data, proportions greater than 15 % indicates questionable data quality, and proportions less than 5 % are exceptionally clean.
- Additionally, densely collected data often provide a subjective indication of quality by demonstrating spatially consistent, and hydrogeologically reasonable distributions. For example, independently-collected closely-spaced parallel ERI planes with strikingly similar patterns suggest good data quality. Revisiting—similar to repetition, but with a time-delay and after removing and replacing the equipment—can provide a similar indication of data quality by providing nearly identical data at the same location at different times. Finally, locations where lines cross should provide similar data.

The data quality for the site was very good by all three measures. Repetition error was generally less than 1% for more than 95% of the data (Figure 3.5-5). As expected, reciprocal error was higher with about 10 percent of the data above 10 percent reciprocal error. The reciprocal dataset was not conducted with each measurement immediately following the next. Instead, an entire file of data was collected in one direction, then the reciprocal was collected. This may have increased the reciprocal errors, but not significantly. Finally, inversion RMS error was very good with a range from 3.0 – 6.2%. The data also demonstrated smooth variations in parallel datasets indicating that the technique was collecting good quality data that provided consistent interpretations of the subsurface.

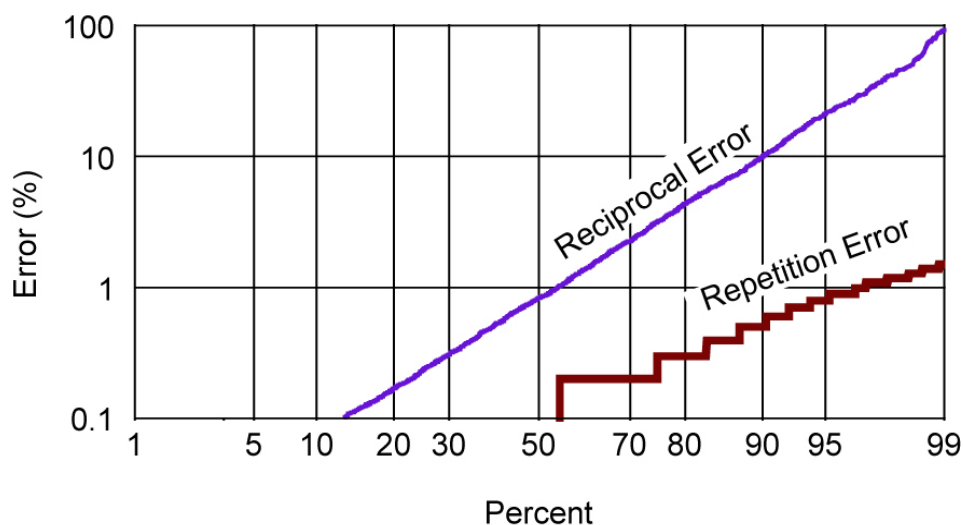


Figure 3.5-5. Reciprocal and repetition error for ERI data collected at the BAZE site. The data represents data for one complete ERI dataset.

3.5.7.6 Calibration Procedures, Quality Control Checks, and Corrective Actions

The instruments used for chemical analysis were calibrated daily from standards prepared from stock solutions. Check samples were run after every 10 samples to validate the repeatability of the instrument. The on-site, real-time instruments like ORP electrodes, pH meters, DO meters and electronic depth meters were calibrated prior to sampling. The ERI instrument was checked prior to each sampling interval for the functioning of data channels and relays, and tested for calibration. The battery voltages were maintain above 12.1 volts to ensure data quality, except during an overnight data collection after injection when the battery voltage went below standards.

3.5.8 Demobilization

Demobilization of ERI equipment involved removing stakes, cables, and flagging from the survey areas. This was relatively straightforward except in the area of the site that was planted with soybeans. Vegetation grew over the period of the demonstration and it became extremely difficult to find the electrode stakes in the field. A few were left in the field and became problematic at harvest time. The field procedures have now been modified to include wire flags at the location of each electrode when working in highly vegetated areas.

3.6 Selection of Analytical/Testing Methods

See Appendices A and B.

3.7 Selection of Analytical/Testing Laboratory

See Appendices A and B.

4. Performance Assessment

4.1 Performance Criteria

Table 4.1-1: Process Performance Criteria

Performance Criteria	Description	Primary or Secondary
Contaminant Reduction	Identify the contaminants that the alternative technology will destroy	Primary: RDX, note that the LC/MS analysis which were used in this demonstration, routinely analyzes for TNT, RDX, HMX and common degradation products Primary: ERI measuring permanganate plume (spatial and temporal)
Contaminant Mobility	Identify any contaminants whose mobility may be increased or decreased (even if not degraded) by the alternative technology	Generally the ISCO process will not affect the mobility of any contaminant in the groundwater. Precipitation of MnO ₂ could reduce hydraulic conductivity but we will be re- measuring hydraulic conductivities before and after the permanganate injection to quantify if any changes occurred.

		The ERI is not intrusive and had no affect on the sampled area.
Hazardous Materials	Identify any hazardous materials that will remain or might be introduced by the alternate technology	ISCO required the injection of NaMnO ₄ as the chemical oxidant. RDX was the primary target of the treatment process. Natural oxidant demand of the aquifer material will eventually consume the permanganate as it move downgradient.
Process Waste	Identify any process waste produced by the technology. If there is such a waste, describe its volume, and hazardous that are associated with it, and how it will be handled.	ISCO is an in-situ process, so little process waste was produced throughout the demonstration. Purge water that was tainted with permanganate was taken to the nearby pump and treat facility where it was run through the activated carbon filters. ERI did not generate any process wastes.
Factors Affecting Technology Performance	Describe how technology performance is affected by operating conditions (e.g., flow rate, feed rate, throughput, temperature, etc.). Describe how matrix effects (e.g., soil type, particle size distribution, groundwater pH, DO, other contaminants, etc.) may affect technology performance.	Flow rate and feed rate will affect the size and time needed to establish a curtain of permanganate between injection wells IW1 and IW2. Environmental variables influencing the rate and extent of contaminant degradation with permanganate in groundwater are: (i) natural oxidant demand of the groundwater matrix; (ii) temperature; (iii) pH and ionic composition of the groundwater.

		<p>ISCO with permanganate can be cost effective at sites that have relatively high saturated permeabilities (conductivity > 10⁻⁴ cm/s); low organic carbon in groundwater (<0.5%); and pH in the optimal range of 7 to 8 (USDOE, 1999). Based on previous evaluations (Woodward-Clyde, 1995), these criteria are met at the Nebraska Ordnance Plant. Secondary: DO, pH and temperature were periodically monitored following permanganate injection.</p> <p>ERI performance was controlled by two factors. First contact resistance between electrodes and the ground can limit either injected current or potential measurements. This can be controlled by the addition of a half liter of salt water around a dry electrode, but was not an issue for the site. The second factor is the electrical contrast between the permanganate plume and the surrounding aquifer. It was anticipated that the injected permanganate mass would generate a strong conductive signature in the subsurface.</p>
Reliability	Issues addressed should include, but not limited to, potential	Breakdowns are limited to the timeframe encompassing the

	breakdowns of the equipment and sensitivity to environmental conditions	<p>permanganate injection. Once the permanganate injection was completed, reliability issues of the ISCO process were minimized.</p> <p>ERI reliability was limited to equipment failure at the site. Spare batteries prevented power source issues, and spare equipment was available to be delivered on an overnight basis if equipment failed.</p>
Ease of Use	Describe the number of people required in the demonstration. Address the level of skills and training required to use the technology. Can technicians operate the equipment, or are operators having higher skills and education required? Is continuous monitoring of the process required? Indicate whether OSHA's health and safety training is required	<p>ISCO required 2 to 3 people to perform the permanganate injection. Note several HAZWOPER-trained graduate students were also be on hand to benefit from this research demonstration.</p> <p>Moderate level training was required for permanganate injection such as: HAZWOPER, operation of pumps, meters, and real-time measurements like pH and ORP meters.</p> <p>ERI measurements required two individuals trained in ERI measurements and a third to help deploy and manage the equipment.</p>
Versatility	Describe whether the technology can be used for other application(s) and whether it	The ISCO technology does not have any specific boundaries of use. Provided groundwater can

	<p>can be used at other locations. If not, could it be adapted? To what extent would the technology have to be adapted so that it can be used in other settings?</p>	<p>be reached by injection wells, any site containing explosive-contaminated groundwater can be treated.</p> <p>The ERI technology can generally reach a depth of up to 100 feet. Typical line length for this depth is 500 feet. The technique can be performed in both consolidated and unconsolidated sediments, hard rock environments, and urban settings. Performance is limited if a sufficient connection cannot be obtained with the subsurface. This would be caused by thick concrete that cannot be drilled through or similar large insulator.</p>
<p>Maintenance</p>	<p>Discuss routine required maintenance, including frequency and labor involved. Described the level of training required for maintenance personnel.</p>	<p>The ISCO and ERI technology is a low or no maintenance in situ process.</p> <p>The ERI equipment is generally removed from the site after a sampling period. A system can be deployed for long term remote sampling, and would require maintenance of the system power and data transmission equipment.</p>
<p>Scale-up Constraints</p>	<p>Describe potential issues of concern (e.g., engineering or throughput constraints, interferences) associated with scaling up the technology for full implementation, and how</p>	<p>Potentially there are no constraints scaling up the ISCO technology. The engineering issue is the number of injection and monitoring wells needed to address the size of the explosive</p>

	the issues of concern will be addressed in the demonstration.	plume. ERI could aid greatly in this process by spatially and temporally tracing the permanganate plume following injection.
--	---	--

4.2 Performance Confirmation Methods

Groundwater samples collected from monitoring wells (MW) will be analyzed weekly by the laboratories listed in Section 3.8. The chemical analysis methods are standard methods approved by US EPA and/or ASTM.

The instruments used for chemical analysis were calibrated before each use from standards prepared from stock solutions. Check standards were run after every 10 samples to validate the repeatability of the instruments.

On-site instruments like ORP electrodes, pH meters, DO meters, and electronic depth meters were calibrated prior to sampling for instrument reliability and repeatability.

ERI instruments were tested for calibration and to ensure that switching relays are performing properly prior to surveying. Voltage on batteries during surveys were maintained above 12.1 volts except on one overnight survey. Data was collected by repeating measurements for each data point collected. Data that was not repeated within 2% was excluded from the datasets. Data QA/QC followed procedures established by OSU and Aestus, LLC.

The experimental control for obtaining baseline data in the ISCO demonstration was from the monitoring well (MW00) that was 30 feet upstream from the injection zone. MW00 was sampled at every sampling to develop baseline RDX concentrations.

Ten percent of the total field samples were collected for QA/QC data completeness as well as accuracy. We determined the initial RDX concentration in the permanganate injection zone and then tracked changes in RDX as the permanganate and RDX moved down gradient. We also monitored MW00 and the injection zone wells throughout the experiment to determine the influx of RDX. Table 4.2-1 summarizes the expected performance levels of the ISCO/ERI demonstration project and the analytical methods to evaluate ISCO/ERI effectiveness.

Table 4.2-1: Project Performance Confirmation Methods

Primary Criteria	Expected Performance Metric (pre demo)	Performance Confirmation Method*
PRIMARY CRITERIA (Performance Objectives) (Qualitative)		
Contaminant mobility	ISCO/ERI does not have any influence on contaminant mobility	Analysis of samples from monitoring wells using EPA's SW846-8330 and UNL Water Sciences Laboratory LC/MS methods.
Faster remediation	A decrease in RDX concentration from ~70 µg/L to <2 µg/L, which is the HA for RDX.	Analysis of samples from monitoring wells using EPA's SW846-8330 and UNL Water Sciences Laboratory LC/MS methods.
Ease of Use	Implementation of ISCO/ERI will complement each other in determining permanganate location and RDX destruction rates	A comparison of RDX destruction with ERI images of permanganate concentrations will confirm or reject whether ERI can complement ISCO.
PRIMARY CRITERIA (Performance Objectives) (Quantitative)		
Target Contaminant - % Reduction - Regulatory standard	RDX Removal by 97% Achieve US EPA's HA concentration (2 µg/L) for RDX	Comparisons of RDX concentration between samples from monitoring wells and initial RDX concentrations.
Hazardous Materials	None	Degradation products of RDX will be screened by LC/MS using Cassada et al., 1999
Process Waste	None	Observations in the field
Factors Affecting Performance		

- Throughput	Not a concern, as most of the time for injection and sampling is fixed.	Sample analysis at flow rates present at each sampling interval, which may be differ.
- Media size	NOP aquifer material is sandy.	ERI measurements yielded a spatial distribution (2-D) of the permanganate plume. This 2-D image will verify how well permanganate was injected.
- Media constituents	Media constituents will not affect ISCO/ERI process as the permanganate is soluble in water and has no affinity for sorption	Analysis of permanganate concentrations from monitoring wells using UV detection.

SECONDARY PERFORMANCE CRITERIA

(Qualitative)

Plume size	RDX size in demonstration area will get smaller Permanganate plume size will dissipate and decrease in concentration as it moves down gradient	Analysis of samples from monitoring wells using EPA's SW846-8330 and UNL Water Sciences Laboratory LC/MS methods. ERI 2-D images of permanganate plume was to confirm
Reliability	No breakdowns	Record keeping
Safety - Hazards - Protective clothing	Oxidants Modified Level D PPE (see Sec. 3.6.8)	Experience from demonstration operation
Versatility - Intermittent operation	No, oxidant will be added only	

- Other applications	once. ISCO/ERI process can be applied to any explosives contaminant aquifer with slight modifications on quantity and frequency of amendment addition.	ISCO/ERI results will confirm
Maintenance - Required	None, except for pump or other equipment breakdown	Experience from demonstration operation
Scale-Up Constraints - Engineering - Flow rate - Contaminant concentration	None, only more wells may be needed depending on plume shape and size Flow rate will control timeframe needed for permanganate injection Not a concern.	Monitor during demonstration operation. Experience from demonstration operation Experience from demonstration operation

4.3 Data Analysis, Interpretation, and Evaluation

4.3.1 ERI Data

During the course of the experiment, two spacings were used for ERI lines. The 3-meter spacings resulted in ERI datasets (pseudosections) that were 165 meters long and 33 meters deep. The 6-meter spacings resulted in datasets that were 330 meters long and 66 meters deep. The datasets indicate a shallow conductive layer less than 100 ohm-meters that extends between 4-5 meters (13-16 feet) depth (Figures 4.3-1 and 4.3-2) to an elevation of approximately 350 meters. Beneath that layer is a highly variable layer that extends 20-30 meters deep with a range in resistivity from 100-10,000 ohm-meters. The layer ends at an elevation of approximately 320 meters.

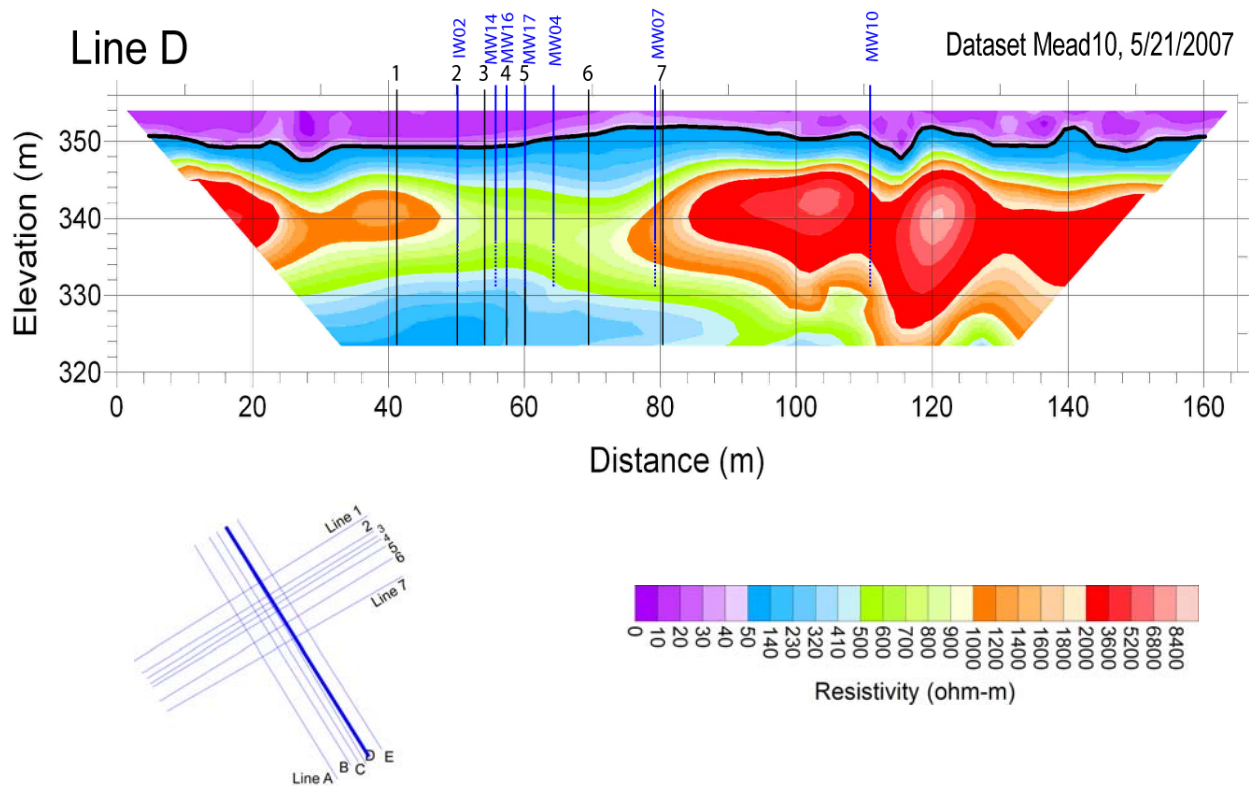


Figure 4.3-1. 2D ERI pseudosection of ERI line D with location of wells on the line. The location of crossing lines are indicated with black vertical lines.

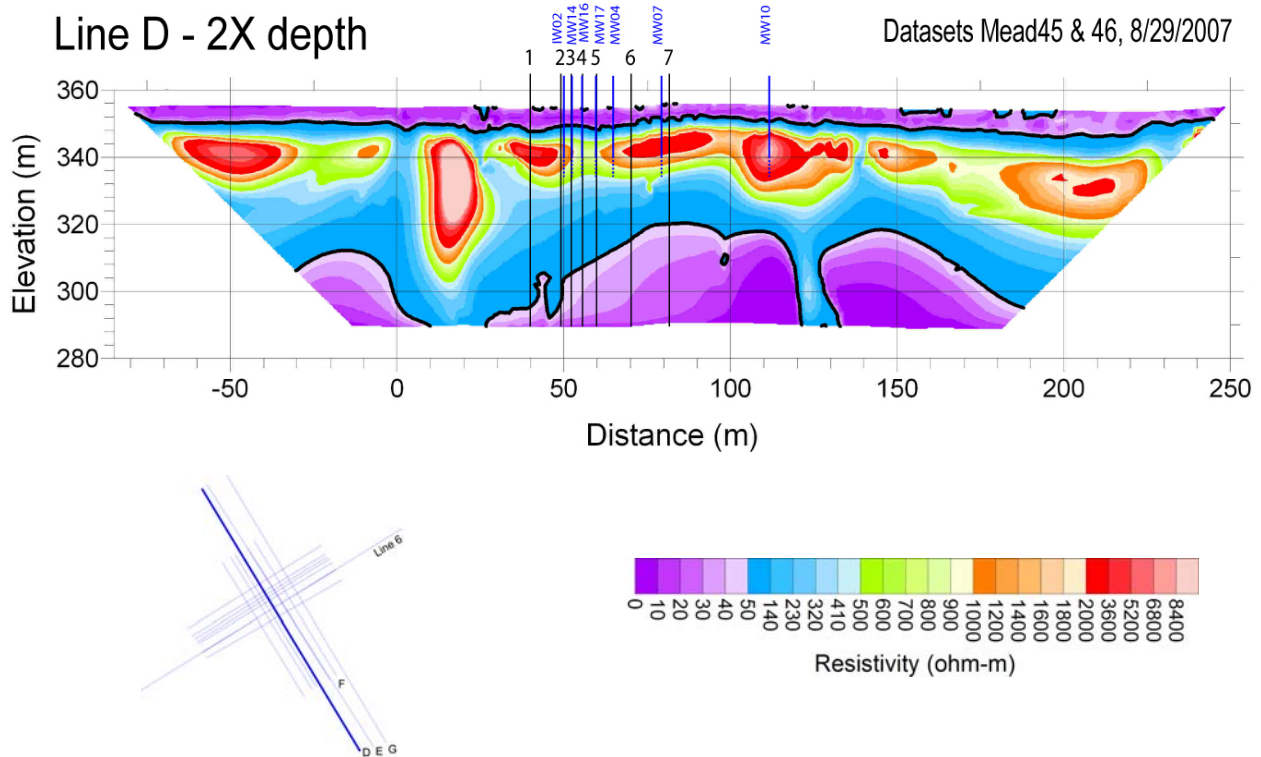


Figure 4.3-2. Six-meter 2D ERI pseudosection of ERI line D with location of wells (if present) on the line. The location of crossing lines are indicated with black vertical lines.

The ERI dataset compare well with hydraulic conductivity data for the monitoring well system at the site. A significant increasing trend exists between the geometric mean ERI data for the screened intervals of the monitoring wells and the hydraulic conductivity data at the wells (Figure 4.3-3). Although a simple logarithmic trend is possible, the tracing results as well as the hydraulic conductivity data suggest that above approximately 3000 ohm-meters, the hydraulic conductivity decreases. This is interpreted as a decrease due to either compaction or cementation that caused higher resistivity and slightly lower hydraulic conductivity.

When compared to direct push EC logging, the first layer is comparable to the result from EC logging in that the large increase in conductivity is observed in the same location. When compared to sediment cores, a distinct difference is noted (Figure 4.3-4A). While the upper conductive layer corresponds well to the thickness and expected resistivity of the Peoria Loess, the Todd Valley Formation is logged as a divided unit in the sediment logs at an elevation of approximately 336 meters. The ERI datasets indicate that this is a break point, but that the electrical layer extends much deeper. The ERI datasets and the sediment logging agree again on

the location of the Dakota Group, which appears to exist at an elevation of approximately 320 meters, although as part of this study, no core was available to that depth.

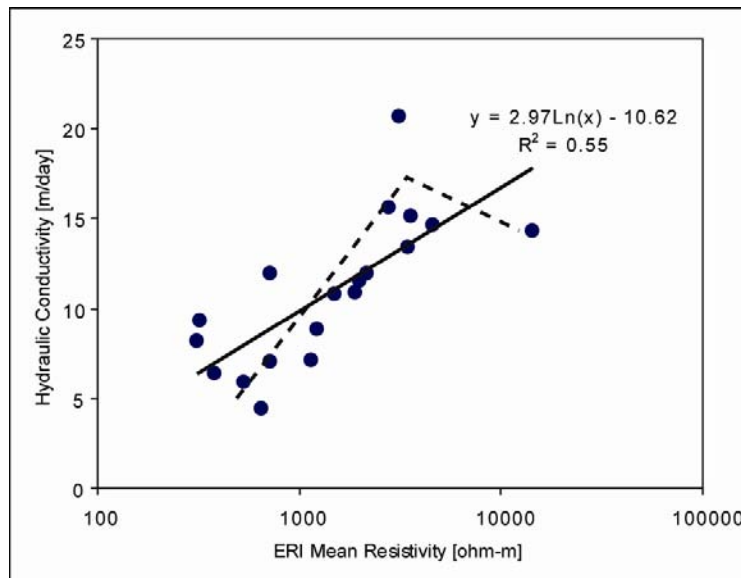
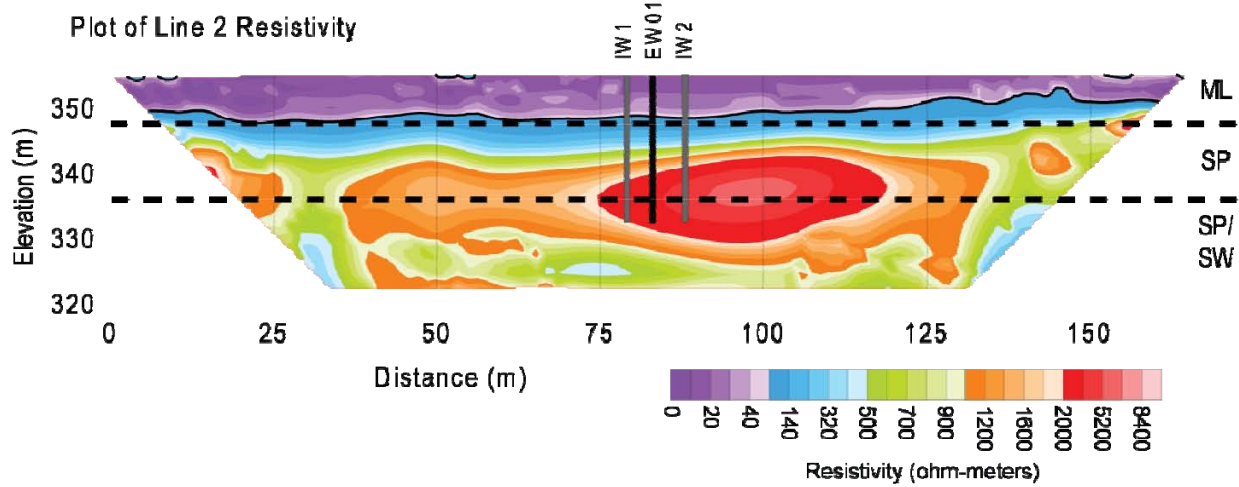


Figure 4.3-3. Geometric average of ERI datasets for location of screened intervals of monitoring wells compared with the hydraulic conductivity at the wells. The trend (solid black line) indicates a general increase in hydraulic conductivity with increases in resistivity. The dashed line indicates the expected trend when factoring in the results of the tracer test which supported a conclusion that the high resistivity areas (>3000 ohm-m) were less hydraulically conductive.

The resistivity images show no appreciable differences post injection. The amount and conductivity of the injectate was expected to cause significant changes to the resistivity images. As this did not occur, differencing was performed to evaluate changes in the resistivity between time periods. Only differencing between pre-injection and immediately post-injection showed any discernable changes. The majority of these changes were observed on the lettered lines B-D. The other orientation provided signal only for locations where the stakes were not moved between surveys (Lines 2 and C) (Figures 4.3-4 and 4.3-5). At these locations, both positive and negative changes occurred. The changes ranged from -13% to 13% which was much smaller than expected. The location of the changes indicates that significant changes occurred above the water table. The other changes occurred upgradient of the injection wells and vertical below and to the southwest of the injection wells. These changes were consistent with a conductive injectate being placed in the aquifer. The changes exist over the entire injection wall domain.

The positive changes are associated with the location of the on-site road (Figure 3.4-4 B) and some areas near the water table, which may indicate areas that drained during the injection phase.

A)



B)

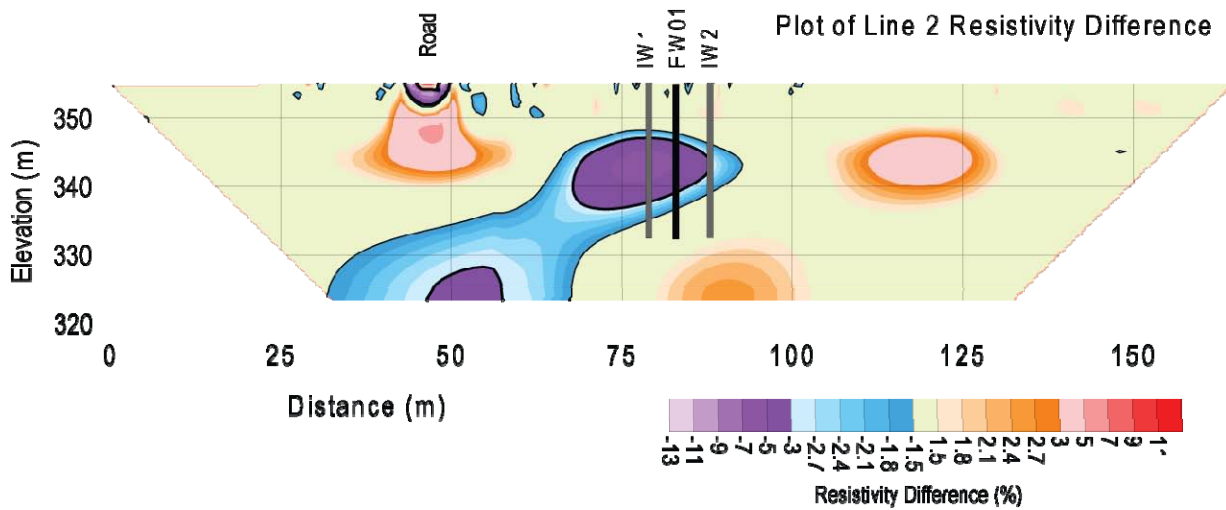


Figure 4.3-4. A) Resistivity of ERI Line 2 (through injection plane) showing location of wells used to develop permanganate curtain, and the lithology develop for the site using other techniques B) Resistivity difference after injection.

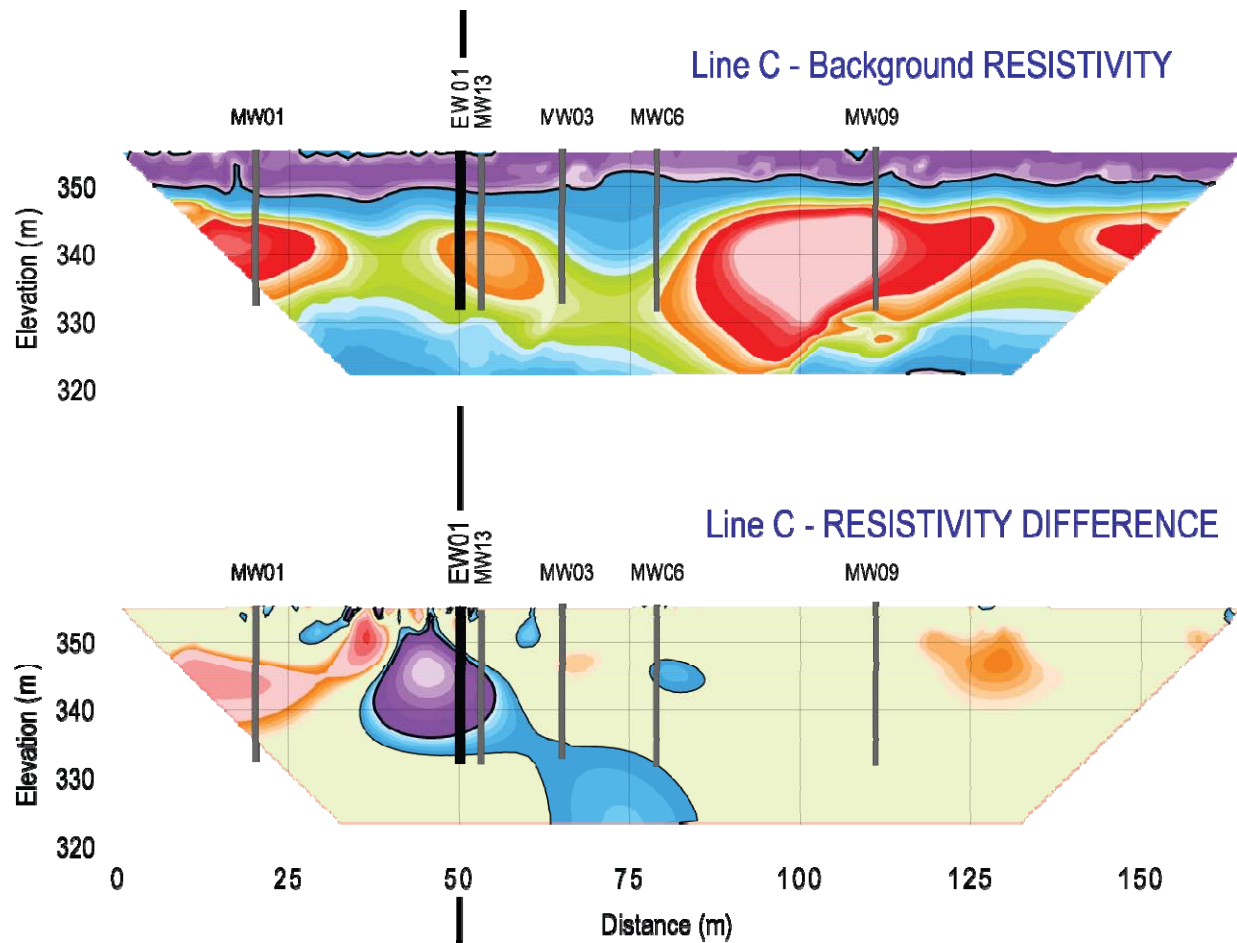


Figure 4.3-5. A) Resistivity of ERI Line C (parallel to natural gradient) showing location of extraction well used to develop permanganate curtain and monitoring wells. B) Resistivity difference after injection.

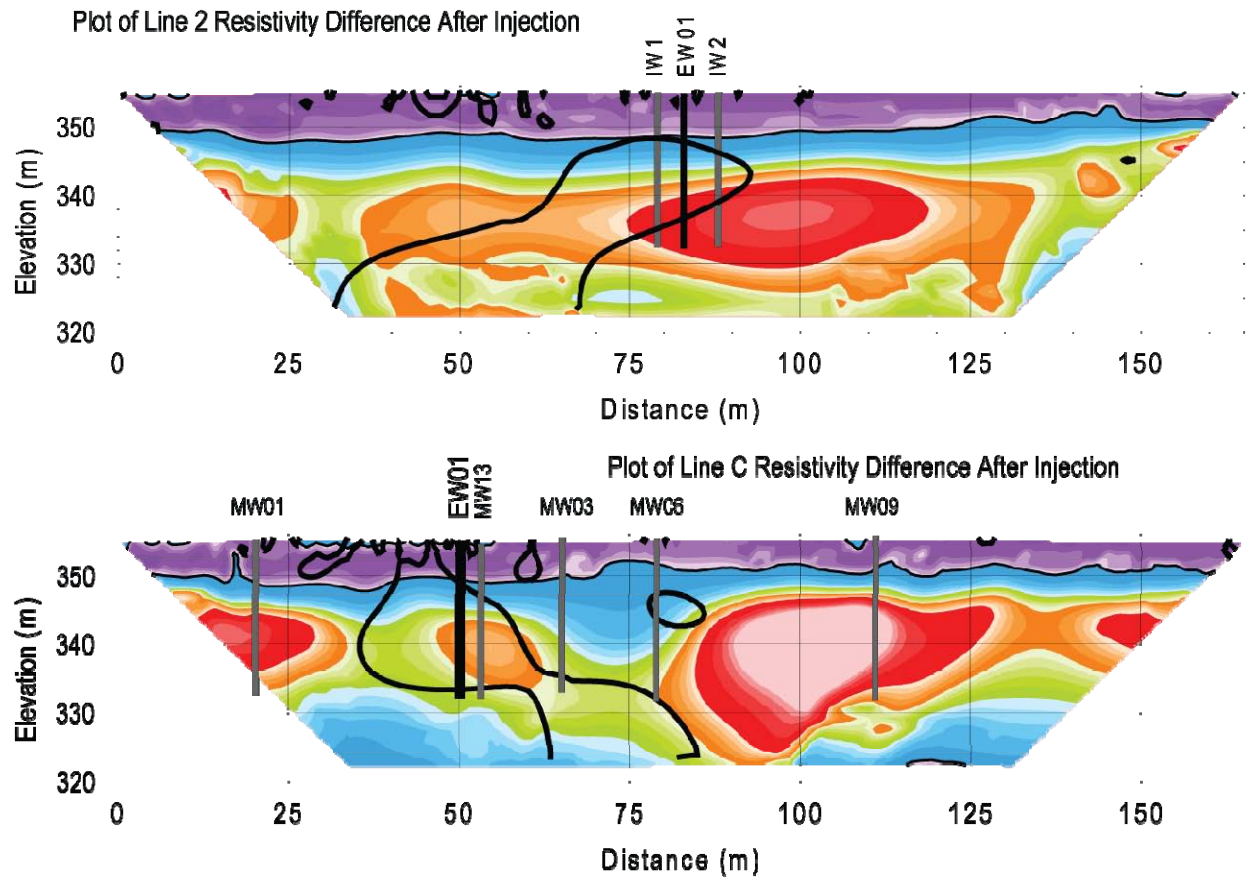


Figure 4.3-6. A) Resistivity of ERI Line 2 (parallel to injection curtain) showing location of extraction and injection wells used to develop permanganate curtain. Heavy overlay indicates area of greatest resistivity change after injection. B) Resistivity of ERI Line C (perpendicular to injection current) showing location of extraction well used to develop permanganate curtain and monitoring wells. Heavy overlay indicates area of greatest resistivity change after injection.

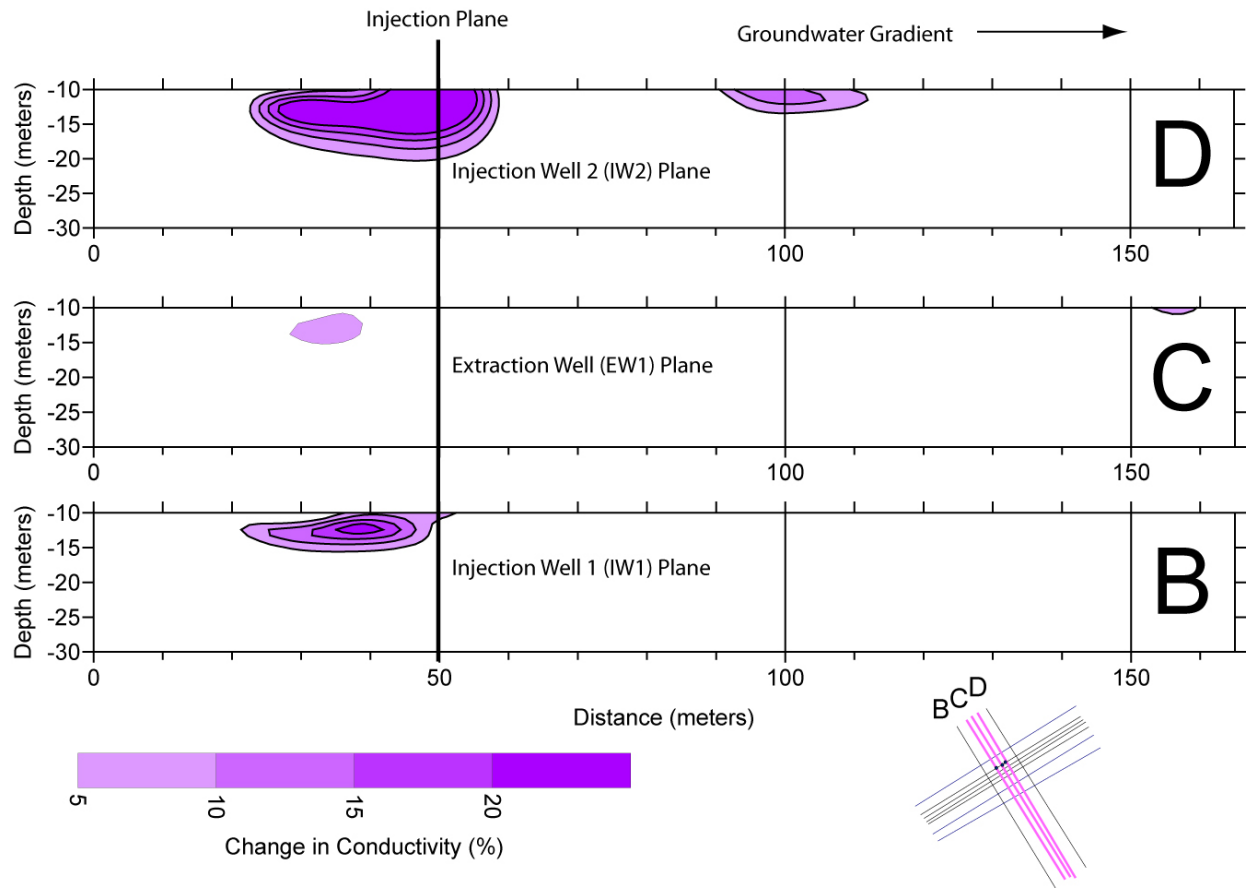


Figure 4.3-7. ERI differences along ERI lines B, C, and D. Data collected for lines B and D by differencing datasets where stakes were replaced instead of being held constant.

The areas of increased conductance correspond to the higher hydraulic conductivity areas mapped by the ERI technique (Figures 4.3-3 and 4.3-6). The increased conductive area appear to move away from the highly resistive zone in line 2 at 100 meters lateral distance (Figure 4.3-6A) and appear to move under the low resistivity area at 75 meters and the high resistivity area at 100 meters on line C (Figure 4.3-6B). Differencing of line B and D indicate that line C was the smallest change of all three lines. The injection well locations have a much larger signal than the extraction well location, approximately twice as high (Figure 4.3-7). The other orientation showed no consistent pattern for changes except for the line 2, which left the electrodes in place during the injection.

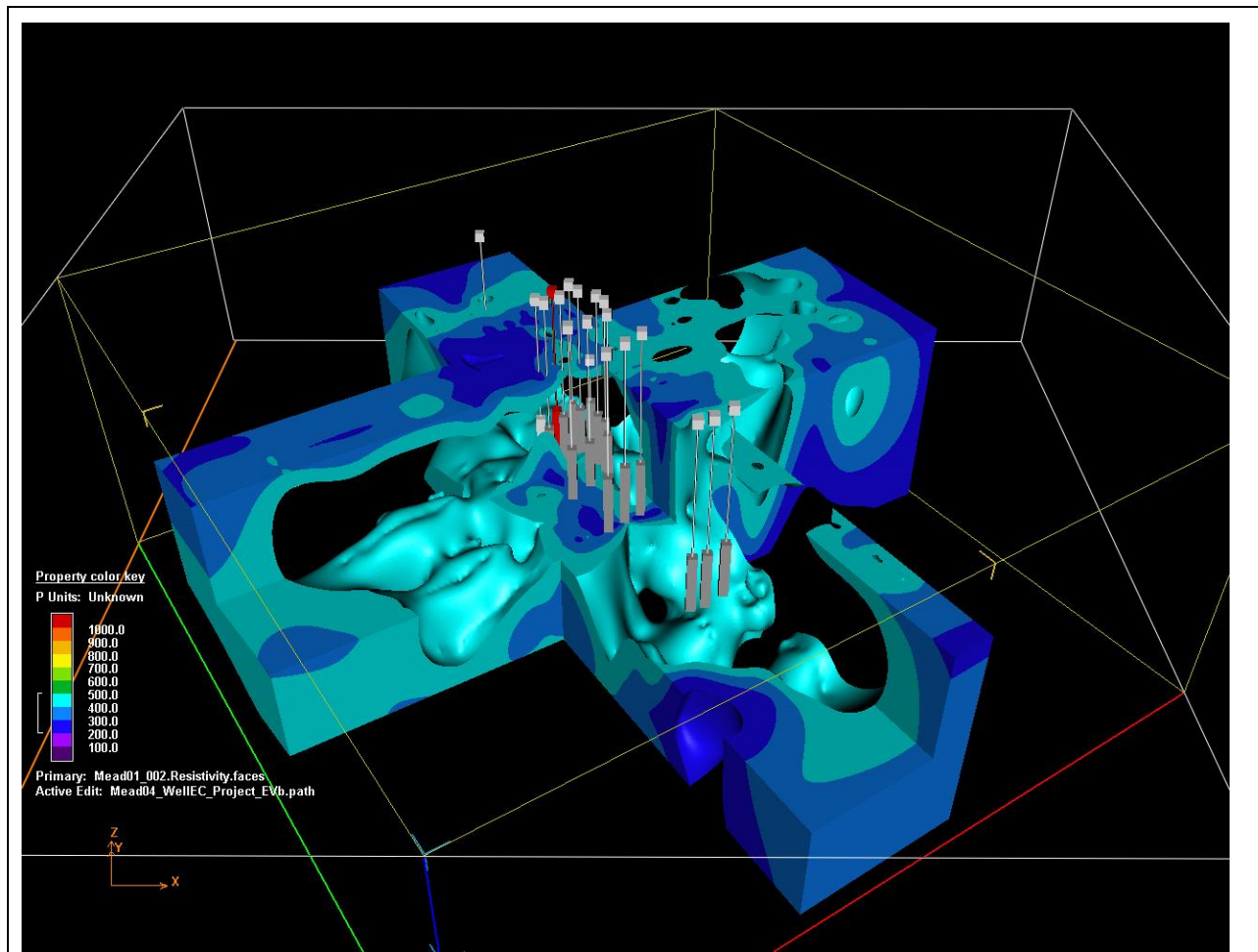


Figure 4.3-8. 3D representation of full 3 meter ERI datasets of BAZE site. Transparent areas are interpreted to correspond to areas of higher hydraulic conductivity and thus preferential pathways for the injection.

4.3.2 Injectate Data

Based on our modeling efforts (Eq 3.4-1 – 3.4-6), and assuming piston-type flow (i.e., no dispersion), approximately seven hours of pumping (extraction-injection) would have been required to complete the permanganate curtain. Initial permanganate breakthrough at the extraction well, however, was observed within 77 min (1.3 h). Once all the permanganate had been injected into the injection wells (IW-1 and IW-2) ($t = 6.88$ h), the sodium permanganate concentration in the extraction well (EW-1) had only reached 2386 mg/L, indicating that a uniform curtain of permanganate was not established across the injection wells. Electrical resistivity imaging (ERI) conducted during the injection process indicated that our conceptual curtain failed to develop. The ERI data indicated that the sodium permanganate migrated upgradient in the vadose zone due to preferential flowpaths. The ERI data also showed that the sodium permanganate was not substantially drawn towards EW-1. Moreover, we observed different head buildups in the injection wells during the permanganate injection. IW-1 had a maximum buildup of 3 m of permanganate while IW-2 was at 7 m (23 ft) near the end of the injection. IW-1 and IW-2 head differences were previously encountered during a 30 min pre-injection test using water but not to the extent observed during the permanganate injection. The differential head buildup observed between injection wells also likely contributed to a less than uniform distribution of permanganate.

RDX concentrations temporally decreased in wells closest to the injection wells (IW-1, IW-2, Fig. 3.4-9) as the permanganate migrated down gradient. We observed RDX degradation rates of 0.12/d in MW-12 and 0.087/d in MW-14. These rates were lower than what was observed under batch conditions at 11.5°C and likely a result of a lower initial permanganate concentration (6000 versus 15000 mg/L). RDX concentrations decreased nearly 80% (from 64.6 to 13.1 $\mu\text{g/L}$) in MW-12, 70 % in MW-14 (from 54.3 to 16.2 $\mu\text{g/L}$), 73% in MW-15 (from 87.3 to 23.5 $\mu\text{g/L}$), and 75% (from over 45 to 11 $\mu\text{g/L}$) in MW-16 before permanganate breakthrough was complete. We observed a slight decrease in RDX in MW-17 and MW-4 (data not shown). The permanganate concentrations sampled in MW-17 and MW-4 did not show a true breakthrough, which corresponds to the scattering RDX concentrations measure in both wells.

When permanganate and bromide breakthrough curves were normalized to the maximum concentrations observed, the $\text{MnO}_4^-/\text{Br}^-$ BTC in wells MW-12, MW-14, and MW-15 were nearly identical and indicated that permanganate consumption by native SOD was minimal (Fig. 3.4-10). By integrating the $\text{MnO}_4^-/\text{Br}^-$ BTC, we estimate permanganate consumption was between 0.25 to 0.76% for wells MW-12, MW-14, and MW-15 indicating low permanganate consumption after a linear distance of 6 m (20 ft). These data are also supported by the fact that

sodium permanganate fingers were also observed while multilevel sampling via direct push at concentrations in excess of 900 mg/L 72 d after injection and at a linear distance of >14.5 m from IW-2 (Fig. 3.4-11). The low oxidant demand of both aquifer and groundwater (i.e., RDX concentration) indicate that permanganate could potentially oxidize a large volume of RDX-contaminated groundwater within the Todd Valley Aquifer. Also note in Figure 3.4-11 that some of the multilevel sampling seem to indicate that less conductive region of the aquifer (layers where permanganate was not found) were void of RDX, meaning that both permanganate and RDX appear to take similar flow paths.

Permanganate breakthrough was observed in all wells within the field site except MW-2 and MW-3. Fluid electrical conductivity measurements conducted prior to groundwater sampling also provide evidence that the permanganate plume did not uniformly enter the monitoring well screens but followed preferential flow paths found during multi-level slug testing of MW-15 prior to permanganate injection (Fig. 3.3-6). Monitoring wells only captured fingers of permanganate, that when sampled mixed treated and non-treated groundwater during pumping, therefore, diluting permanganate/bromide concentrations within the well and possibly increasing RDX concentrations due to mixing (Fig. 4.3-12)

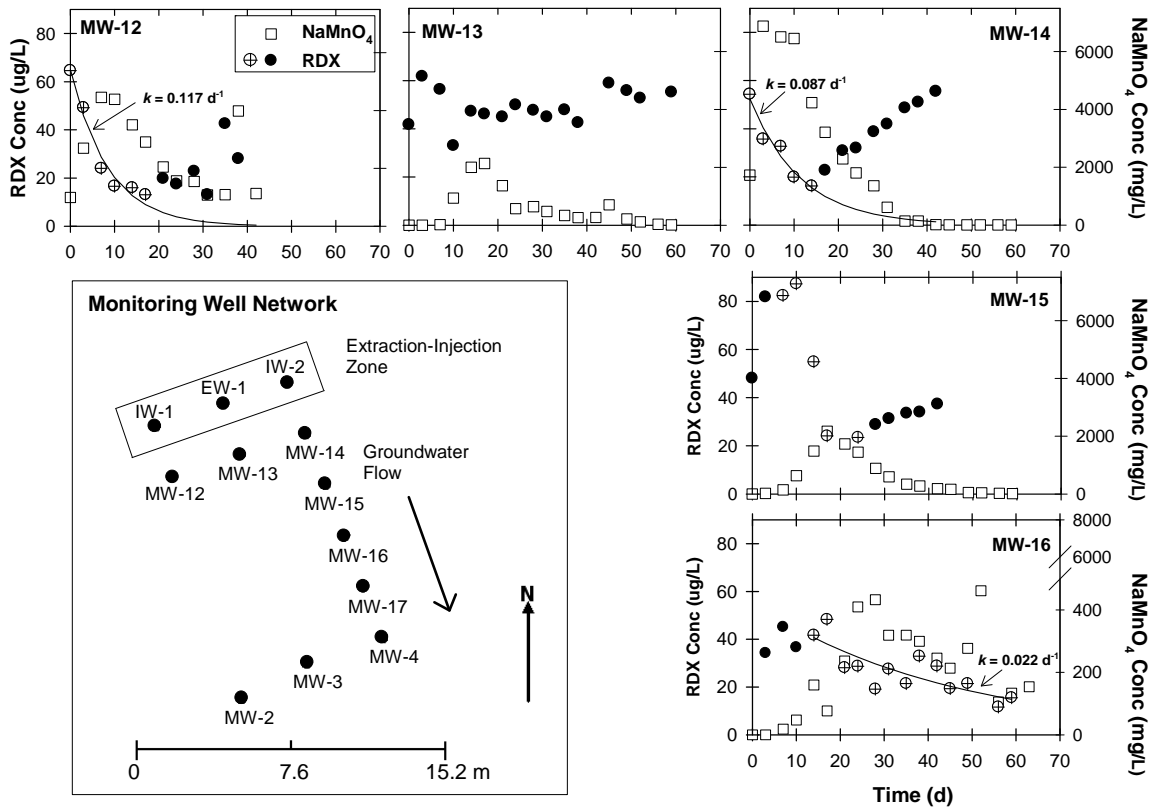


Figure 4.3-9. RDX and permanganate breakthrough curves observed in field monitoring wells. Open circle symbols with crosses were used to calculate RDX degradation kinetics (i.e. fitted lines).

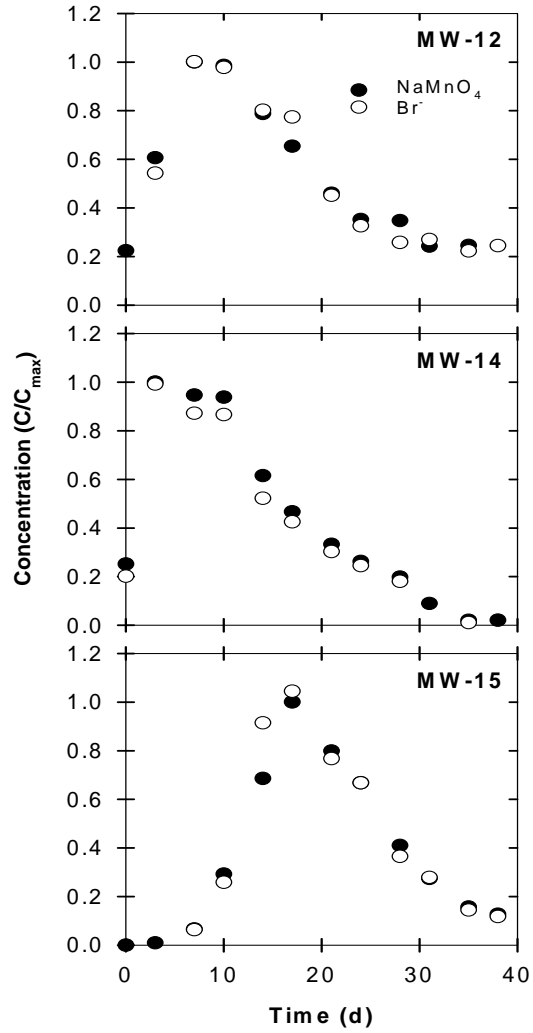


Figure 4.3-10. Sodium permanganate and Bromide breakthrough curves obtained from MW-12, MW-14, and MW-15.

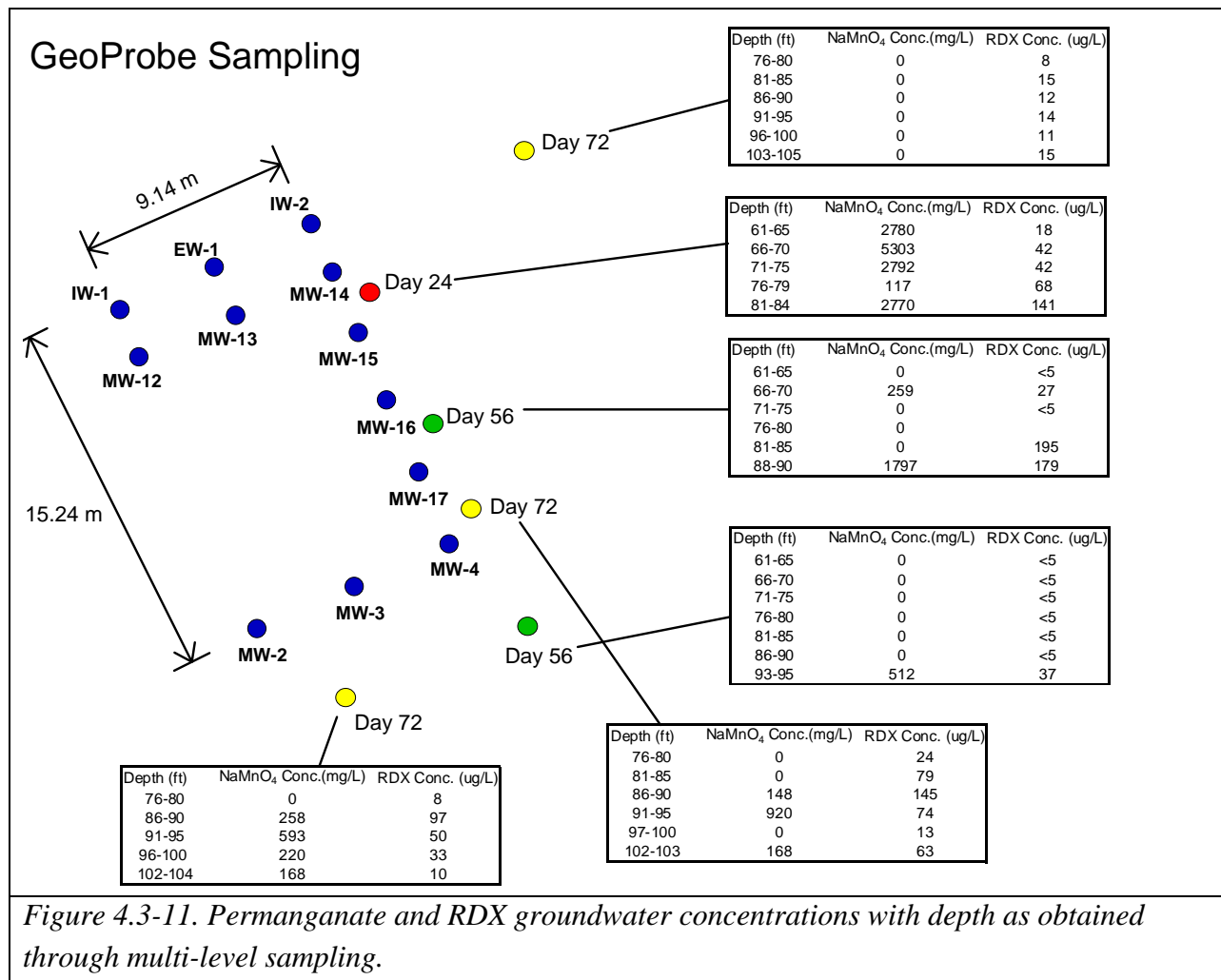


Figure 4.3-11. Permanganate and RDX groundwater concentrations with depth as obtained through multi-level sampling.

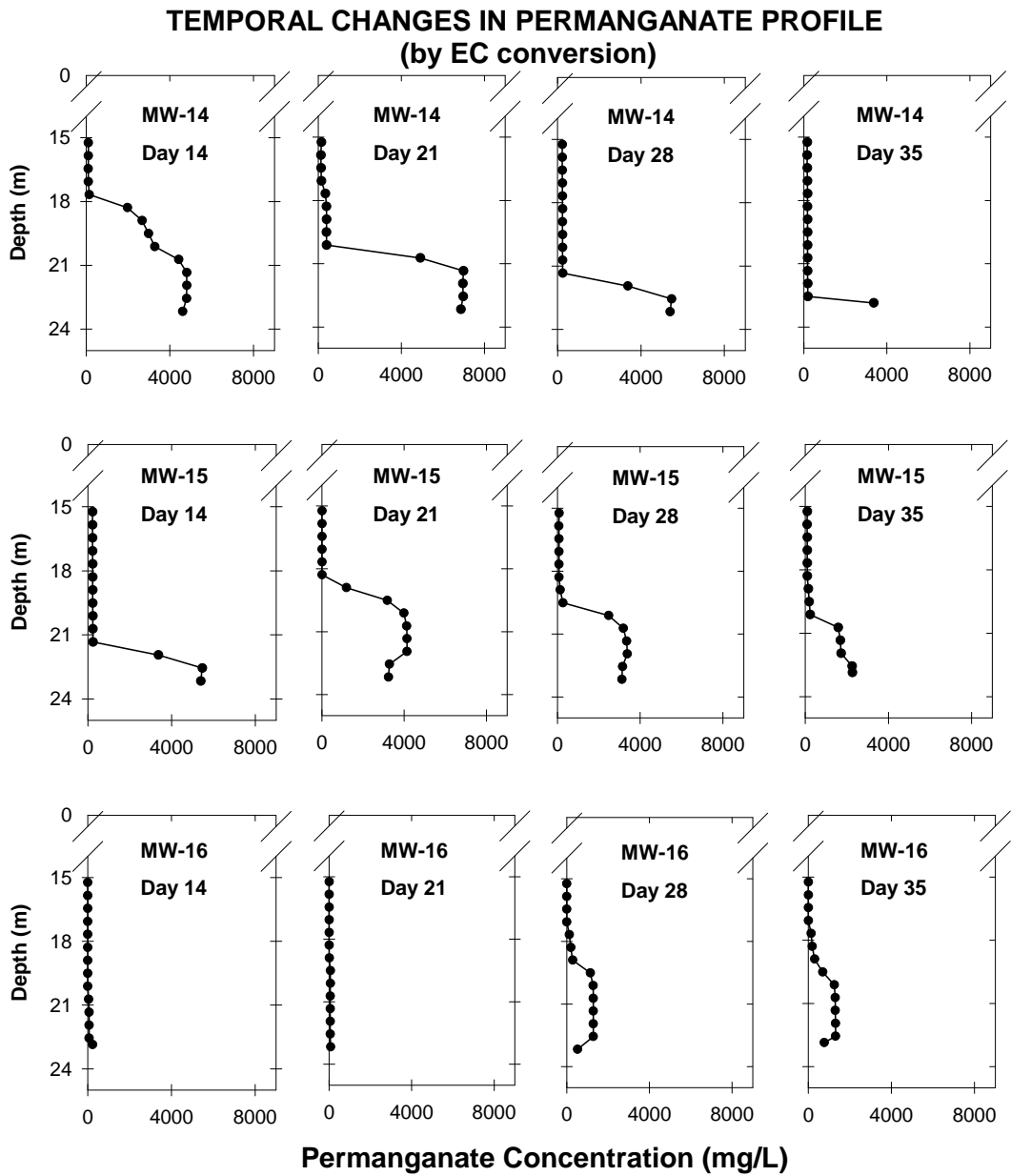


Figure 4.3-12. Permanganate profile concentrations in monitoring wells prior to pumping for groundwater sampling.

4.3.3 Data Comparison

The results of ERI and groundwater sampling clearly indicate that the predicted injection did not move in the anticipated directions and rates. For the chemistry, the areas that were sampled performed similarly to laboratory experiments, but the samples were more difficult to obtain as much of the injectate appeared to move below the monitoring well system. Without installing additional piezometers, the thin fingers of injectate could not be monitored to further assess the degradation process.

The ERI data provided a quantitative assessment of the hydraulic conductivity field of the site allowing an understanding of the variability observed in multilevel slug tests. This quantitative comparison indicates that ERI or similar geophysical data (i.e. helicopter electromagnetic data), may be useful in assessing the aquifer for sampling or planning remediation programs.

The ERI data was intended to be quantitatively compared with well data as part of the transient analysis of the dataset. Unfortunately, with the results found, the injectate location and the wells did not correspond. The data suggested that the injectate moved upgradient approximately 15 meters in preferred pathways in the vadose zone. An asymmetrical curtain of injectate appeared to form upgradient from the injection/extraction well system. The injectate then appears to move vertically downward and beneath the monitoring wells. It is not clear if this movement was a density effect or the effect of vertical gradients on the site as no data on vertical hydraulic gradients are available. As the only time period that was cleanly detectable was immediately after injection, the signal included wetting of the vadose zone by the cone of injection, thus the signal was comprised of both injectate and changes in moisture content in the vadose zone.

Aside from the unexpected movement of the injectate, two properties appeared to affect the ERI analysis, the general formation properties and geometry, and the fluid distribution. The aquifer geometry can electrically be approximated as a two layer system. The upper conductive layer of silt provided suppression of the signal due to the large contrast with the aquifer material. The upper layer resistivities were on the order of 10 ohm-meters (lower than expected) while the aquifer was on the order of 1000 ohm-meters (higher than expected). This yields a ratio of approximately 100 between the two layers. Additionally, the upper layer thickness of approximately 6 meters gives a ratio with the electrode spacing of 3 meters of 0.5 which makes the interpretation more difficult (Telford et al., 1990).

Direct push sampling of the injectate indicated that the fluid was moving as fingers less than 1.2 meters (4 feet) in thickness. As the resolution of the technique is 1.5 meters as performed, the fluids were moving in fingers that were below the resolution of the technique. While this does not eliminate the possibility of detecting the material, it limits the expected signal strength.

For the technique, the site provided a challenging geometry that limited the ability to quantitatively assess the injection, but did provide an ability to observe the injectate in locations where monitoring wells were unavailable. In other aquifers, the signal can be much stronger and provide better controls over the injection process (Sima et al., 2008).

Following the injection, permanganate samples were collected from the monitoring wells for 63 days. During this time, between five and eight wells contained measurable quantities of permanganate. The ERI data, EC monitoring data, and direct push samples all indicate that the majority of permanganate went below the monitoring well screens. A spatial and temporal analysis of the relationship between ERI resistivity values and permanganate concentration was performed to determine if there was correlation between the two datasets. The statistical power of the data are limited as there were few wells that had injectate appear.

The spatial relationship between ERI values at monitoring wells and permanganate concentrations was variable in the first two weeks after the injection. After that period, the plume appeared to stabilize and from day 14 to 45, the relationship between ERI resistivity and sodium permanganate concentration was stable with a logarithmic relationship (average R^2 factor of 0.45). This relationship is illustrated from the sampling data collected one month after the injection occurred (Figure 4.3-13). During this time period the slope, intercept, and R^2 values of the relationship remained stable (Figures 4.3-14 – 4.3-16). Later, as the concentration dropped, the relationship began to change. These limited data indicate that the ERI mapping allows a monitoring of the spatial distribution of permanganate by providing a mapping of the hydraulic conductivity distribution. Modifications to the monitoring protocol would be required to provide a direct mapping of concentration.

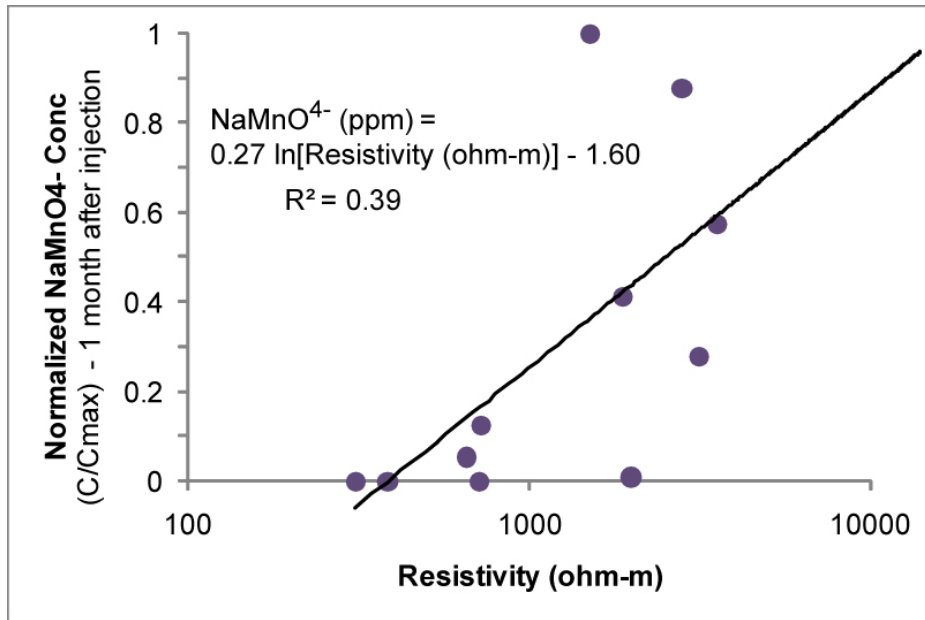


Figure 4.3-13. ERI resistivity versus sodium permanganate concentrations in monitoring wells one month after injection. Best fit line represents slope, intercept and R² value for the single time period.

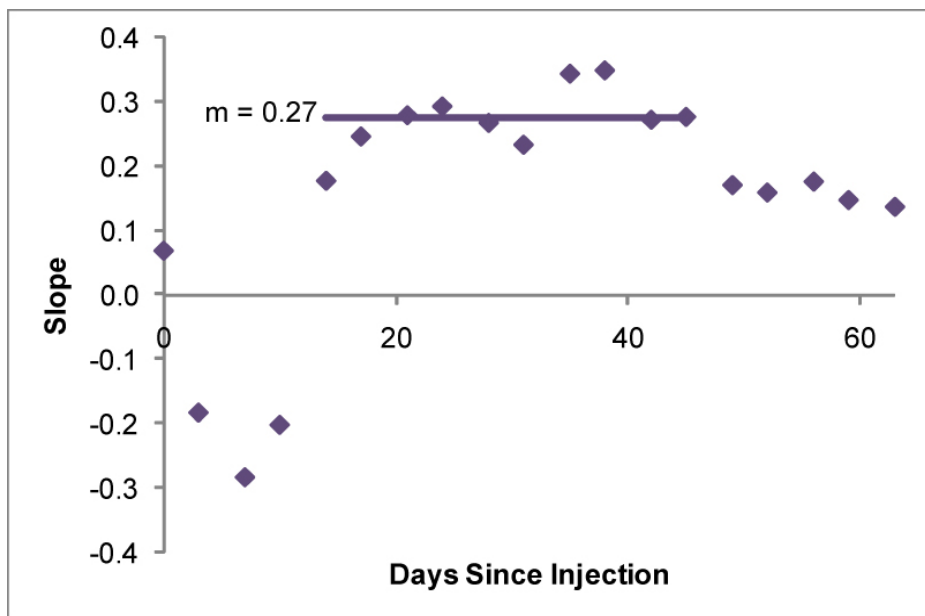


Figure 4.3-14. Slope of best fit line for ERI resistivity versus sodium permanganate concentrations in monitoring wells from the time of injection to 63 days following injection. The average slope value from 14 to 45 days is highlighted with a thick line.

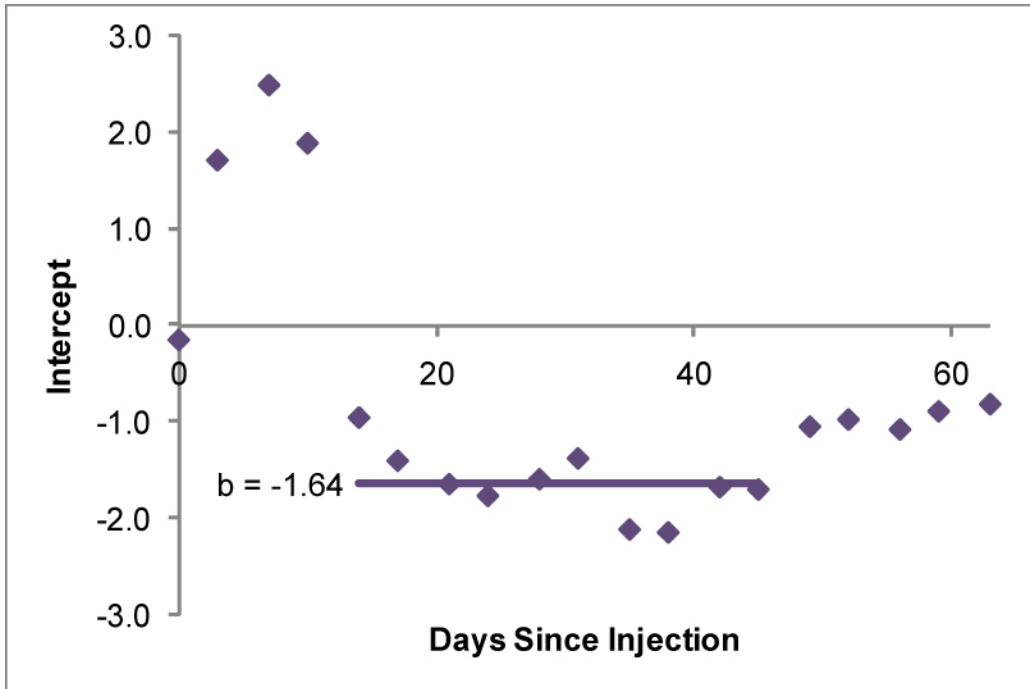


Figure 4.3-15. Intercept of best fit line for ERI resistivity versus sodium permanganate concentrations in monitoring wells from the time of injection to 63 days following injection. The average slope value from 14 to 45 days is highlighted with a thick line.

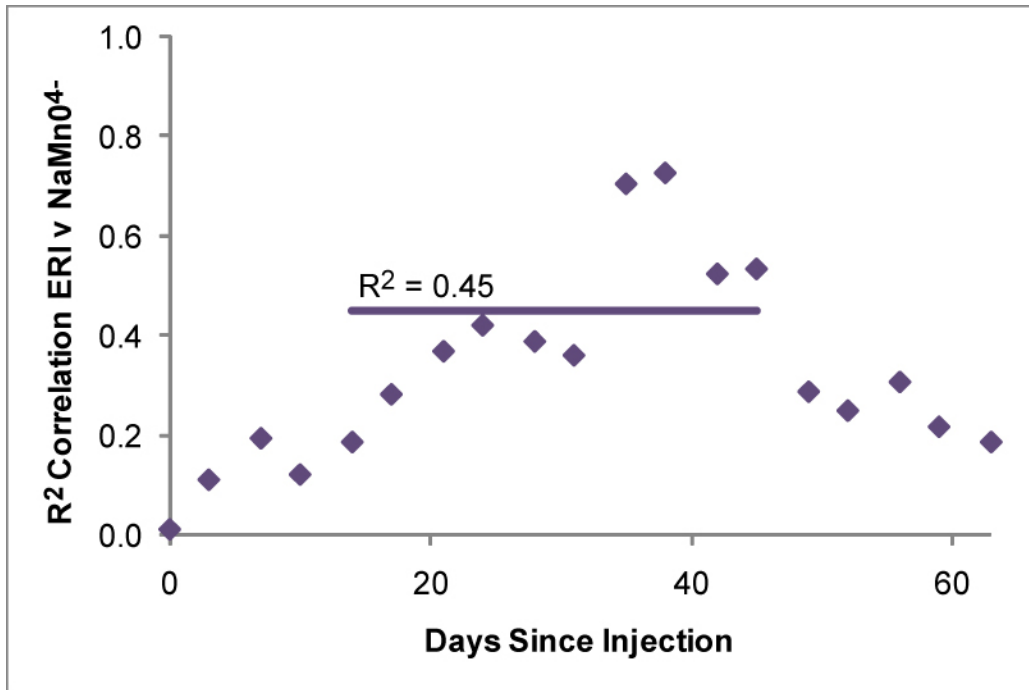


Figure 4.3-16. R^2 values for best fit line for ERI resistivity versus sodium permanganate concentrations in monitoring wells from the time of injection to 63 days following injection. The average slope value from 14-45 days is highlighted with a thick line.

For future monitoring experiments, several protocol modifications can be made to improve results. First, semi-permanent electrodes can be installed at the surface for the duration of the experiment. While this will not improve the results dramatically, they can provide an increase in signal to noise ratio that can be important. Secondly, any monitoring system should include smaller piezometers screen lengths to ensure less fluid mixing occurs in the samples for geophysical calibration. Third, imaging for only fluid movement should be included at the same flow rates and locations as the planned injection. This will potentially enable the vadose zone changes to be separated from the injectate signals. This can be done with or without electrical tracers such as chloride or bromide solutions. Finally, injection curtains should be established at lower pumping rates to control fingering. The lower head changes in the aquifer will increase injection costs, but will likely improve delivery to the zones of interest. These changes are detailed in section 6.4

5. Cost Assessment

5.1 Cost Reporting

Table 5.1-1: Cost Tracking

COST CATEGORY	SUB CATEGORY	DETAILS
START-UP COSTS	Site Characterization	Measurements of background ERI of groundwater
	Mobilization	Includes (but not limited to) planning, contracting, personnel mobilization, transportation and site preparation
CAPITAL COSTS	Capital Equipment Purchase	ERI equipment: Resistivity Instrument Switchbox Cables Stakes Laptop computer
	Ancillary Equipment Purchase	Sampling Pumps DO Electrode/Meter ORP Electrode/Meter Conductivity Electrode/Meter
	Modifications	None expected
	Structures, Installation	Injection and monitoring wells
	Engineering	Monitoring and injection well design. Note this is same as BAZE system
OPERATING COSTS	Capital Equipment Rental	Pump and injection equipment
	Ancillary Equipment Rental	A small dumpster and portable outhouse will be rented and placed on site during permanganate injection and

		initial ERI measurements. 700W generator for pumps
	Supervision	
	Operator Labor	ISCO: two personnel for 1 week (40 h) ERI: three personnel for 2 d (16 h) per sampling
	Operator Training	ISCO: HAZWOPER
	Maintenance	Periodic pump maintenance during permanganate injection
	Utilities	None at demonstration site
	Raw Materials	None expected
	Process Chemicals	Sodium Permanganate Potassium Bromide (see Sec. 3.6.3)
	Nutrients	None
	Consumables, Supplies	Teflon tubing for sampling, Glassware for sampling Shipping containers
	Residual Waste Handling	None expected
	Offsite Disposal	None expected
	Sampling and Analysis	
Indirect Environmental Activity Costs	Environmental and Safety Training	HAZWOPER
	OSHA Ambient Environmental Sampling	Not required
Demobilization	Injection equipment removal	Removal of inflow permanganate injection equipment

5.2 Cost Analysis

5.2.1 Cost Comparison

The most commonly used technologies for remediating RDX in groundwater is pump-and-treat with GAC adsorption. Unique to this project is that because we are using the exact location of the BAZE project, costs of this ISCO/ERI project can be directly compared. Similar comparison between pump and treat and ISCO with permanganate have been previous published (Cronk and Marvin, 2004).

5.2.2 Cost Basis

Our results provided proof-of-concept that permanganate could be used for in situ chemical oxidation of RDX-contaminated groundwater. Important criteria in evaluating ISCO remediation technology is the cost. This cost estimate is based on our field trials; therefore, the cost of a full-scale application will decrease due to the economics of scale. The majority of costs belong to chemical and operational costs (e.g., injecting, labor, and equipment rental costs). We used 40% (w/w) sodium permanganate (NaMnO_4) for this demonstration.

Although factoring in labor, capital outlays and equipment depreciation is complicated, chemical and operational expenditures per volume of treated groundwater (or mass of treated RDX) is straightforward. According to our design calculation, we would have initially treated approximately 16,088 gallons of groundwater (i.e., 60,900 L). Given that the groundwater was treated with 40% (w/w) NaMnO_4 , and cost of NaMnO_4 (including delivered) was \$9,950, we calculated the cost of NaMnO_4 at \$0.618 per gallon of groundwater (Table-1). Another important cost was incurred for injecting NaMnO_4 into the pumped groundwater using a continuous proportional feed mixing system. These costs are often price-quoted depending upon the site characteristics. Aquifer Solutions, Inc., a well-known company in ISCO applications, estimated charges of \$17,463. Therefore, it costs \$1.703 to treat one gallon of groundwater (Table5.1-2).

Table 5.1-2 Permanganate and Contractor Costs

Description	Unit	Quantity	Cost	\$ per gallon of contaminated groundwater (16,088 gallons)
Sodium Permanganate	Gal	451	\$9,950	\$0.618
ISCO Applications (Contractor)	L.S.	1	\$17,463	\$1.085
				\$1.703

Based on the volume of groundwater treated, we also estimated the cost per milligram of RDX destroyed. From four monitoring wells (i.e., MW-12, MW-14, MW-15, and MW-16), amount of treated-RDX concentrations ranged from 34.0 ug/L to 63.8 ug/L (i.e., average 46.9 ug/L). If 16,088 gallons of groundwater was treated uniformly, we would have destroyed approximately 2,853 mg RDX. In conclusion, the permanganate and injection costs per mg of RDX was \$9.608. Ideally, we would have preferred to treat a source zone of RDX, with much higher RDX concentrations, but the characteristics of the NOP site did not allow for such a demonstration.

For ERI analysis, the comparison is not as simple as it is often compared against monitoring wells alone. For this project the ERI costs are equipment, labor, and processing. The equipment and labor can generate approximately four lines of data per day. Commercially, this is performed at a cost between \$5000 to \$8000 per day including reporting. If additional visualization is performed, additional charges of \$2000 to \$5000 are incurred depending on the amount of visualization required. If additional correlations and analysis are performed, other than posting well locations and concentration data, additional time is involved with additional costs. For this project, there were 13 field data collection days and a 3D visualization performed. This would cost \$84,500 plus visualization and analysis.

These costs were compared against using standard monitoring wells. To collect a comparable number and distribution of data would require approximately 204 wells or boreholes spaced every 10 meters in the core data area to a depth of 30 m (98 ft). At a cost of \$3,500 per hole, the well installation would cost \$714,000 before sampling. This would not include the examination for the deeper aquifer portions, nor multilevel wells to obtain vertical data. If the larger areas evaluated were included the costs would be much higher.

However, ERI cannot be performed to quantitatively assess hydrogeology without using wells. The well placement can be greatly improved by focusing on areas of high and low hydraulic conductivity in this case and provide samples that demonstrate the range of possible values in the subsurface. Once this process has been performed, the ERI tool can be used to scan other locations and provide similar information without needing the large number of monitoring points required.

Comparing ERI assessment with direct push is also difficult as they are not a direct comparison. The common case is to employ ERI when either wells or direct push methods fail to provide data that allows the site data to be well understood. In this case, the ERI data that is collected is an additional cost that then needs confirmation from further direct push work. This is generally due to the ERI data providing narrow targets of investigation that were missed in previous data collection periods.

If collected during the initial site characterization, ERI data allows direct push evaluation to be highly targeted toward providing a correlation with the ERI dataset. This is similar to the petroleum and mining industries use of seismic datasets. A “Common Earth” approach is employed to evaluate difference between the data types as contradictory data will exist between the ERI and the direct push data. Generally, this approach lowers the overall cost of direct push data collection, but increases the overall cost of site characterization.

5.2.3 Cost Drivers

The primary cost drivers for the demonstration are site construction, principally well placement (Capital cost), permanganate, and sampling and analysis (groundwater monitoring and ERI).

For ERI characterization and monitoring, the cost drivers are defined by the site conditions and the overall objectives. Each driver is discussed separately.

Mobilization: The ERI equipment can be palletized and shipped worldwide. If the location is accessible by truck, additional equipment can be mobilized to the site for traffic control or other contingencies.

Monitoring Periods: For transient analysis of ERI data, the number of monitoring periods define what type of equipment can be cost effectively employed. The costs decrease with an increasing number of periods as permanent cables can be installed in the shallow subsurface instead of repeatedly installing cables at the surface. Additionally, if a site is to be monitored for a large number of monitoring periods, a dedicated system can be installed for the life of the project that can be monitored remotely.

Traffic Control: Costs increase if a site requires traffic control. This can be achieved through overnight surveying, traffic controls and lighted barricades, and traffic rated cable ramps. This largely just increases the time to deploy cables to achieve project objectives.

Ground Surface Characteristics: Empty grass fields with soft soil and no buildings are faster and easier locations to collect data from than urban environments, concrete pavements, or thick scrub. In concrete, to avoid data ambiguity and increase data quality, 3/8" diameter holes are drilled to allow the electrodes to contact native soil. If the concrete must remain intact, conductive gels can be employed to collect data. The technique has been employed in environments ranging from jungle floors to refinery complexes. The technique can be used across water and solid rock. The cost is defined by the rate of data collection and what factors slow the acquisition of data.

Survey Line Length: For surface only ERI surveys, the total line length affects the time for acquisition. Generally, for 3 meter spacings on a 56 electrode survey (165 meter total line length), four lines of data can be collected per day. For longer spacings, the number of lines decrease to 1 to 2 per day as the distance becomes more difficult to manage.

Survey Resolution: In noisy urban environments or for monitoring injections, additional time is required for data collection. This decreases the number of lines possible per day.

Number of correlation sites: Data correlation with ERI datasets generally involves a large portion of data which correlates well with other datasets. There are almost always discrepancies due to well mixing processes, long screened intervals causing averaging, data collected at much different times, and other causes. The larger the datasets are, the more time and cost required to correlate the datasets.

Data Visualization Requirements: Visualization of datasets is a time consuming process. All datasets must be converted to x,y,z,t coordinates which is somewhat time consuming for ERI datasets, but is generally much more time consuming for archival datasets for comparison. If a well-maintained and complete site database exists, visualization can be quite rapid, but this is not often the case in spatial and temporal coordinates.

5.2.4 Life Cycle Costs

ISCO/ERI is an in-situ process that does not require any installation or demobilization of large equipment or reactors. The major capital cost is construction of injection and monitoring wells. Pumps will be needed for sampling and other on-site real-time instruments for recording the Eh, pH, and DO of groundwater aquifer. Given the time-frame in which this project was performed, there were no major depreciation costs over the project life cycle.

6. Implementation Issues

6.1 Environmental Checklist

An injection permit is usually required for permanganate injection but given that the NOP is a Superfund site and this a research project, the State of Nebraska only required approval of the injection work plan. The ISCO work plan was approved by Nebraska's DEQ on April 17, 2007.

Other issues specific to the ISCO/ERI project was that the cuttings from the monitoring wells needed to be barreled and contained until they were analyzed by a certified EPA laboratory. If cuttings were below 1 mg RDX/kg, the cuttings were left on site or taken to the ARDC landfill. Likewise, water obtained during well installation was contained and taken to the pump and treat facility where it will be run through the GAC system.

6.2 Other Regulatory Issues

After completion of the ISCO/ERI demonstration, the performance and cost analysis will be shared with regulatory agencies such as US EPA, Army Corps of Engineers, Nebraska Department of Environmental Quality, and other agencies for information dissemination and future application of ISCO/ERI process on full-scale levels.

6.3 End-User Issues

At sites where munitions were manufactured or assembled, soil contamination has typically resulted from the once common practice of releasing explosive-tainted wastewater to drainage ditches, sumps, settling ponds, or impoundments. TNT manufacturing, for example, required large volumes of water for purification. The aqueous waste produced from this process, known as red water, has been found to contain up to 30 additional compounds besides TNT (Urbanski, 1984). Similar practices occurred at loading, packing and assembling plants, where wastewater (also known as pink water) generated during plant operations was routinely discarded outside into sumps and drainage ditches. Left untreated, surface soils laden with wastewater constituents eventually became point sources of ground water contamination. One study showed that of the numerous sites sampled, >95% contained TNT and 87% exceeded permissible ground water concentrations (Walsh et al., 1993).

The primary end-user for this innovative in-situ technology will include federal ordnance sites with explosives contaminated groundwater plumes. Currently there are 583 sites with confirmed explosive-contaminated groundwater at 82 installations nationwide. At 22 other installations, 88

additional sites are suspected of groundwater contamination with explosives and organics (Defense Environmental Network and Information Exchange, DENIX 2003).

6.4 Lessons Learned for ERI Monitoring of Injections

For future monitoring experiments, several protocol modifications can be made to improve results. The modifications are listed first as modifications to the ERI approach. Secondly, modifications to the injection and well sampling protocols are listed.

ERI Modifications:

- 1) First, semi-permanent electrodes can be installed at the surface for the duration of the experiment. While this will not improve the results dramatically, they can provide an increase in signal to noise ratio that can be important. This would have been difficult at the Mead site as part of the site was being actively farmed for soybeans, another for corn, and the remainder was actively mowed to limit the height of grasses. This can either be performed by installing graphite rods and attaching cables to them during each interval, or installing cables in shallow trenches below the depth of surface activities. If this approach is used somewhat regularly, having semi-permanent cables installed would be the more cost effective option.
- 2) All ERI monitoring should be done assuming that transient data will be the only source of monitoring data. The assumption with the experiment was that data in the resistivity domain would allow a calibration to the injection fluid. However, the most sensitive data is obtained in the transient ERI mode, and should be assumed to allow the most rapid ability to modify protocols in the event that the injection is very different to the proposed injection plan.
- 3) Third, imaging for only fluid movement should be included at the same flow rates and locations as the planned injection prior to injection of permanganate or other compounds. This was not possible with this experiment as it was designed to amend an already existing experiment. By monitoring a test of the injection system with only water and tracer, vadose zone and conservative tracer changes can be separated from the injectate signals. This can be done with or without electrical tracers such as chloride or bromide solutions depending on the setting.

Injection Modifications:

- 1) First, assume that the injectate will primarily move up into the vadose zone. This was observed during this experiment and at two additional commercial sites using this technique. If the material is to be delivered to the phreatic zone only, injection rates and monitoring should be adjusted to catch vertically upward movement of injectate.
- 2) Secondly, any monitoring system should include smaller piezometers screen lengths to ensure less fluid mixing occurs in the samples for geophysical calibration. This is often difficult as

injections are often performed on preexisting sites, but if smaller screens are an option, they should be installed based on the property distribution defined by ERI data.

3) Injection curtains should be established at lower pumping rates to control fingering. The lower head changes in the aquifer will increase injection costs by increasing delivery times, but will likely improve delivery to the zones of interest.

4) Finally, vertical gradients near injection zones need to be established to assist in predicting the movement of injectate. If piezometers are available to determine vertical gradients, they can also be used during injection to determine if significant vertical movement is occurring.

7. References

- Adam, M.L., S.D. Comfort, M.C. Morley, D.D. Snow. 2004. Remediating RDX-contaminated ground water with permanganate: Laboratory investigations for the Pantex aquifer. *J. Environ. Qual.* 33:2165-2173.
- Adam, M.L., S.D. Comfort, T.C. Zhang, and M.C. Morley. 2005. Evaluating Biodegradation as a Primary and Secondary Treatment for Removing RDX (Hexahydro-1,3,5-trinitro-1,3,5-triazine) from a Perched Aquifer. *Bioremediation Journal*, 9:9-19.
- Albano, J.A., 2009. Aquifer characterization for an ISCO treatment of a RDX-contaminated aquifer. M.S. thesis, University of Nebraska-Lincoln, Lincoln, NE
- Andrew Curtis Elmore, T. G. (2001), A Case Study of the Beneficial Reuse of Treated Groundwater, *Remediation Journal*, 11(3), 49-62.
- ASTM Standard D 7262-07. Standard Test Method for Estimating the Permanganate Natural Oxidant Demand of Soil and Aquifer Solids, ASTM International, West Conshohocken, PA, www.astm.org.
- Bouwer, H., Rice, R.C., 1976. A slug test for determining hydraulic conductivity of unconfined aquifers with completely or partially penetrating wells, *Water Resources Research*. 12 (3), 423-428.
- Cassada, D.A., S.J. Monson, D.D. Snow, and R.F. Spalding. 1999. Sensitive determination of RDX, nitroso-RDX metabolites, and other munitions in ground water by solid-phase extraction and isotope dilution liquid chromatography-atmospheric pressure electro-spray ionization mass spectrometry. *J. Chromatog. A*, 844:87-95.
- Choekejaroenrat, C., 2008. Laboratory and pilot-scale investigations of RDX treatment by permanganate. M.S. thesis, University of Nebraska-Lincoln, Lincoln, NE
- Clayton, W.S., Harris, S.T., Marvin, B.K., and Struse, A.M., 2001. In-Situ oxidation treatment of high explosives in groundwater using potassium permanganate. In proceedings of the 2001 International Containment and Remediation Technology Conference, Institute for Cooperative Environmental Research, Florida State University,
- Comfort, S.D., 2005. Remediating RDX and HMX contaminated soil and water. In M. Fingerman and R. Nagabhushanam (eds) *Bioremediation of Aquatic and Terrestrial Ecosystems*. Science Publishers, Enfield, NH. pp. 263-310.

- Condra, G. E., Reed, E.C., 1943. The geological section of Nebraska: Nebraska Geol. Survey Bull. 14, 82.
- Cronk, G., Marvin, B., 2004. "Economic Evaluation of Long-Term Pump and Treat Versus In Situ Chemical Oxidation", Remediation of Chlorinated and Recalcitrant Compounds. Ed. Gavaskar A.R. and Chen A.S.C., Proceedings of the Fourth International Conference on Remediation of Chlorinated and Recalcitrant Compounds Monterey, CA; Columbus, OH: Battelle Press.
- Daily, W., Ramirez, A., Binley, A., and D. LaBrecque, 2004. *Electrical resistance tomography*. Leading Edge 23(5):438-442.
- Defense Environmental Network and Information Exchange (DENIX). 2003. *Enhanced alternative and in situ treatment technologies for explosives in groundwater*. URL: <http://www.denix.osd.mil/denix/DOD/Policy/Army/Aerta/Report/a12a.html>.
- de Marsily, G., 1986. Quantitative Hydrogeology: Groundwater Hydrology for Engineers. Academic Press, INC., Sand Diego, CA.
- Environmental Protection Agency, 2006. Standard Test Method for Determining the Permanganate Soil Oxidant Demand (Screening Phase, PSOD-1). http://www.epa.gov/ada/research/waste/research_52.pdf
- Environmental Protection Agency. 1998. Field applications of in situ remediation technologies: chemical oxidation. EPA 5421-R-98-008. United States Environmental Protection Agency, Office of Solid Waste and Emergency Response, Technology Innovation Office. Washington, DC.
- Etnier, E. and W.R. Hartley. 1990. *Comparison of water quality criterion and lifetime health advisory for hexahydro-1,3,5-trinitro-1,3,5-triazine (RDX)*. Regulatory Toxicol. Pharmacol. 11:118-122.
- Halihan, T., and V.A. Zlotnik, 2002, Asymmetric dipole-flow test in a fractured carbonate aquifer, *Ground Water*, 40(5), 491-499.
- Halihan, T. and T. Fenstemaker, 2004. *Proprietary Electrical Resistivity Imaging Method. 2.0 ed.* Oklahoma State University Office of Intellectual Property, Stillwater, OK.
- Halihan, T., S. Paxton, I. Graham, T. Fenstemaker, and M. Riley. 2005. Post-Remediation Evaluation of a LNAPL Site Using Electrical Resistivity Imaging, *Journal of Environmental Monitoring*, v 7., p. 283-287. DOI: 10.1039/b416484a
- Haselow, J. S., Siegest, R. L., Crimi, M., and Jarosch, T., 2003. Estimating the total oxidant demand for in situ chemical oxidation design. *Remediation*. v. 13, no. 4, 5-16.

- Hundal, L.S., J. Singh, E.L. Bier, P.J. Shea, S.D. Comfort, and W.L. Powers. 1997. Removal of TNT and RDX from water and soil using iron metal. *Environ. Poll.* 97:55-64.
- IT Corporation and S.M. Stoller Corporation. 2000. *Implementation Report of Remediation Technology Screening and Treatability Testing of Possible Remediation Technologies for the Pantex Perched Aquifer*. Pantex Environmental Restoration Department, USDOE, Amarillo, TX.
- ITRC, 2001. Technical and Regulatory Guidance for In Situ Chemical Oxidation of Contaminated Soil and Groundwater. Interstate Technology and Regulatory Cooperation Work Group, June 2001.
- Kam, A. 2002. Personal communication between M. Morley (UNL) and Alvin Kam, U.S. Army Corps of Engineers, Omaha, NE,.
- Lowe, K.S., F.G. Gardner, and R.S. Siegrist. 2002. Field evaluation of In Situ chemical oxidation through vertical well-to-well recirculation of NaMnO₄. *Ground Water Mon. Rem.*, 22:106-115.
- Love, K.S., Gardner, F.G., Siegrist, R.L., and Houk, T.C., 2000. Field pilot test of in situ chemical oxidation through recirculation using vertical wells at the Portsmouth Gaseous Diffusion Plant. EPA/625/R-99/012. U.S. EPA Office of Research and Development, Washington, D.C. 20460. pages 42-49
- Mumford, K.G., Lamarche, C.S., and Thomson, N.R., 2004. Natural oxidant demand of aquifer materials using the push-pull technique. *Journal of Environmental Engineering*, v. 130, no. 10, 1139-1146.
- Nyquist, J.E., Carr, B.J., and Davis, R.K., 1999, DC Resistivity Monitoring of Potassium Permanganate Injected to Oxidize TCE In Situ: *Journal of Environmental and Engineering Geophysics*, v. 4, p. 135-147.
- Oberle, D. W., and Schroder, D. L., 2000. Design consideration for in-situ chemical oxidation, in *Proceedings of the Second International Conference on Remediation of Chlorinated and Recalcitrant Compounds*, v. C2-6., Monterey, CA: Battelle Press, Columbus, OH, 397-403.
- Piskin, R., 1971. Hydrogeology of the University of Nebraska field laboratory at Mead, Nebraska: University of Nebraska PhD Dissertation.
- Ramirez, A., W. Daily, D. LaBrecque, E. Owen and D. Chesnut. 1993. *Monitoring an Underground Steam Injection Process Using Electrical Resistance Tomography*. *Water Resources Research*. 29:73-87.

- Reynolds, J.M., 1997. *An Introduction To Applied And Environmental Geophysics*, John Wiley, Chichester, New York, 796 p.
- Riley, C. (1997) Milan Army Ammunition Plant Operable Unit One, Performance Evaluation of the Groundwater Treatment System, Draft Document. ICF Kaiser Engineers, Report #SAV-04-001 for U.S. Army Corps of Engineers, Contract #DADA21-96-D-0010, Delivery Order 0004.
- Schnarr M., Truax C., Farquhar G., Hood E., Gonullu T., and Stickney B., 1998. Laboratory and controlled field experiments using potassium permanganate to remediate trichloroethylene and perchloroethylene DNAPLs in porous media. *Journal of Contaminant Hydrology*, v. 29, iss. 3, 205-224.
- Schuett, E. C., Jr., 1964. Petrology and the water mineral relationship of two Quaternary fills in eastern Nebraska: University of Nebraska, M. S. Thesis.
- Schroth, M. H., Oostrom, M., Wietsma, T. W., and Istok, J. D., 2001. In-situ oxidation of trichloroethene by permanganate: effects on porous medium hydraulic properties. *Journal of Contaminant Hydrology*, v. 50, 79-98.
- Seol, Y., Zhang, H., and Schwatz, F. W., 2003. A review of in situ chemical oxidation and heterogeneity. *Environmental and Engineering Geoscience*, v. 9, 1, 37-49.
- Siegrist, R. L., Urynowicz, M. A., West, O.R., Crimi, M. L., and Lowe, K. S., 2001 *Principles and practices of in situ chemical oxidation using permanganate*. Battelle Press, Columbus, OH.
- Siegrist, R. L., Urynowicz, M. A., Crimi, M. L., and Lowe, K. S., 2002. Genesis and effects of particles produced during in situ chemical oxidation using permanganate. *Journal of Environmental Engineering*, v.128, 11, 1068-1079.
- Sima, A. M., Halihan, T., Thompson, K., Fox, G., and Storm, D., 2008. Transient Electrical Resistivity Imaging of a Tracer Test, Tahlequah, OK, GSA South-Central Sectional Meeting, Hot Springs, AK, April 2008, Geological Society of America *Abstracts with Programs*, Vol. 40, No. 3, p. 7.
- Simmons, C.T., T. R. Fenstermaker, and J.M. Sharp. 2001. Variable-density groundwater flow and solute transport in heterogeneous porous media: approaches, resolutions and future challenges. *J. Contamin. Hydrol.* 52:245-275.
- Singha, K. and Gorelick, S.M. 2006a. *Hydrogeophysical tracking of 3D tracer migration: the concept and application of apparent petrophysical relations*. *Water Resources Research*, 42, W06422, doi:10.1029/2005WR004568.

- Singha, K. and Gorelick, S.M. 2006b. *Effects of spatially variable resolution on field-scale estimates of tracer concentration from electrical inversions using Archie's law*. *Geophysics*, 71(3), p. G83-G91.
- Souders, V.L., 1967, Availability of water in Saunders County, Nebraska, USGS Hydrologic Investigations, Atlas HA-266
- Stanley, K. O., 1971. The tectonic implications of Cenozoic gravel dispersal, Nebraska and adjoining Wyoming: North-Central Section Fifth Annual Meeting, Geol. Soc. Am. Abstr., V. 3, 280.
- Stollar, R.L. and P. Roux. 1975. *Earth resistivity surveys--a method for defining ground-water contamination*. *Ground Water* 13:145-150.
- Struse, A.M., Siegrist, R.L., Dawson, H.E., and Urynowicz, M.A., 2002. Diffusive transport of permanganate during in situ oxidation. *Journal of Environmental Engineering*, v. 128, no. 4, 327-334.
- Struse, A.M., Siegrist, R.L., 2000. Permanganate transport and matrix interactions in silty clay soils. Chemical Oxidation and Reactive Barriers. Ed Wickramanayake, G.B., Gavaskar A.R., and Chen, A.S.C., Columbus, OH, Battelle Press.
- Telford, W.M., Geldart, L.P., and Sheriff, R.E., 1990, *Applied Geophysics, 2nd Edition*, Cambridge University Press, Cambridge.
- Urbanski, T. 1984. *Chemistry and technology of explosives*. Pergamon Press, Oxford.
- U.S. Army Corps of Engineers, 1989, Former Nebraska Ordnance Works, Confirmation study, V. 1, Report and appendices A & B, April 1989.
- U.S. Army Corps of Engineers, 2007. 2007 Groundwater Monitoring Program, Operable Unit No. 2, Former Nebraska Ordnance Plant – Mead, NE.
- U.S. DOE. 1999. In situ chemical oxidation using potassium permanganate. United States Department of Energy, DOE/EM-0496.
- U.S. EPA. 1995. EPA Superfund Record of Decision: Nebraska Ordnance Plant (Former)/ EPA ID NE6211890011/ OU 01/ Mead NE. EPA/ROD/R07-95/083.
- Vance, D.B., 2002. A review of chemical oxidation technology. Available from <http://2the4.net/html/chemoxwp.htm>. November, 2004.
- Van Nostrand, R.G. and K.L. Cook. 1966. *Interpretation of Resistivity Data*. U.S. Geological Survey Professional Paper 499. 310pp.

- Walsh, M.E., T.F. Jenkins, P.S. Schnitker, J.W. Elwell, and M.H. Stutz. 1993. USA Cold Regions Research and Engineering Laboratory CRREL Special Report 93-5. Hanover, NH. pp. 1-17.
- Wani, A.H., Wade, R., Davis, J.L., 2007. Field demonstration of biologically active zone enhancement using acetate as a sole carbon source for in situ reductive transformation of RDX in groundwater. *Practical Periodical of Hazardous, Toxic, and Radioactive Waste Management*. V. 11, No.2, 83-91.
- Webb, G., S.W. Tyler, J. Collord, D. Van Zyl, T. Halihan, J. Turrentine, and T. Fenstermaker, *in press*, Field Scale Analysis of Flow Mechanisms in Highly Heterogeneous Mining Media, *Vadose Zone Journal*.
- Weeks, K.R., Veenstra, S.C., Hill, D.L., and Gregson, B.P., 2003. A study of treatment options to remediate explosives and perchlorate in soils and groundwater at Camp Edwards, Massachusetts. *Remediation Journal*. V. 13, is. 2, 131-143.
- West, O.R., Cline, S.R., Holden, W.L., Gardner, F.G., Schlosser, B.M., Thate, J.E., Pickering, D.A., and Houk, T.C., 1998. A field-scale demonstration of in situ chemical oxidation through recirculation at the X-701B site. Oak Ridge National Laboratory Report, ORNL/TM-13556.
- West, O.R., Siegrist, R.L., Cline, S.R. and Gardner, F. G., 2000. The effects of in situ chemical oxidation through recirculation (ISCOR) on aquifer contamination, hydrogeology, and geochemistry. Oak Ridge national Laboratory, Internal report submitted to the Department of Energy, Office of Environmental Management, Subsurface Contaminants Focus Area.
- Woodward-Clyde, 1995. Engineering evaluation/cost analysis for operable unit No. 2 (groundwater) former Nebraska Ordnance Plant, Mead, Nebraska DACA 41-92-C-0023. Prepared for the Department of the Army, U.S. Army Engineers District, Kansas City District, Corps of Engineers, Kansas City, Missouri, May, 1995.
- Yan, Y.E., and Schwatz, F.W., 1999. Oxidative degradation and kinetics of chlorinated ethenes by potassium permanganate. *J. Contaminant Hydrol.*, v. 37., 343-365.
- Zlotnik, V.A., and McGuire, V.L., 1998, Multi-level slug tests in highly permeable formations: 1. Modification of the Springer-Gelhar (SG) model, *J. of Hydrology*, v. 204, 271-282.
- Zlotnik, V.A., and McGuire, V.L., 1998. *Multi-level slug tests in highly permeable formations: 2. Hydraulic conductivity identification, method verification, and field applications*, *J. of Hydrology.*, 204:283-296.

- Zlotnik, V. and G. Ledder, 1993, Groundwater velocity in an unconfined aquifer with rectangular areal recharge. *Water Resources Research*, v.29, no. 8, 2827-2834.
- Zlotnik, V.A., and B.R. Zurbuchen, 1998, Dipole probe: design and field applications of a single-borehole device for measurements of vertical variations of hydraulic conductivity, *Ground Water*, 36(6), 884-893.
- Zlotnik, V.A. and B.R. Zurbuchen, 2003, Field study of hydraulic conductivity in a heterogeneous aquifer: Comparison of single-borehole measurements using different instruments. *Water Resour. Res.*, 39(4), doi: 10.1029/2002WR001415.
- Zurbuchen, B.R., V.A. Zlotnik, J.J. Butler, Jr., 2002, Dynamic interpretation of slug tests in highly permeable aquifers, *Water Resour. Res.* v 38 (3), DOI 10.1029/20001WR00354, 17.

8. Points of Contact

POINT OF CONTACT	ORGANIZATION Name/Address	Phone/Fax/email	Role in Project
Steve Comfort	School of Natural Resources University of Nebraska 256 Keim Hall Lincoln, NE 68583-0915	402-472-1502 402-472-7904 scomfort@unl.edu	PI
Todd Halihan	School of Geology Oklahoma State University 105 Noble Research Center Stillwater, OK	405-744-6358 405-744-7841 todd.halihan@okstate.edu	Co-PI
Vitaly Zlotnik	Geosciences University of Nebraska 318 Bessey Hall Lincoln, NE 68502-0340	402-472-2495 402-472-4917 vzlotnik1@unl.edu	Co-PI
Mark Burbach	School of Natural Resources University of Nebraska 512 Hardin Hall Lincoln, NE 68583-0995	402-472-8210 402-472-2946 mburbach@unl.edu	Co-PI
Jeff Albano	School of Natural Resources University of Nebraska 255Keim Hall Lincoln, NE 68583-0915	402-730-9170 402-472-7904 albanoj@gmail.com	Graduate Student
Chanat Chokejaroenrat	School of Natural Resources University of Nebraska 255 Keim Hall Lincoln, NE 68583-0915	402-326-8661 402-472-7904 chanatunl@gmail.com	Graduate Student
Wilson Clayton	Aquifer Solutions, Inc. 29025A Upper Bear Creek Rd. Evergreen, CO 80439	303-679-3143 ext#11 303-679-3269 wclayton@ aquifersolutions.com	Contractor
Bruce Marvin	Aquifer Solutions, Inc. 950 Gilman Street, Suite 101B Berkeley, California 94710-1462	510-525-4440 ext #1 510-525-4474 bmarvin@ aquifersolutions.com	Contractor

APPENDICES

Appendix E: ERI 2D and 3D Data

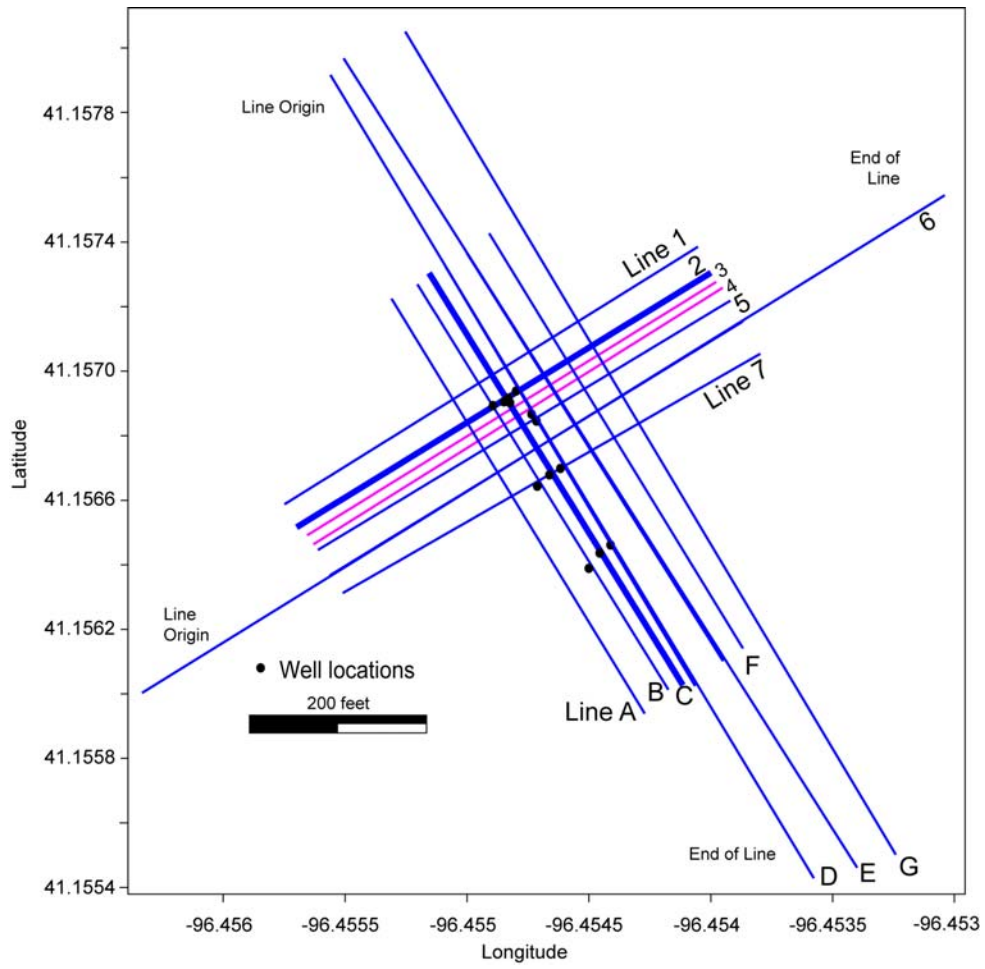


Figure E1. Orientation of ERI datasets at BAZE site.

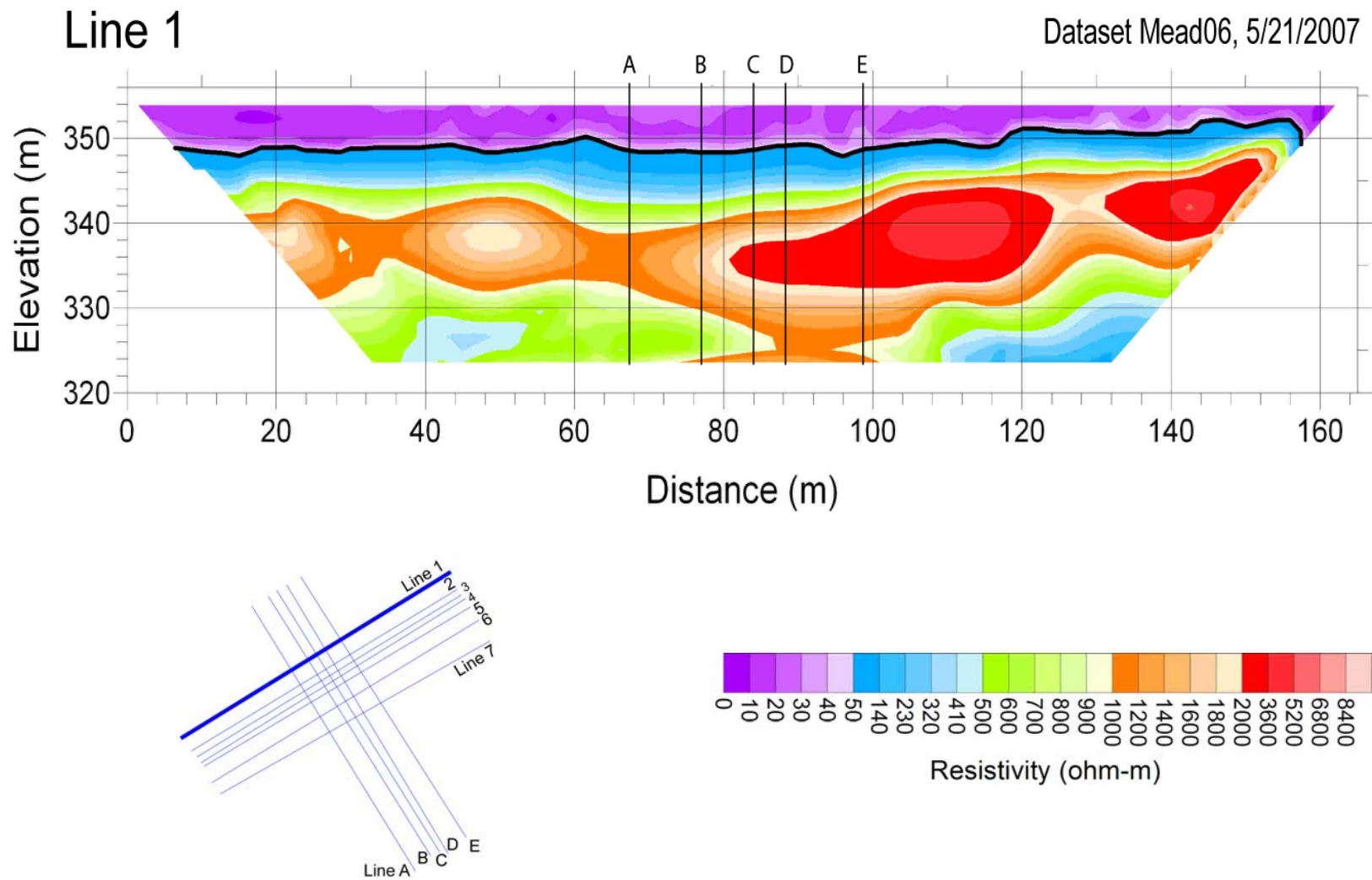


Figure E2. 2D ERI pseudosection of ERI line 1 with location of wells (if present) on the line. The location of crossing lines are indicated with black vertical lines.

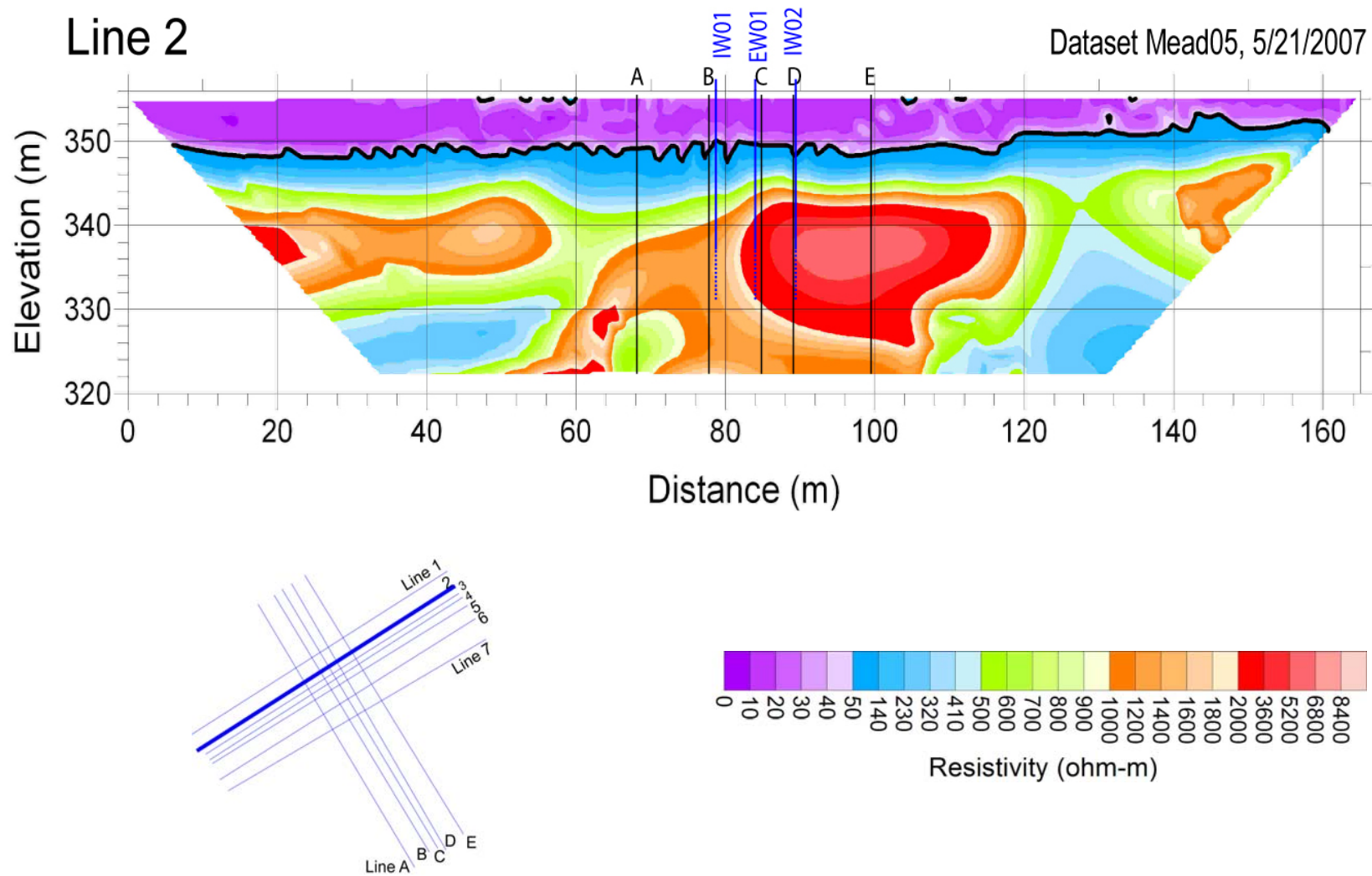


Figure E3. 2D ERI pseudosection of ERI line 2 with location of wells (if present) on the line. The location of crossing lines are indicated with black vertical lines.

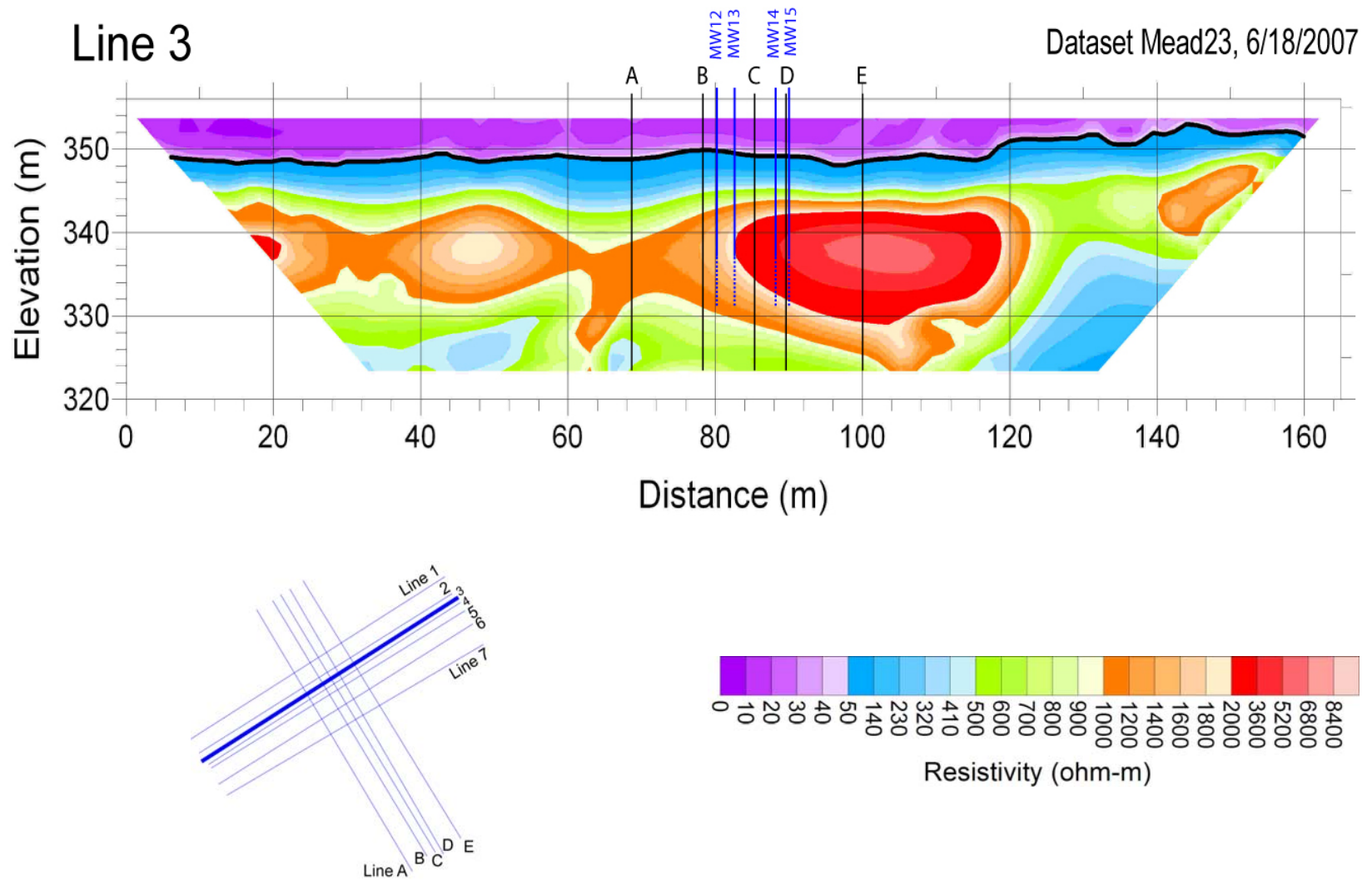


Figure E4. 2D ERI pseudosection of ERI line 3 with location of wells (if present) on the line. The location of crossing lines are indicated with black vertical lines.

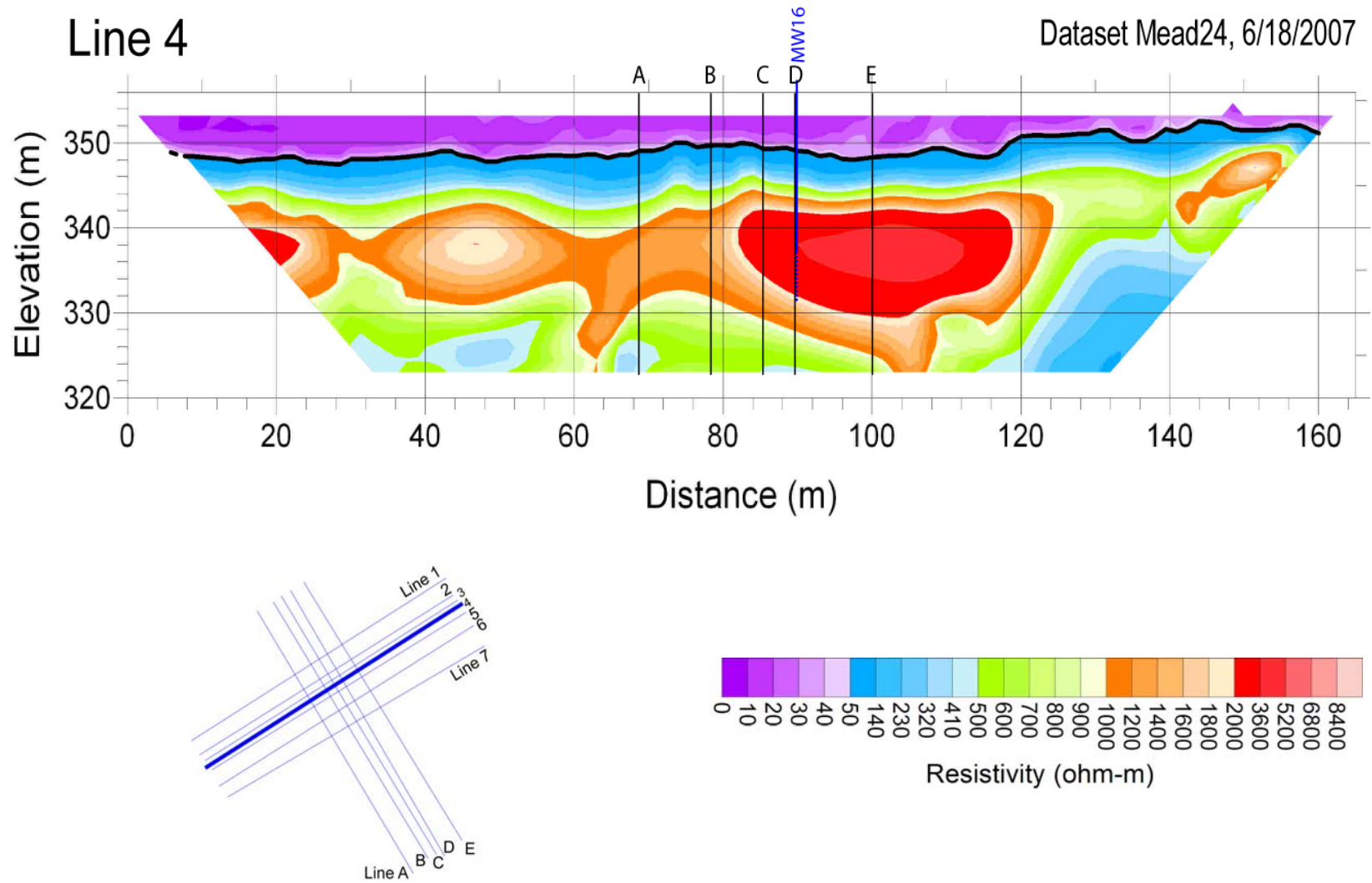


Figure E5. 2D ERI pseudosection of ERI line 4 with location of wells (if present) on the line. The location of crossing lines are indicated with black vertical lines.

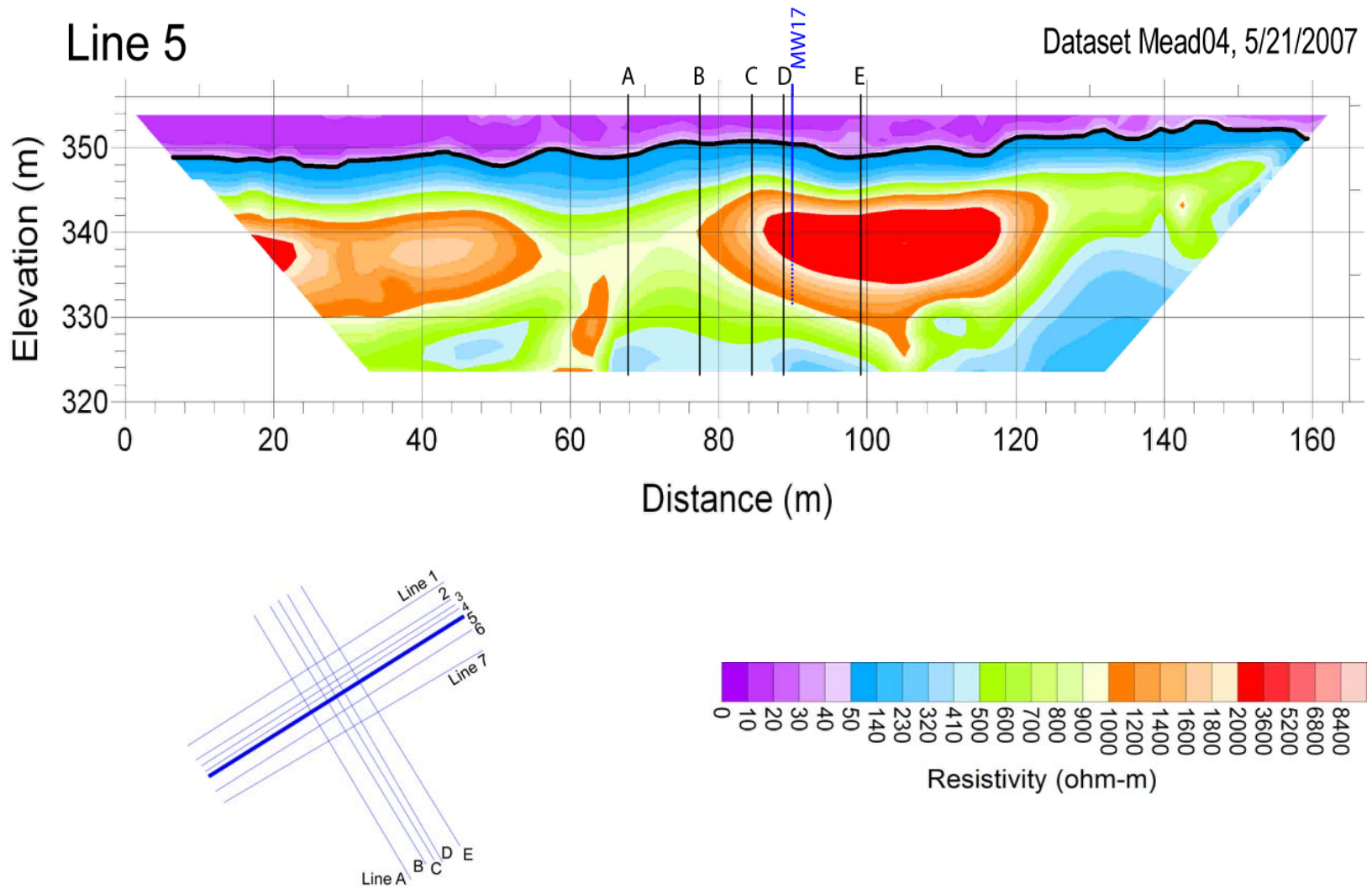


Figure E6. 2D ERI pseudosection of ERI line 5 with location of wells (if present) on the line. The location of crossing lines are indicated with black vertical lines.

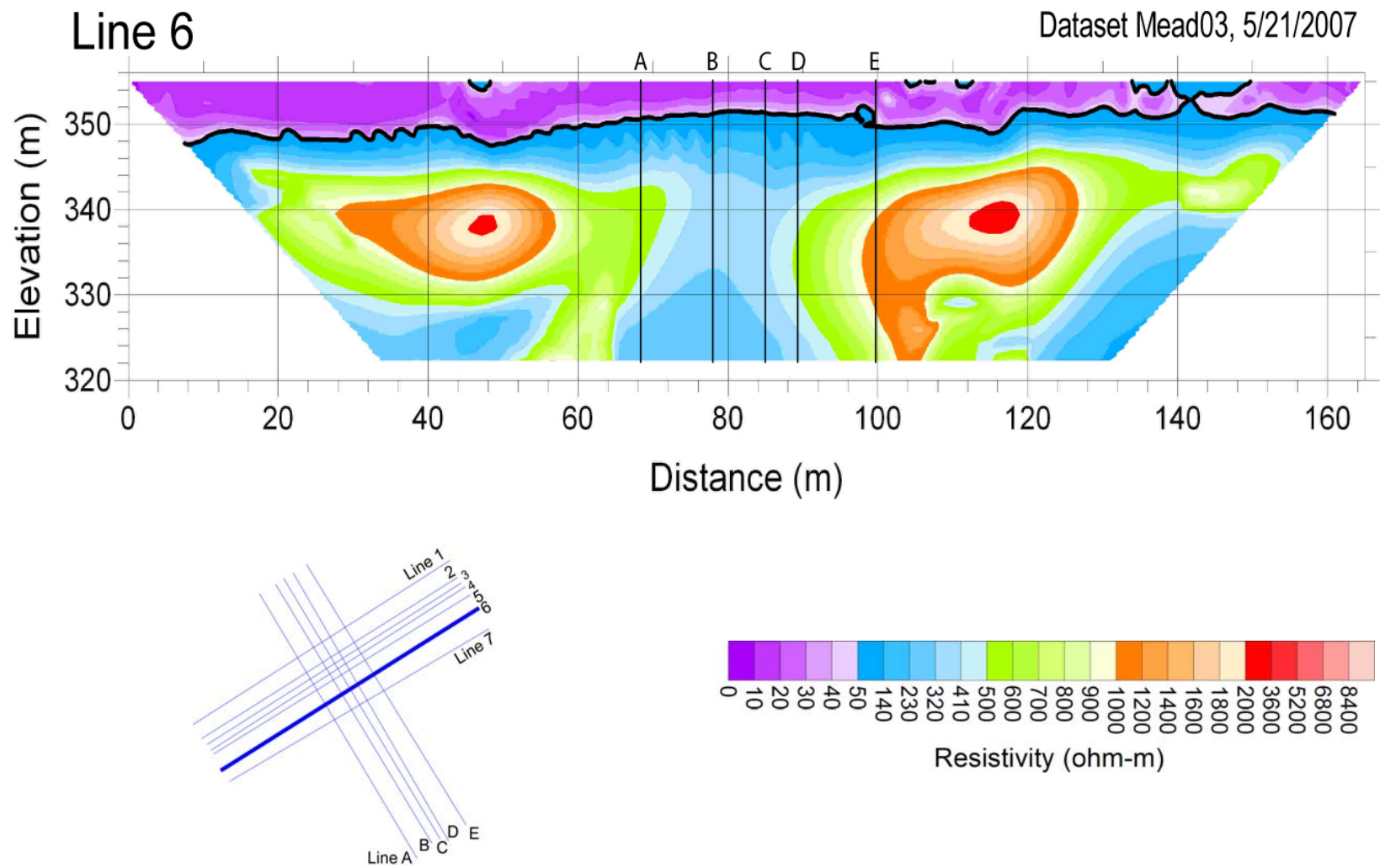


Figure E7. 2D ERI pseudosection of ERI line 6 with location of wells (if present) on the line. The location of crossing lines are indicated with black vertical lines.

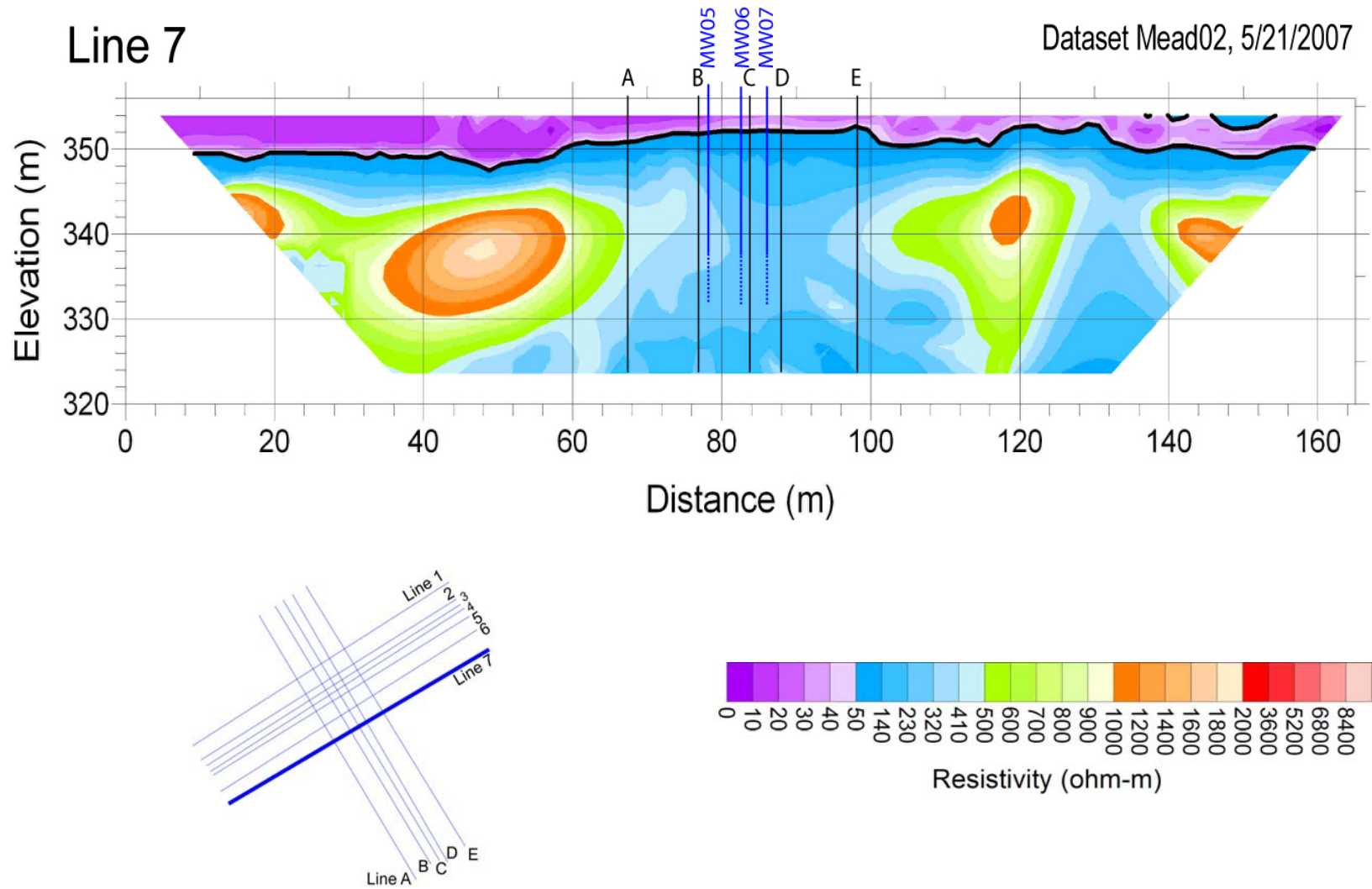


Figure E8. 2D ERI pseudosection of ERI line 7 with location of wells (if present) on the line. The location of crossing lines are indicated with black vertical lines.

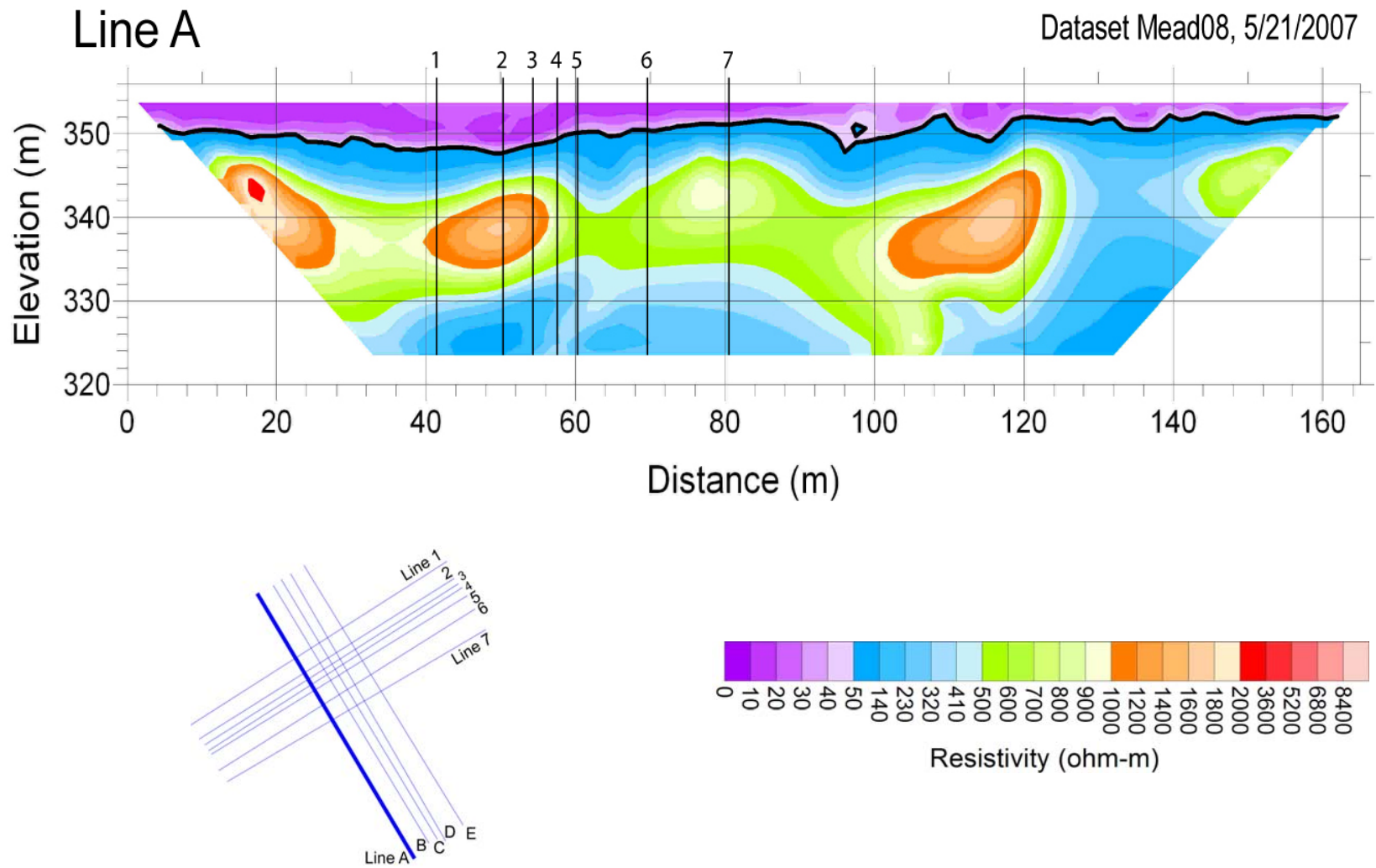


Figure E9. 2D ERI pseudosection of ERI line A with location of wells (if present) on the line. The location of crossing lines are indicated with black vertical lines.

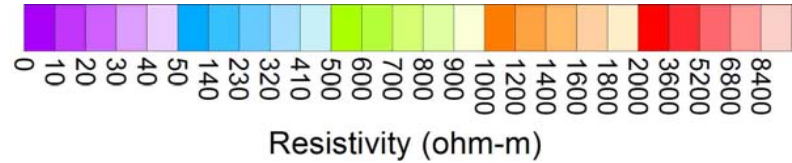
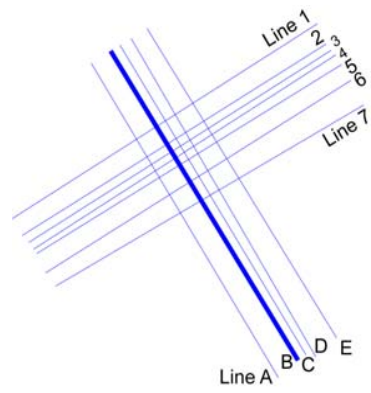
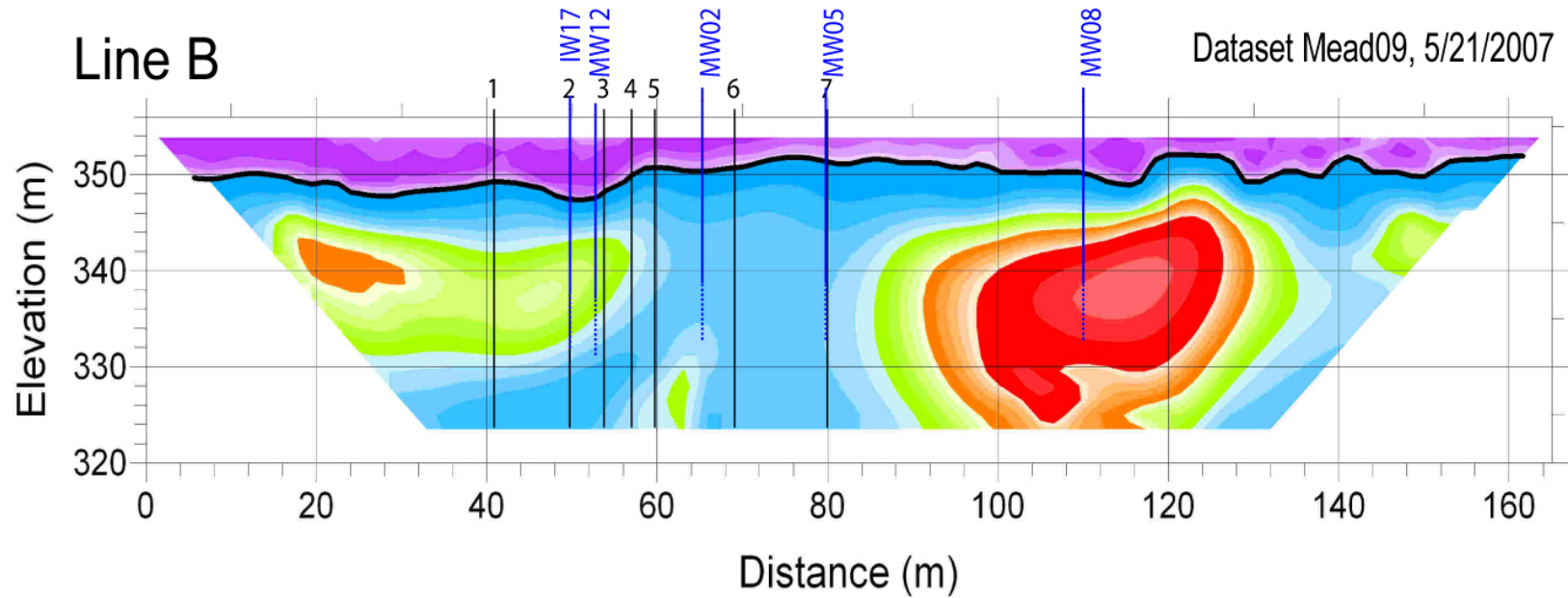


Figure E10. 2D ERI pseudosection of ERI line B with location of wells (if present) on the line. The location of crossing lines are indicated with black vertical lines.

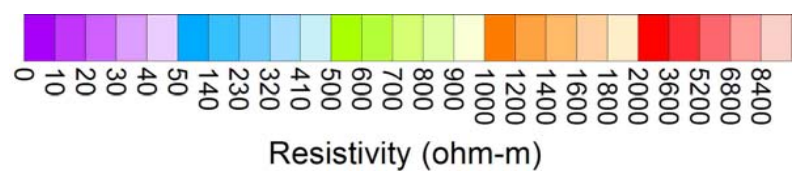
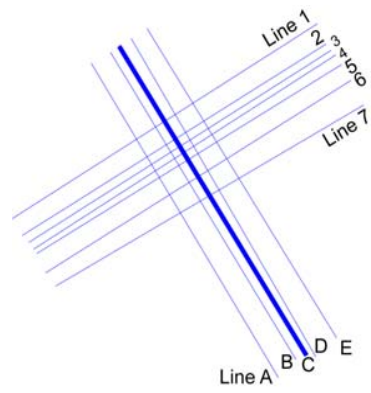
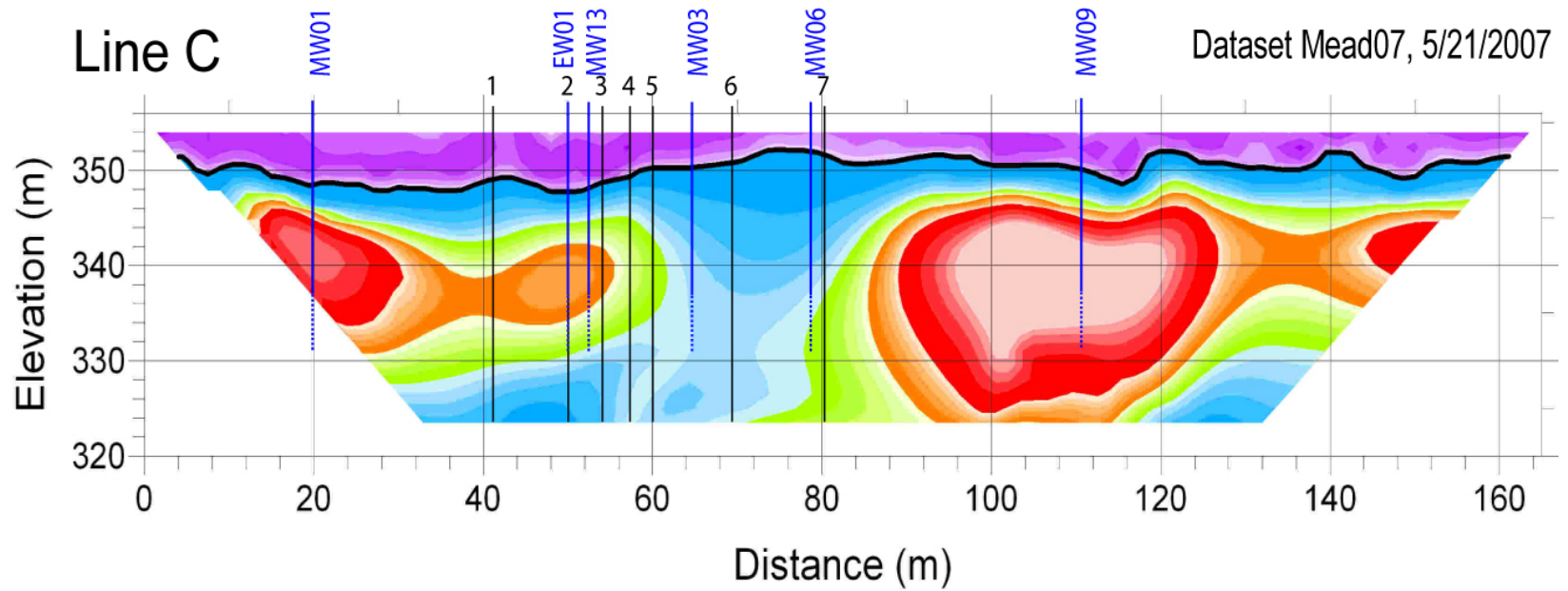


Figure E11. 2D ERI pseudosection of ERI line C with location of wells (if present) on the line. The location of crossing lines are indicated with black vertical lines.

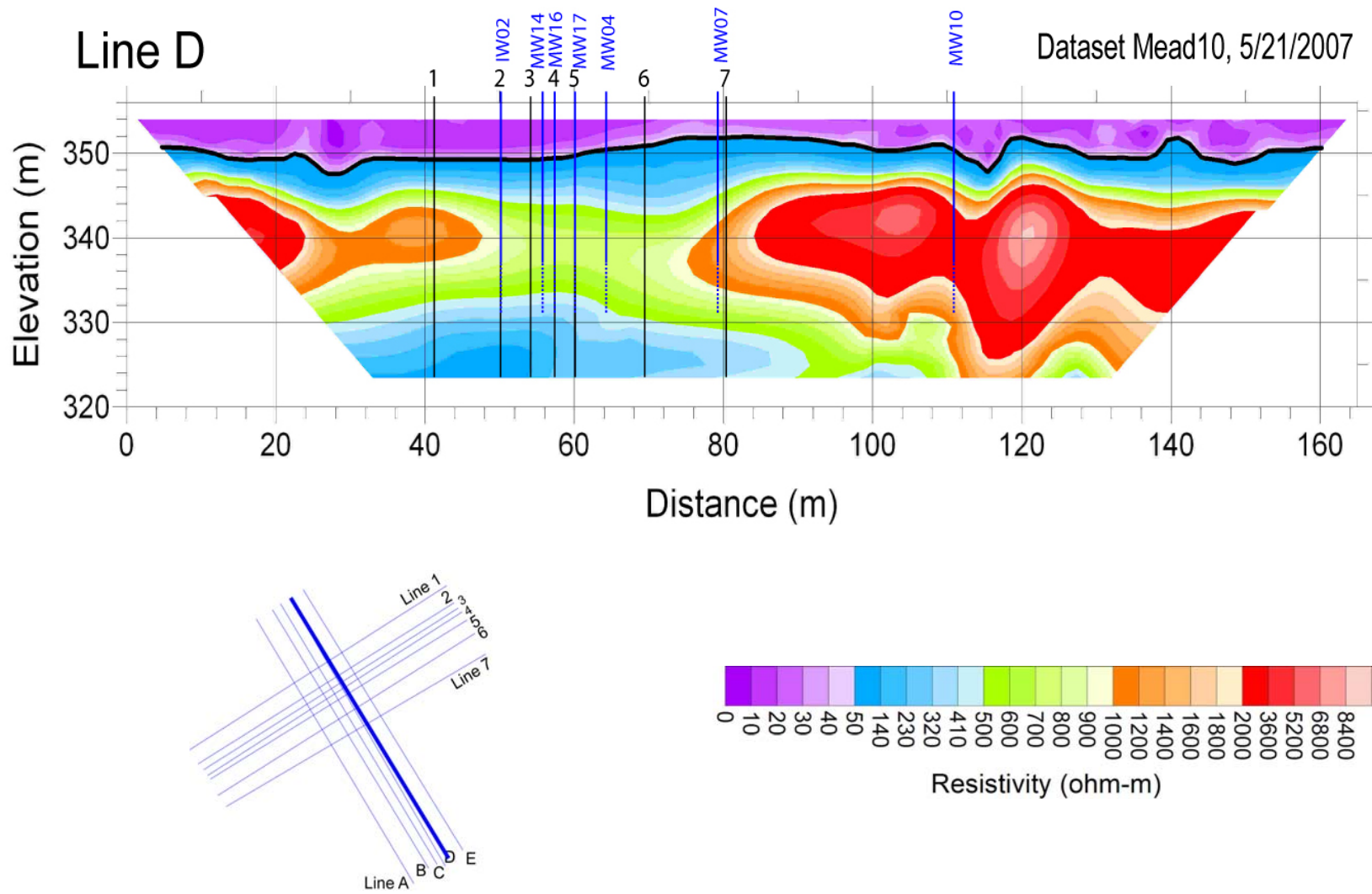


Figure E12. 2D ERI pseudosection of ERI line D with location of wells (if present) on the line. The location of crossing lines are indicated with black vertical lines.

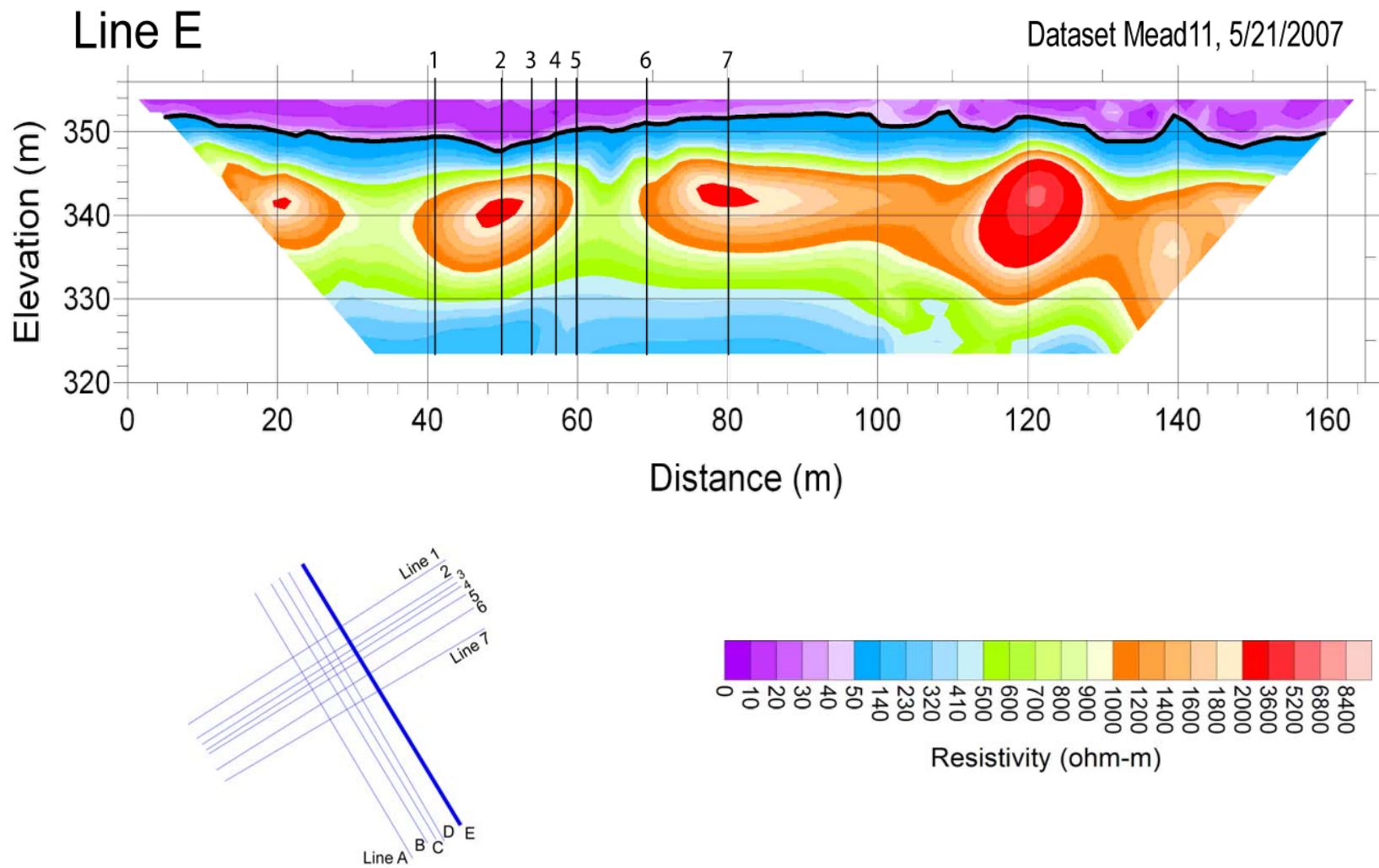


Figure E13. 2D ERI pseudosection of ERI line E with location of wells (if present) on the line. The location of crossing lines are indicated with black vertical lines.

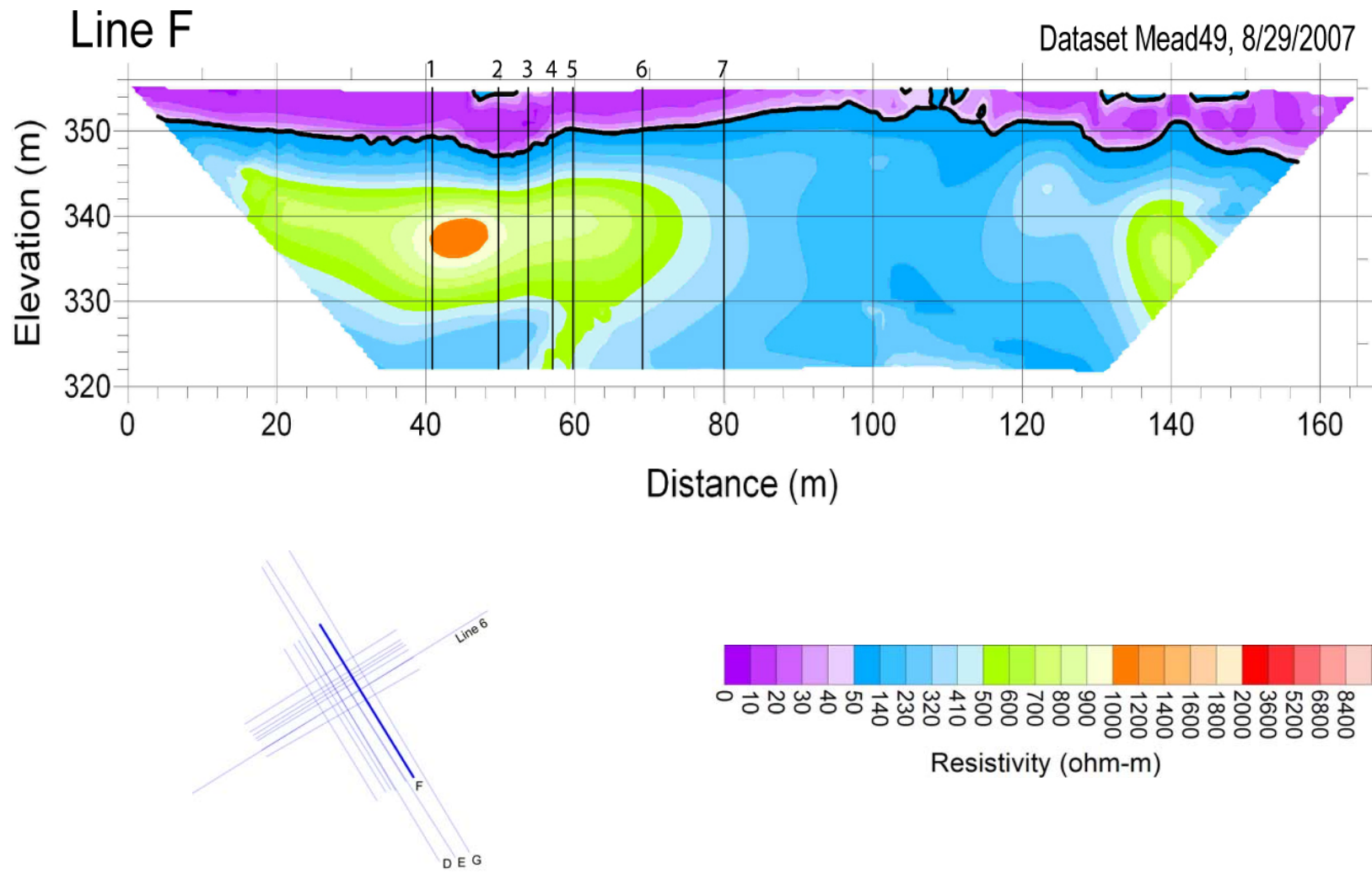


Figure E14. 2D ERI pseudosection of ERI line F with location of wells (if present) on the line. The location of crossing lines are indicated with black vertical lines.

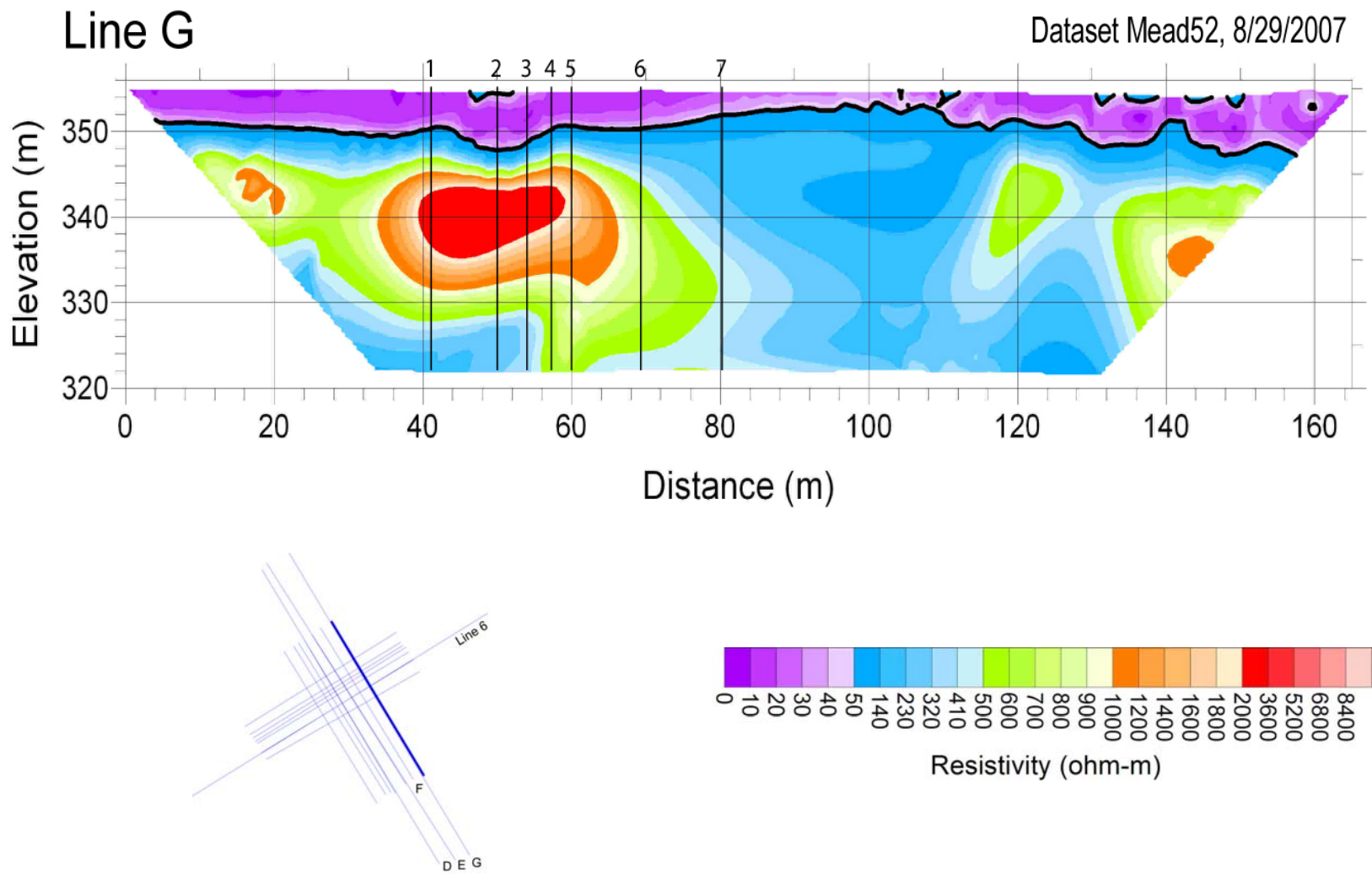


Figure E15. 2D ERI pseudosection of ERI line G with location of wells (if present) on the line. The location of crossing lines are indicated with black vertical lines.

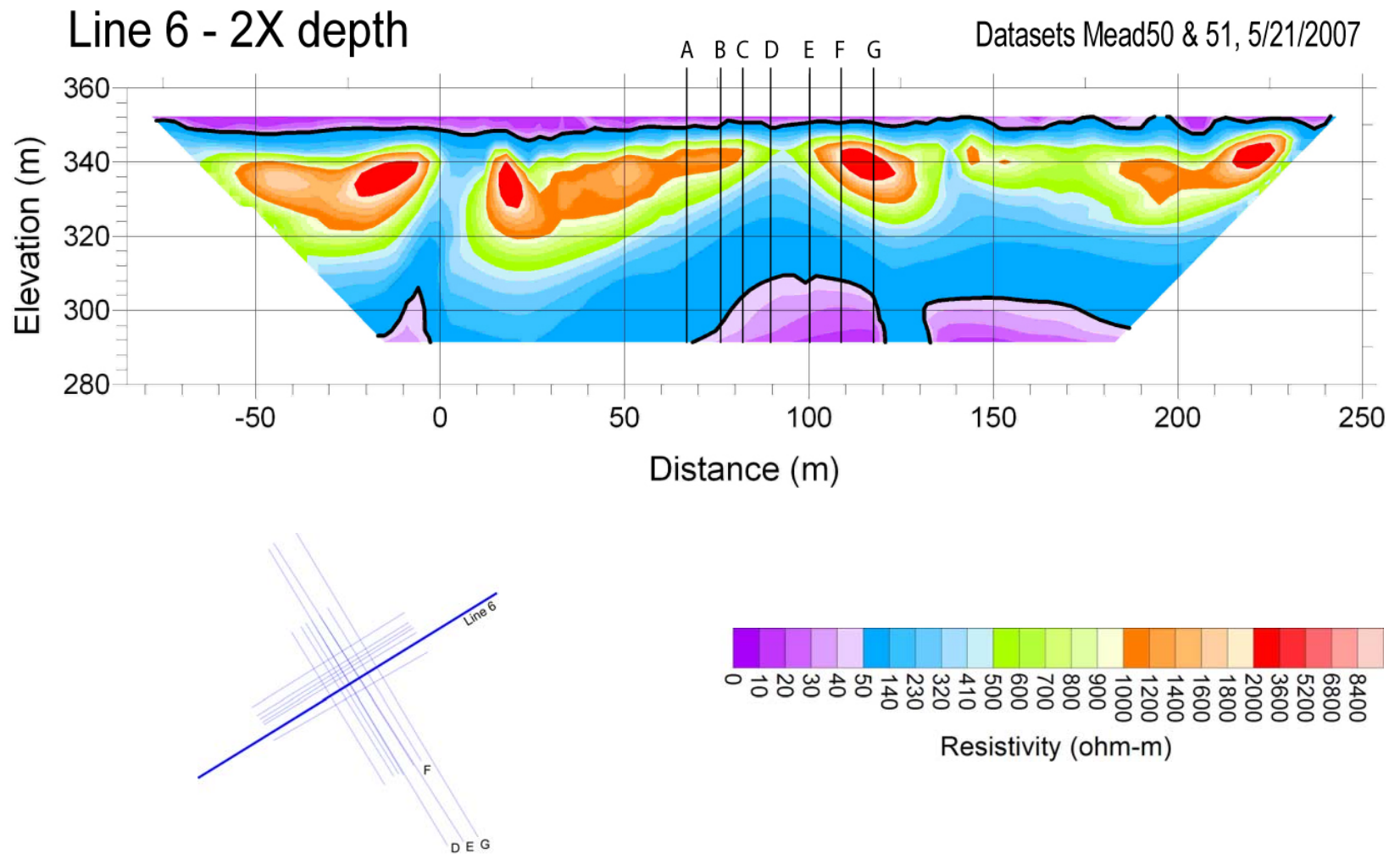


Figure E16. Six-meter 2D ERI pseudosection of ERI line 6 with location of wells (if present) on the line. The location of crossing lines are indicated with black vertical lines.

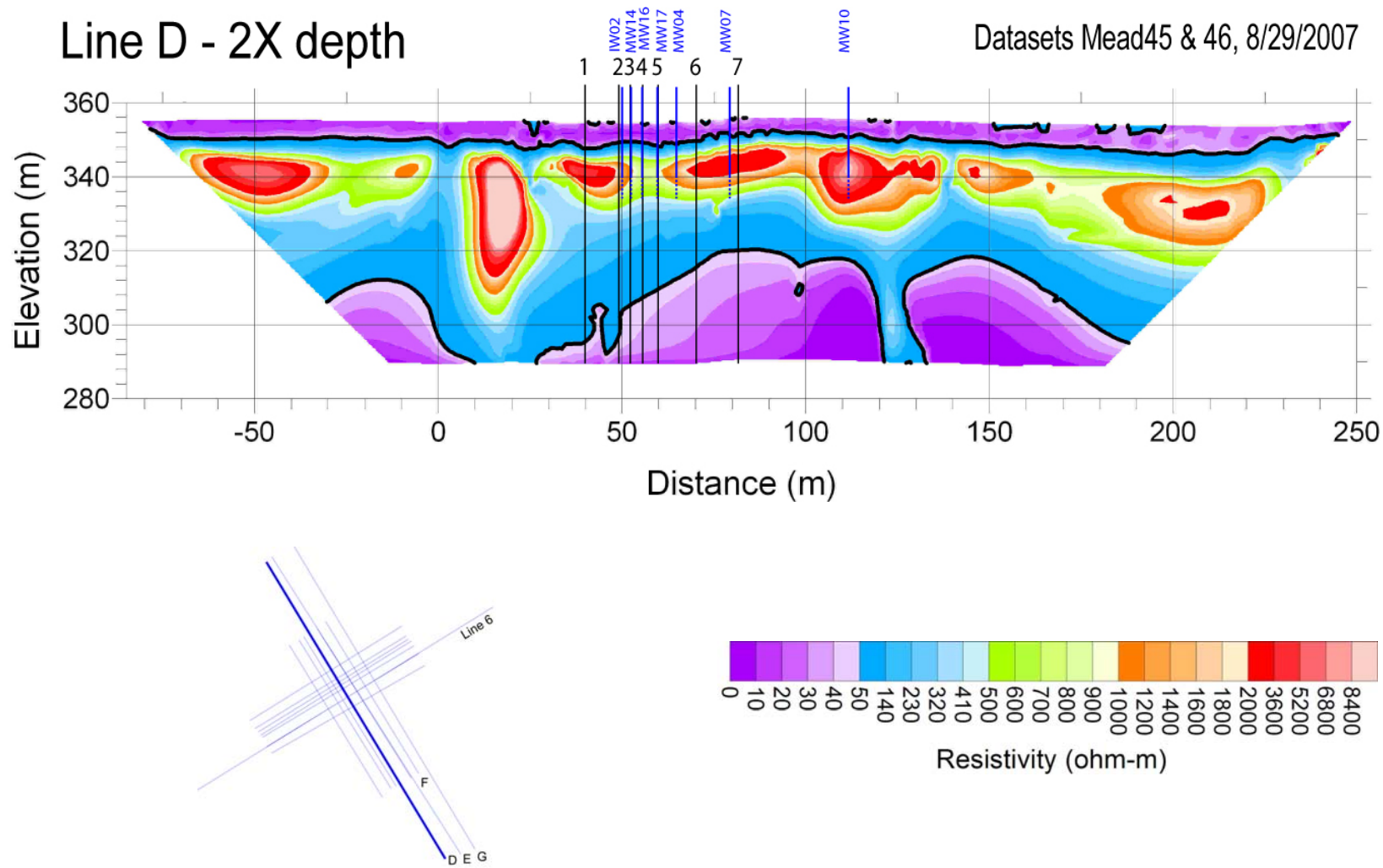


Figure E17. Six-meter 2D ERI pseudosection of ERI line D with location of wells (if present) on the line. The location of crossing lines are indicated with black vertical lines.

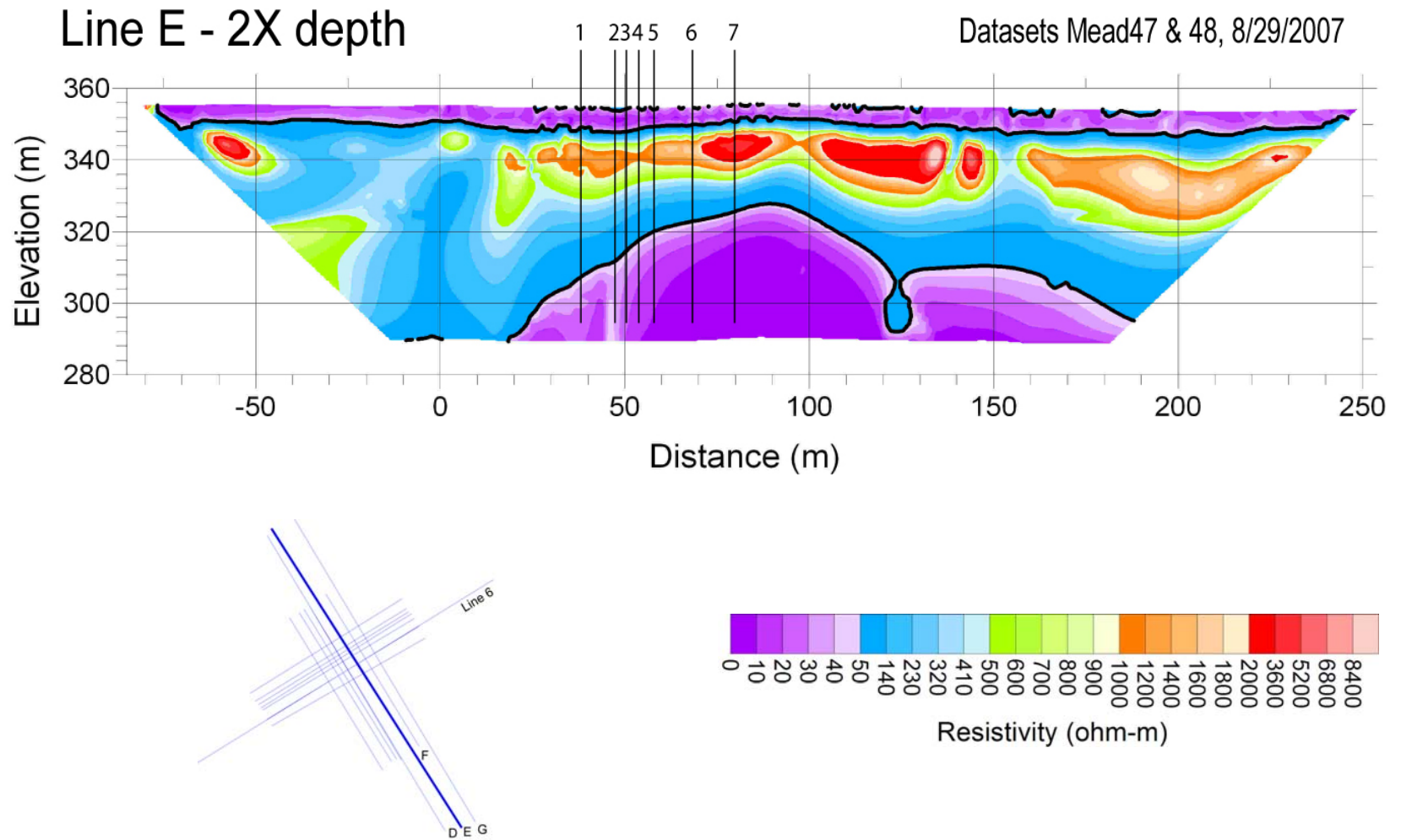


Figure E18. Six-meter 2D ERI pseudosection of ERI line E with location of wells (if present) on the line. The location of crossing lines are indicated with black vertical lines.

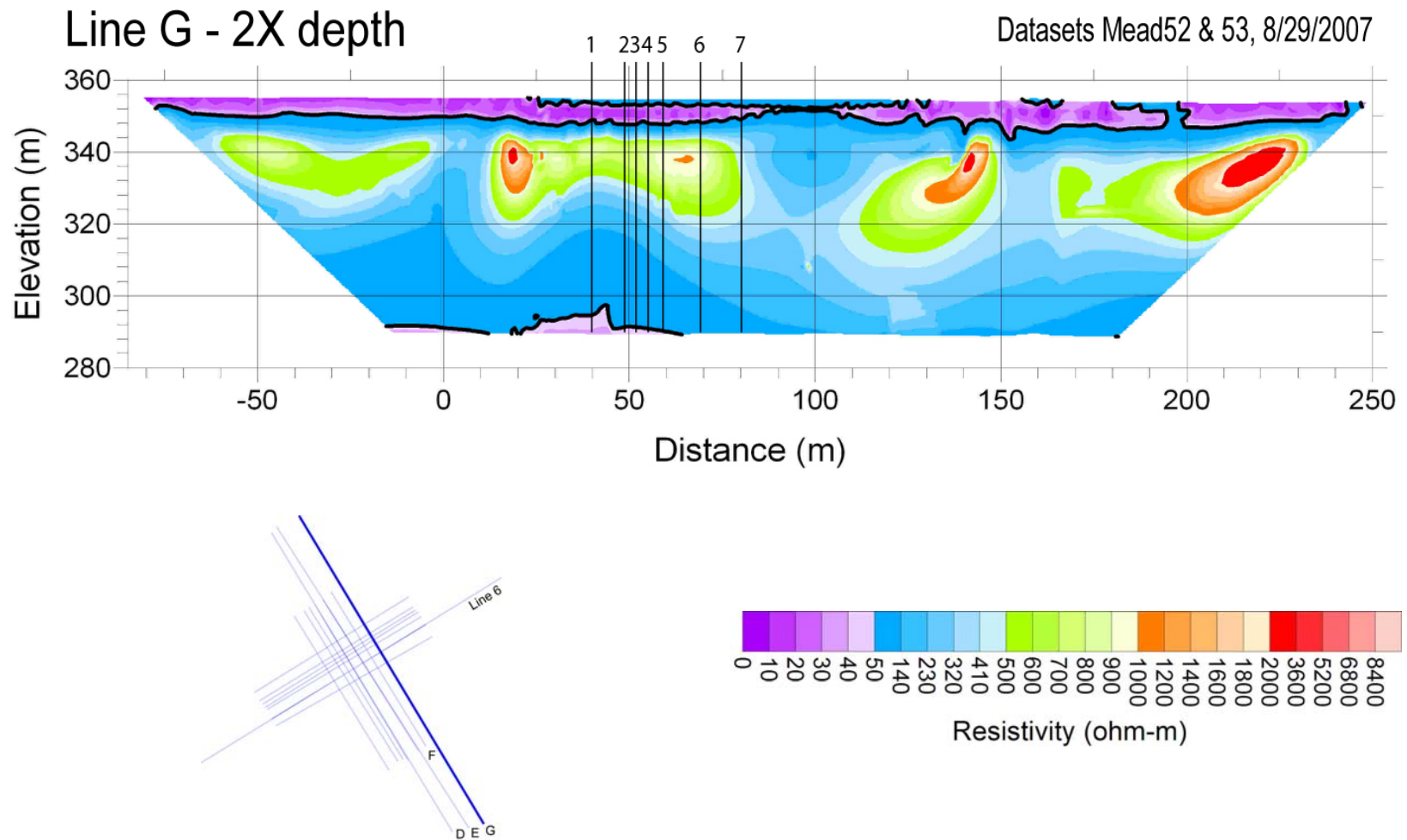


Figure E19. Six-meter 2D ERI pseudosection of ERI line G with location of wells (if present) on the line. The location of crossing lines are indicated with black vertical lines.

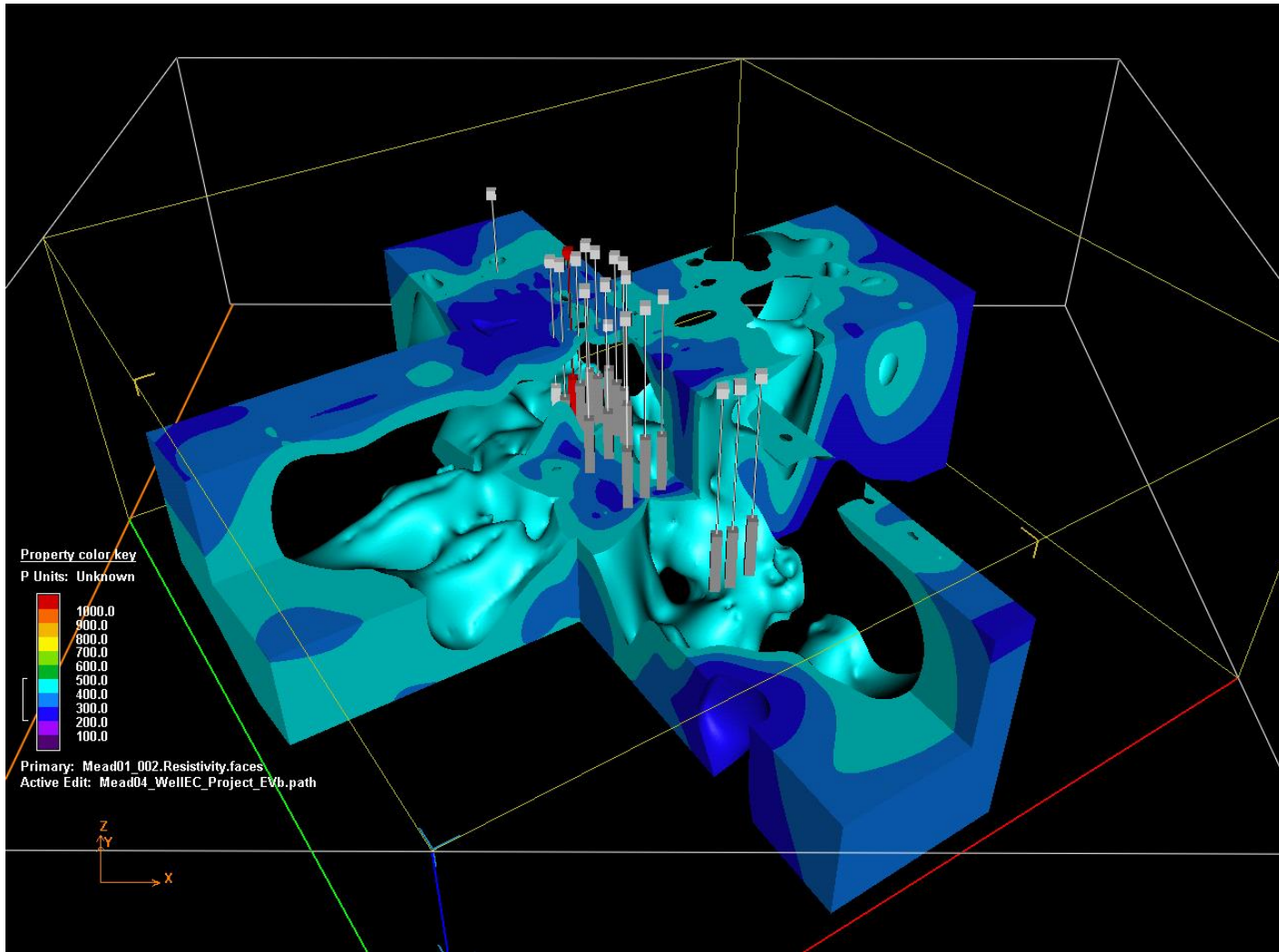
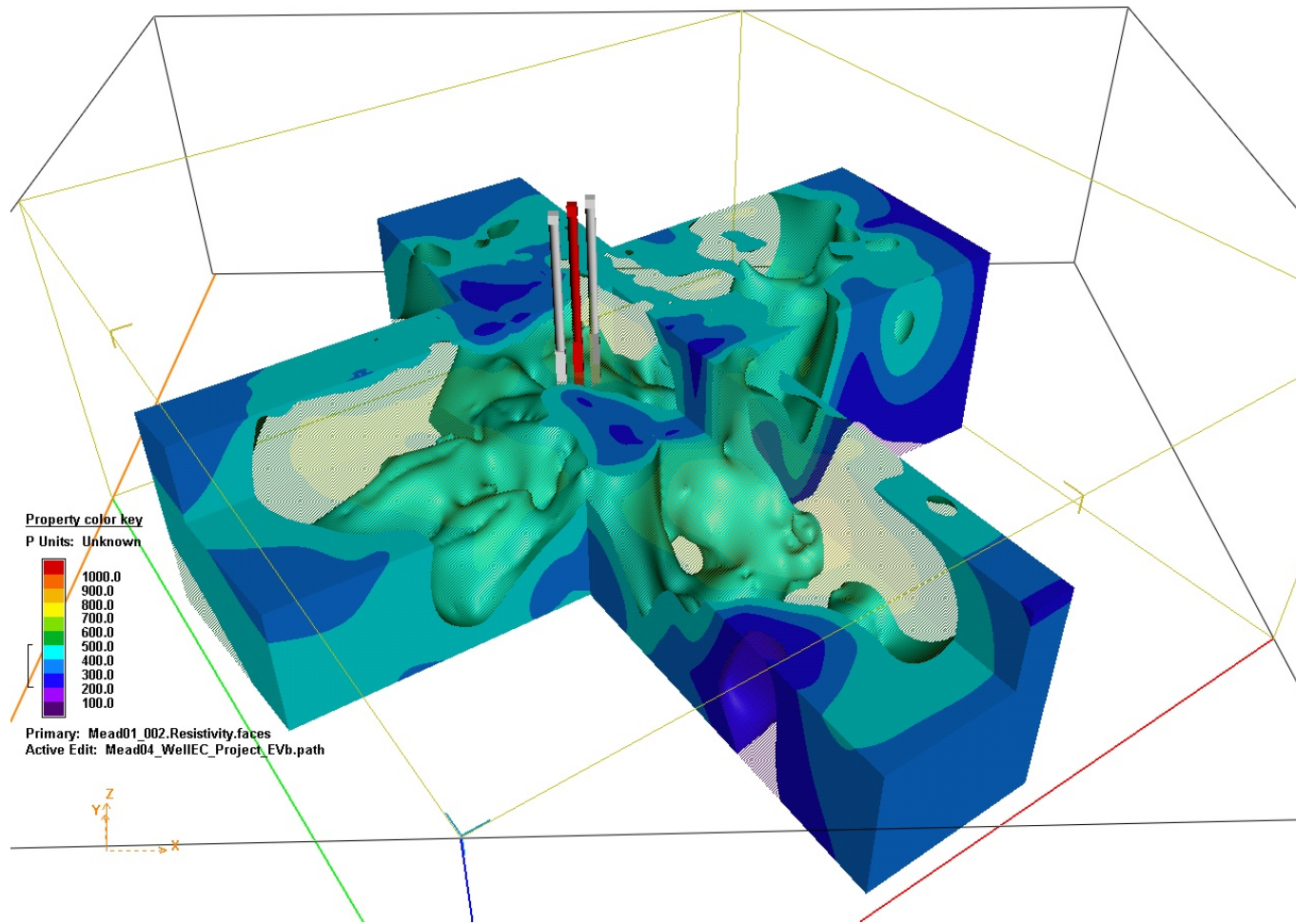
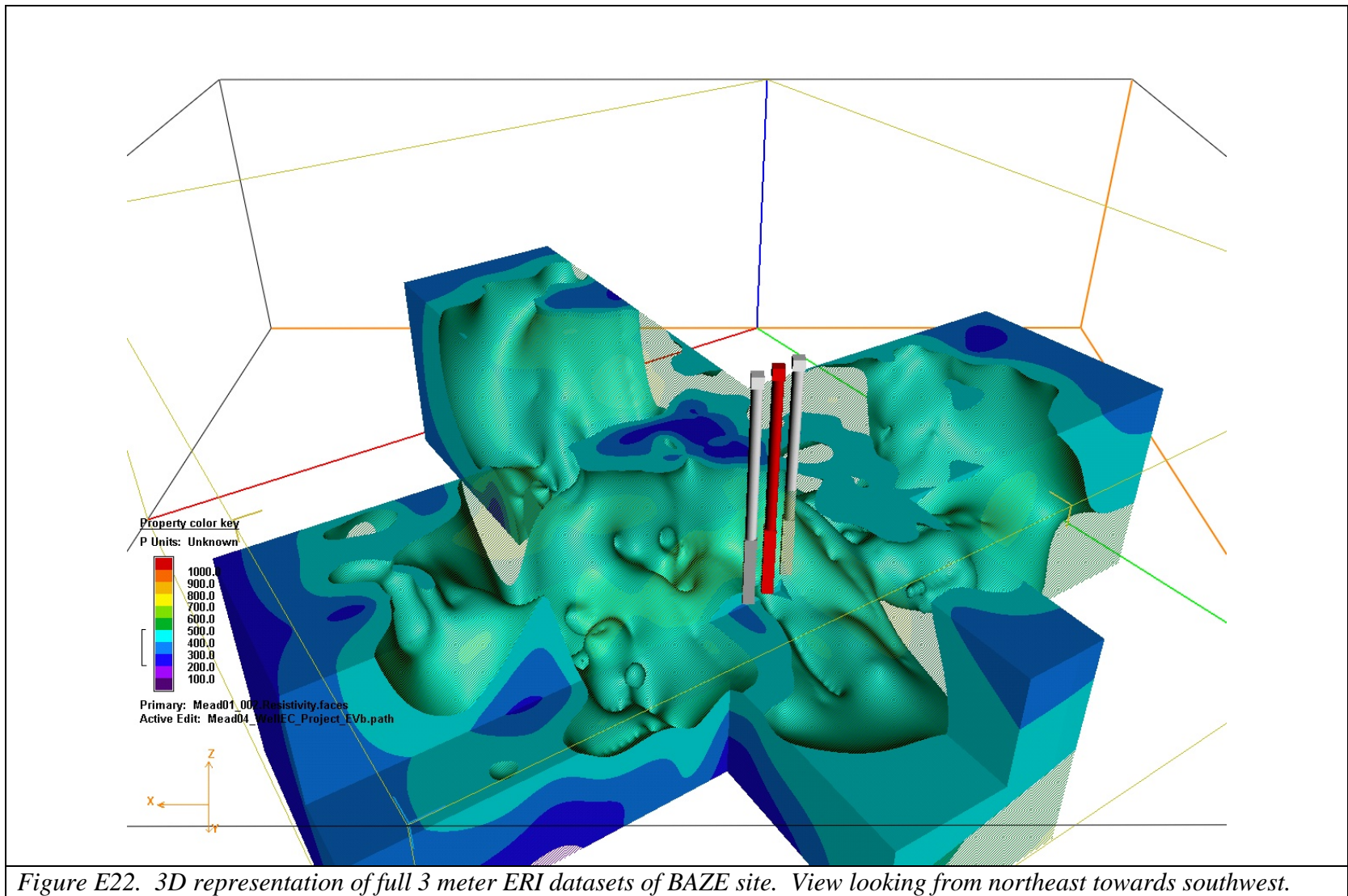


Figure E20. 3D representation of full 3 meter ERI datasets of BAZE site. Transparent areas are interpreted to correspond to areas of higher hydraulic conductivity and thus preferential pathways for the injection.





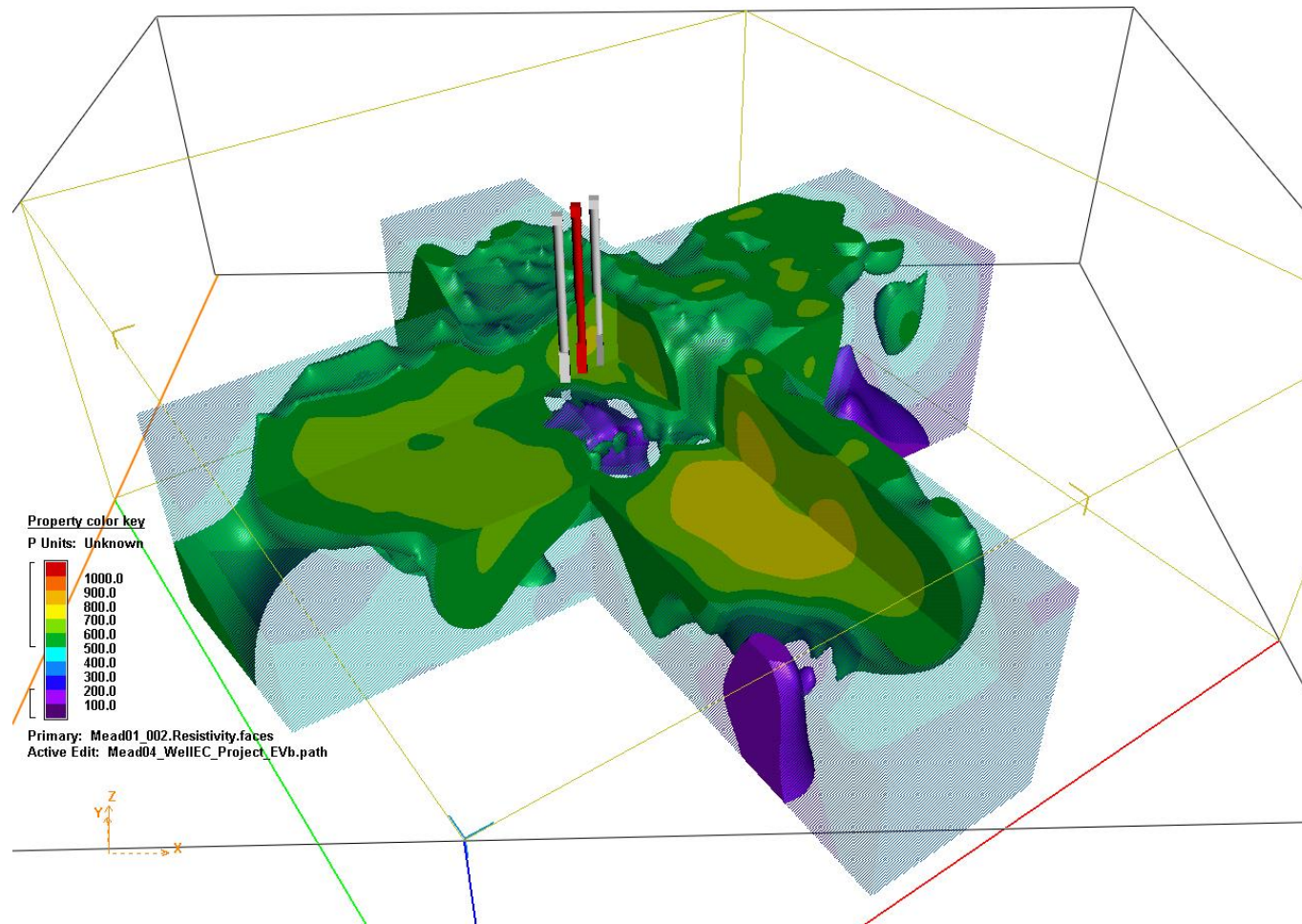


Figure E23. 3D representation of full 3 meter ERI datasets of BAZE site.

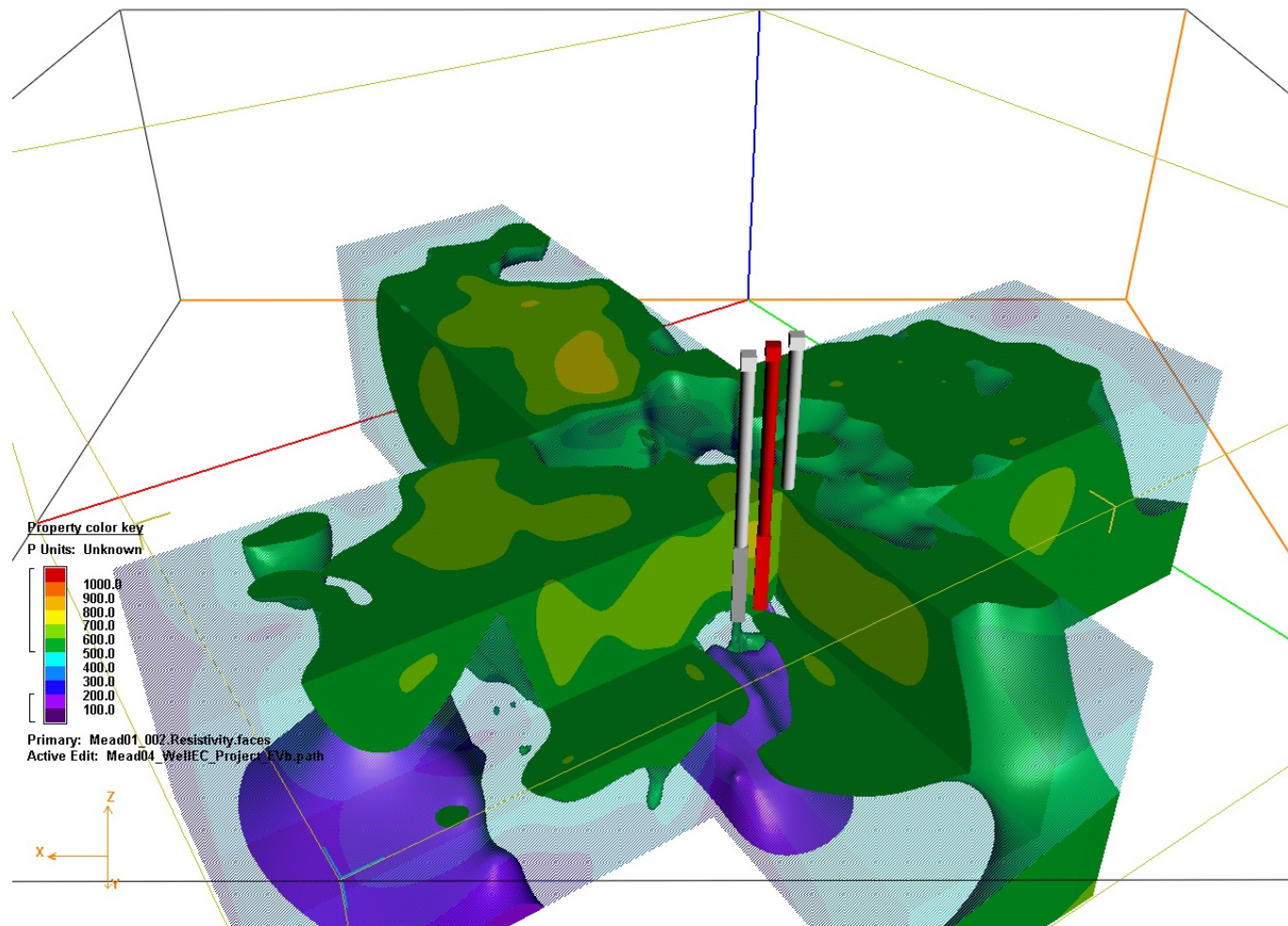


Figure E24. 3D representation of full 3 meter ERI datasets of BAZE site.